U.S. EPA Region III
Regional Center for Environmental Information
1650 Arch Street (3PM52)
Philadelphia, PA 19103

Chesapeake Bay Ecosystem Modeling Program

The Chesapeake Bay Ecosystem Modeling Program explores how water quality, the growth of plants and animals, and the physical and chemical forces of Chesapeake Bay affect each other. Model simulations help predict how things may change over time or under different conditions. The Bay Program's ecosystem models help clarify how the Bay's plant and animal life interact with the environment. Ecosystem models emphasize nutrient and organic matter sources and cycles, interactions among food web connections, and habitat structures. These state-of-the-art models help explain how and why the things we observe in Chesapeake Bay happen.

The *Strategy for the Restoration and Protection of Ecologically Valuable Species* directs Bay Program partners to pursue development of simulation models of the Chesapeake Bay ecosystem. Simulation models are part of a bigger package designed to restore and protect Bay species, at all trophic levels. Meeting the *1987 Chesapeake Bay Agreement* goal to "provide for the restoration and protection of the living resources, their habitats and ecological relationships" requires understanding the physical, chemical, and biological processes at work in the Bay. The Ecosystem Modeling effort is developing a series of interlinked models that address relationships in the Bay by simulating critical habitats of Chesapeake Bay. These simulations will be used for management decisions concerning land use, nutrient loadings, and fish production.

ECOSYSTEM MODELS OF CHESAPEAKE BAY

1994 - 1996

Progress reports
prepared for the

Living Resources Subcommittee
Chesapeake Bay Program

August 1997

Printed on recycled paper by the U.S. Environmental Protection Agency
for the Chesapeake Bay Program

TABLE OF CONTENTS

Summary 1

Empirical Ecosystem Models 6

Wetlands

Modeling the Lower Chesapeake Bay Littoral Zone and Fringing Wetlands: Ecosystem Processes and Habitat Linkages 21

Submerged Aquatic Vegetation

Trophic Control of SAV Responses to Nutrient Enrichment: Simulation Modeling of Mesocosms Experiments 52

A Model of SAV Feedback Effects on Water Quality 58

Marsh

Simulation Model of Biogeochemical Processes in Marsh Mesocosms 72

Zooplankton

Zooplankton Process Model for Chesapeake Bay 78

A Stage-Structured Model of Zooplankton Dynamics in Chesapeake Bay 86

Plankton-benthos

Planktonic-Benthic Interactions in Mesohaline Chesapeake Bay: Model Simulations of Responses to External Perterbations 95

Fish

Fish Bioenergetics: Relating Nutrient Loading to Production of Selected Fish Populations 106

Ecosystem Models of Chesapeake Bay
Summary

Chesapeake Bay is a very complex and diversified estuarine ecosystem. Freshwater pours into the Bay from five major river systems. The ocean penetrates the Bay's mouth, with saltwater sliding under the freshwater. Salinity, which affects everything that lives in the Bay, varies from source to mouth, top to bottom, and year to year. Although much of the Bay is fairly shallow, a deep trench stretches down the mainstem where the ancestral Susquehanna flowed. Water temperatures fluctuate, depending on depth and season. Plants and animals crucial to the ecosystem are often small or hidden. Microscopic phytoplankton and zooplankton inhabit the water column, providing food for fish and utilizing nutrients. Bottom dwellers are important links in the food web, not only as predators and prey, but because they help recycle nitrogen and carbon. Submerged aquatic vegetation (SAV) or Bay grasses growing along the edges of the Bay supply oxygen to the water and capture suspended sediments. SAV also provides habitat for young fish and crabs. The Bay's hydrological and biochemical processes are complex and interrelated with each other as well as the biota. Models use mathematical relationships to summarize and analyze these relationships. Once created, models can help project future biotic responses, based on environmental factors.

In addition to natural processes, human effects can't be ignored when examining the Bay's ecosystem. Activities on land affect water temperatures, oxygen levels, and the amount of sediment and nutrients in the Bay. If water quality improvements are to be sustained and restoration of plants and animals successful, the Bay's natural processes and how they affect each other must be understood. Human activities can then be factored into those processes. The Chesapeake Bay Program depends on the scientists who gather information about the Bay, but resource managers need to quickly apply what is learned to the Bay's pressing problems. Ecosystem models can help managers and decision-makers direct restoration of Chesapeake Bay.

In 1984, the Bay Program initiated several long-term monitoring programs which provide information on water quality, hydrology, and living resources in the Bay. The Chesapeake Bay Ecosystem Modeling Program was a natural extension of these monitoring efforts. Ecosystem models explore how water quality, the growth of plants and animals, and the physical and chemical forces of Chesapeake Bay affect each other. Models provide a picture of the Bay's relationships and simulations by the models help predict how things may change over time or under different conditions.

A key component of the Ecosystem Modeling Program is effective integration of modeling approaches. The ecosystem process models use nutrient loading and other information to predict the quality and quantity of food and habitat available to fish populations. The fish bioenergetics models use this food and habitat information to predict the potential production of striped bass, bluefish, weakfish, Bay anchovy, menhaden, spot and white perch. The models will be combined to incorporate ecological feedbacks associated with top-down control by fish of their prey and ecosystem components, such as SAV and water quality. The two modeling frameworks for Chesapeake Bay -- fish bioenergetics and ecosystem process models -- will also be merged with hydrodynamic models to evaluate changes in habitat conditions, flow, and nutrient loading on living resources.

The Chesapeake Bay Ecosystem Modeling Program for 1994-1996 included models for: submerged aquatic vegetation (SAV); littoral areas, marshes and wetlands; plankton-benthos; zooplankton; and ecosystem and fish bioenergetics. "Box models" describe ecosystem processes

as they change through time and space. Empirical modeling helps to determine responses of the ecosystem to nutrient loading on various time-scales. Elements of the ecosystem models are also being combined with the Chesapeake Bay Water Quality Model.

Model Specifics

Empirical Ecosystem Models explore the large-scale driving forces that influence plant and animal growth. The models link growth of plants and algae, oxygen conditions of the water, nitrogen concentrations, deposits from decaying plants, and the amount of water flowing from rivers into the Bay. Important features of the empirical ecosystem models are linked with vegetation and fish models to help explain how the growth of these living resources changes through space and time.

To demonstrate the ecological connections and interactions, the ecosystem is broken down by important components into boxes. Collectively, these box models portray regions of the estuary as a network with patterns of physical exchange. Model simulations make it possible to determine how residence time of biochemical, chemical and biological components vary seasonally, with river flow, and spatially within the estuary. For example, empirical model results indicated that 88% of the variability in freshwater residence time for Patuxent River could be predicted by the freshwater input rate to the Patuxent. Previous reports described a strong positive relationship between river flow and hypoxia in the Bay's mainstem. The new box models showed that the stratification associated with river flow and the oxygen demand associated with nutrient and organic matter loading created this relationship between flow and hypoxia.

These empirical ecosystem models offer some surprising results. They confirmed earlier conclusions that phytoplankton biomass decreased in the upper estuary as river flow increased. However, in the upper estuary, model results contradicted the conventional nutrient enrichment concepts that phytoplankton biomass would be highest when river flow and nutrient loading was lowest. According to the models, in dry years when nutrient loading was lower, water quality tended to degrade rather than improve. In middle estuary simulations, phytoplankton biomass and production did conform to traditional theories.

The ***Littoral Zone and Wetland Model*** describes the dynamic exchange of primary production, particulate and dissolved substances, and smaller biological components among the mosaic of different habitats in shallow-water areas. Littoral environments of Chesapeake Bay exhibit patterns of aquatic productivity, sediment processes, and biogeochemical cycling distinct from those of adjacent channel waters.

Model results indicated that the biomass of diatoms and other plankton in each of the habitats modeled was greatly influenced by inter-habitat exchanges. The magnitude of exchange among habitats was much greater than exchanges associated with production and loss of components such as carbon, chlorophyll *a*, and nitrogen with habitats. Estimates of annual primary production by phytoplankton, sediment microalgae, and plants, however, is essential to understanding shallow-water ecosystems. Phytoplankton contributed about 15% of littoral zone/fringing wetlands production. Over one-third of annual littoral zone production was from sediment microalgae. Production rates for microalgae were greater in nonvegetated sites than in vegetated habitats. Eelgrass productivity accounted for 15% of total production, with productivity from shoots four times that from epiphytes. Cordgrass productivity accounted for almost 36% of the littoral zone ecosystem's production. Among the four different habitats

modeled, the vegetated intertidal habitat, which was the smallest habitat, accounted for 43% of total productivity from the entire littoral zone and wetlands modeled.

The ***Marsh Model*** is currently in the early stages of development. Twelve artificial marshes, called mesocosms, were created to determine the effects of time and biological community complexity on marsh functions. The model and mesocosm experiments are interactive; feedback from each is helping to refine both the experiments and the marsh model. To date, the marsh model reasonably duplicates east coast salt marsh behavior. The model is proving useful as an interactive tool for designing mesocosm experiments. Preliminary model results indicated that permanent nitrogen loss through denitrification was dependent on productivity of the marsh plants, but the importance of nitrogen removal vs. nitrogen storage in plant tissues has not been determined.

Submerged Aquatic Vegetation (SAV) Models describe the complex feedbacks that affect SAV growth. One model explores how the effects of nitrogen on SAV depends on both the amount of nitrogen and the level of Bay grasses present. The model showed that the presence of vegetation significantly affected nutrient levels in grass beds. Bay grasses reduced nitrogen levels in water by 50%, compared with unvegetated sites. However, at high nitrogen loads, beds were eventually eliminated and acted like unvegetated sites. The effects of nutrient loading were increased because impaired SAV had less ability to clear sediments from the water. This impaired self-cleaning resulted in more suspended sediment and an even lower light environment.

Another SAV model examines the consequences to grasses of interactions among fish and invertebrate grazers at different nutrient levels. Preliminary results showed that grazing amphipods could not control epiphytic blue-green algae. Fish grazing produced complicated results: adding fish increased nitrogen cycling in moderate nutrient conditions and decreased cycling in high nutrient conditions.

Zooplankton Models explore the interactions among different species and sizes of phytoplankton and zooplankton. Zooplankton feed on phytoplankton and smaller zooplankton, as well as cannibalize juveniles. In turn, they provide food for smaller fish. Two models will be linked to help understand how nutrient loading interacts with this trophic level. One model uses size-frequency distribution and stage-specific zooplankton abundances to estimate food availability for planktivorous fish. A second model examines the environmental factors that influence zooplankton developmental stages. Both models are in the early stages of development. To date, patterns of species abundance and progression through developmental stages have been successfully modeled for mesohaline regions of the Bay.

Plankton-Benthos Process Models examine the ways that plankton and benthos are affected by environmental factors. Eutrophication and associated bottom water hypoxia can cause dramatic shifts in microbial metabolism, as well as seasonal mortality of benthic animals. Hypoxic conditions also inhibit the nitrification-denitrification activities of the benthos. The plankton-benthos model helps predict complex interactions among fish, plankton, nutrients and bottom oxygen.

Model results indicated that most of the nitrogen for production came from river flow in spring and from regeneration in summer. Most of that regenerated nitrogen came from organisms in the water column. The physical activities of benthic deposit feeders stimulated

nitrification-denitrification. Fish grazing on phytoplankton created mixed results, depending on season. When fish increased, the subsequent increased nutrient release stimulated phytoplankton production. Model results suggested that fish feeding, whether on benthos or plankton, had little effect on primary production or sedimentation. However, benthic suspension feeders had a potentially significant effect.

Fish Bioenergetics Models look at the growth rate of important fish under specific environmental conditions. They describe habitat suitability and use by specific fish species. Bioenergetics models are complete for striped bass, bluefish, and weakfish, and two of their preferred foods, bay anchovy and Atlantic menhaden. Bioenergetics models estimate how much food fish will consume, based on growth rates, temperature history, and type of food. Preliminary models also describe growth of two bottom-feeders, white perch and spot. Traditional models of fish population production are usually based on average conditions over large areas and assume constancy of environment. Because habitat quality in Chesapeake Bay is fragmented, three-dimensional (3-D) modeling of the Bay is necessary. Spatial model results of carrying capacity for menhaden showed a large degree of patchiness, depending on season.

Fish success is gauged by the number of individuals in a population, over time, and the growth rates of individuals. Growth rate is species- and size-specific, depending on temperature and food availability. Growth rate is also closely linked to female reproductive capabilities. Completed models indicated that smaller striped bass generally had fewer areas in the Bay that supported positive growth, compared with larger striped bass, except during the winter. As striped bass aged, they increased their use of open-water food sources. Weakfish and bluefish tended to utilize food resources on the bottom and their growth was affected by dissolved oxygen and temperature. It appeared that migration of older striped bass to coastal waters and the restricted use of Chesapeake Bay by older weakfish and bluefish may be due to conditions created by certain combinations of lower temperatures and limited food supply.

In another modeled scenario, striped bass growth rate potential was modeled as a function of the fish's horizontal position and water column depth in Chesapeake Bay. Simulations indicated a dramatic seasonal/spatial difference in growth rate potential. During May, the best growth potential stretched from the western shore to midchannel areas and in shallow regions along the eastern shore of the Bay. During July, growth rate potential was good only in a small region where the salty and freshwater layers meet and near the bottom on the eastern shore. According to the model, striped bass growth was limited in July by two things: higher temperatures and anoxia.

Models for Atlantic menhaden, bay anchovy and spot highlight the importance of understanding each aspect of Chesapeake Bay's food web. Atlantic menhaden and bay anchovy consume different types of plankton; spot feed on small bottom-dwellers. Bay anchovy numbers do not appear to be limited by one particular food type.

Atlantic menhaden spend only a short part of their life in the Bay. Menhaden are an important food for larger, commercially valuable fish. However, model results showed menhaden impact on the bay, represented by how much plankton they consumed, was small. In addition to being an important food source for larger fish, Atlantic menhaden are also commercially harvested. The Fish Bioenergetics Models could be an important link to understanding how commercial fishing affects the sportfish that feed on menhaden.

The Big Picture

Bay researchers are linking ecological models to relate fish production and water quality in Chesapeake Bay and its tributaries to changes in nutrient and organic material inputs. This involves developing the individual models mentioned above and analytical tools, like spatial modeling and Geographic Information Systems (GIS). Connections among model types and with the analytical tools will make it possible to view Chesapeake Bay as the complex ecosystem it really is.

Ecosystem processes, habitat, and plankton, benthos and fish models will be linked with the Bay Program's Time Variable Water Quality Model. This will create a dynamic, three-dimensional, simulation package capable of showing the effects of spatial variation in water quality and living resources . A user-friendly model interface, complete with user-guide, is slated for the final stages of the project (1997-1998). With it, scientists and managers will be able to map habitat and living resources information and simulate management scenarios. Display possibilities include: maps of the surface later of the Bay for any factor on any date; plots of shore outline; specific user-defined locations; and animation of output for any variable, over time, at the surface layer, bottom layer, or 3-D view of the Bay.

Empirical Ecosystem Models

J.D. Hagy and W. R. Boynton

Chesapeake Biological Laboratory
University of Maryland
Solomons, MD

Background

Reports in past years (e.g. Kemp *et al.* 1992, Brandt *et al.* 1995) demonstrated the potential to describe relationships between nutrient loading and responses of estuarine ecosystems in a relatively simple, direct, and empirical way. Some ecosystem responses were localized in particular regions of Patuxent River estuary (e.g. winter, spring and summer phytoplankton, summer hypoxia), suggesting that a careful investigation of spatial patterning would improve the empirical ecosystem models developed earlier. The data interpolation and visualization software developed for spatial patterning did slightly improve the models. The software also expanded the scope of the models beyond individual stations to regions of the estuary. Moreover, the interpolator also made it possible to calculate volume-based parameters, such as the hypoxic volume-days parameter used for hypoxia, and included these parameters in the empirical ecosystem models.

The broad empirical relationships indicate that, on seasonal to annual time scales, Patuxent River estuarine ecosystem responds to nutrient loading predictably. In particular, during years with high river flow, chlorophyll a concentrations tend to be higher in the middle estuary and summer hypoxia tends to be more intense and longer in duration. The responses are substantial with respect to ecological reference points, such as the habitat criteria for Bay grasses. Water quality in high-nutrient load years tends to violate submerged aquatic vegetation (SAV) habitat requrements more often and over a larger area of the estuary than in low-load years. Despite these initial successes, several questions remained, including: (1) how and why do ecosystem responses to nutrient loading vary regionally within estuaries, among estuaries, and throughout the seasons of the year; (2) what is the relative impact of freshwater input rates and the highly correlated nutrient loading rates on estuarine ecosystems; and (3) what is the usefulness of the empirical models in a predictive mode and how can it be improved?

The ecosystem models developed most recently (Hagy 1996) utilized a range of empirical approaches in addition to regression. "Empirical ecosystem models," as opposed to "ecosystem regression models" (the term used earlier within the ecosystem modeling component of the Chesapeake Bay Program) best describe current ecosystem modeling work. Additionally, box models have been added to the range of models used. These primarily descriptive models are related to ecosystem process models in an interesting way: process models use an understanding of ecosystem processes to investigate how both state variables and ecosystem processes change through time and space; box models use the direct measurements of state variables through time and space to calculate how rates of ecosystem processes changed through time and space. Thus, box models "hindcast" important ecosystem rates into the past, permitting a whole new set of predictive empirical ecosystem models, including regression models, to be developed. This is a substantial extension from past work which primarily investigated responses of state variables

such as chlorophyll a or hypoxia (an exception is sediment nutrient fluxes) to nutrient loading and other independent variables. These new box models permit much more interpretation of mechanisms responsible for the empirical relationships we observe.

Box Models for Patuxent River

The box models for Patuxent River were developed for the following purposes, each of which was successfully addressed with the models:

(1) Estimate residence times for several different regions of the estuary-- during each month of the year, under a range of river-flow conditions.

(2) Estimate the transport of materials of interest (i.e. organic carbon, inorganic nitrogen, dissolved oxygen) among different regions of the estuary and between the surface and bottom layer.

(3) Estimate the net production or consumption of the same materials in different regions of the estuary -- at different times of the year and under different river flow/nutrient loading conditions.

Essentially, a box model is a system of linear equations describing the balance of salt and water within each of several regions, or boxes. Collectively, the boxes portray a network of regions of the estuary with an assumed pattern of physical exchange (i.e. two-layer estuarine circulation). The equations can be solved to estimate coefficients describing the physical exchanges. Transport of other materials can be estimated as the product of concentration times water flow, and net production or consumption of the same material can then be calculated by mass balance. Box models were first described by Pritchard (1969) and the technique was extended substantially by Officer (1980). Taft *et al.* (1978) described a notable application of box modeling to Chesapeake Bay. The box models developed for Patuxent River and a large portion of the results obtained from them were described in detail in Hagy (1996); however, essential features of the models will be described here along with selected results.

Model Structure

The Patuxent River box models divided the estuary into six regions along the longitudinal axis of the estuary. Five of the regions were subsequently divided at the pycnocline into two layers (Figure 1). For any one box, the possible exchanges included: lateral advective and non-advective exchanges in two directions; vertical advective and non-advective exchanges; and freshwater input. The salt balance is described as:

$$V_m \frac{ds_m}{dt} = Q_{m-1} s_{m-1} + Q_{vm} s'_m - Q_m s_m + E_{vm}(s'_m - s_m) + [E_{m-1,m}(s_{m-1} - s_m) + E_{m,m+1}(s_{m+1} - s_m) \quad (1)$$

and the water balance is:

$$Q_m = Q_{m-1} + Q_{vm} + Q_{fm} \quad (2)$$

where the terms are defined as follows:

Q_m	Advective transport to the down-estuary box
Q_{m-1}	Advective transport from the up-estuary box
Q_{vm}	Vertical advective transport into the box
Q_{fm}	Freshwater input into the box
$E_{m-1,m}$	Non-advective exchange with the up-estuary box
$E_{m,m+1}$	Non-advective exchange with the down-estuary box
E_{vm}	Vertical non-advective exchange
s_m	Salinity in the box
s_{m-1}	Salinity in the up-estuary box
s_{m+1}	Salinity in the down-estuary box
s'_m	Salinity in the vertically adjacent box
V_m	Volume of the box

For the model to be solvable when the water column was stratified, it was necessary to eliminate two unknown coefficients by assuming that salt transport by horizontal dispersion was negligible compared with horizontal advection. This was a common assertion in this type of model (Officer 1980) and appeared reasonable for Patuxent River much of the time. Each of the exchange coefficients shown in Figure 1 was estimated for each month of the 1985-1992 average year and for each month between January 1985 and December 1992.

Residence Times

Estimates of hydraulic residence times were one of the objectives of the box modeling effort. Hydraulic residence times were the average amount of time that a parcel of water spent in the estuary. This was equivalent to the time required to reduce the concentration of a conservative dissolved material by one exponential factor. The residence time for water entering at the head of the estuary was the freshwater residence time. Residence times were useful for interpreting both the time available for biogeochemical transformations to take place in the estuary and the rates of dilution of the reactants and products of these reactions (related concepts). Residence times were estimated from the estimated physical transport by a simple simulation in STELLA.

Using the simulations, is was possible to determine how residence time varied seasonally, with river flow, and spatially within the estuary (Figure 2). For example, residence time was shorter if a material entered the outflowing lower estuary surface water than if it entered with the inflowing bottom water or upstream at the head of the estuary. Note that these models were not hydrodynamic simulations models.

The model results indicated that 88% of the variability in freshwater residence time for Patuxent River could be predicted by the freshwater input rate to Patuxent River (Figure 2). The relationship was described by the hyperbolic function:

$$T = \frac{1}{0.009 + 0.04 Q_f}, \qquad r^2 = 0.88 \qquad (3)$$

where T = the freshwater residence time in days and Q_f = the freshwater input rate in units of $m^3\ s^{-1}$. Other residence times for Patuxent River did not relate as well to freshwater

input rates to Patuxent River (Figure 2). In fact, for the lower estuary, flushing was better predicted by the rate of inflowing bottom water, gravitationally driven flow, and tidally driven flow. These flows were determined by the density structure of the water column at the mouth of Patuxent River (Figure 3). Therefore, the middle and lower reaches of Patuxent estuary showed no increase in flushing rate during high river flow to mitigate the effects of the high-flow induced, high nutrient loading from Patuxent River.

Nonconservative Box Models

In addition to the residence time estimates, box models estimated a range of nonconservative nutrient and organic matter fluxes for the period between 1985 and 1992. The net nonconservative flux of materials in any box was calculated from the mass balance equation for that material in the box. Many of these conclusions are discussed in detail in Hagy (1996).

The box models were used to estimate the net production of total organic carbon (TOC) and dissolved inorganic nitrogen (DIN; which included ammonium, nitrate, and nitrite) in a 10 km reach of Patuxent estuary located between St. Leonard's Creek and Broomes Island. The box model-based estimate of annual TOC production was amended with estimates of organic matter deposition to sediments and transfer of organic matter to fish. These estimates were then converted to nitrogen to estimate the inorganic nitrogen demand associated with net organic matter production (Figure 4). An estimate of inorganic nitrogen uptake made it possible to estimate, by difference, the amount denitrified. Denitrification in the middle Patuxent was estimated at approximately 736 mmol N m^{-2} y^{-1}. This amount was within the range of denitrification values reported in the literature, but was three times greater than the denitrification rate estimated for Patuxent River by Twilley and Kemp (1985) suggests that denitrification may be a greater sink for nitrogen in Patuxent River than previously believed. However, other sinks for nitrogen, such as marshes, were also significant and may have accountted for some of the difference.

Eleven years of high quality monitoring data are now available. Therefore, it may be possible to make this calculation for years with different levels of nutrient loading and model how nutrient loading has affected denitrification rates in Patuxent River. If in fact denitrification becomes a "free" source of nitrogen reduction in Chesapeake Bay as oxygen conditions improve, this positive feedback may already be apparent in the water quality record for Patuxent River.

New Predictive Models

New empirical models relating external forcing of the Patuxent River ecosystems to ecosystem responses were possible as a result of the flux estimates generated by the box models. Special attention was given to: (1) bottom layer oxygen demand and its relation to river flow and hypoxia; and (2) net phytoplankton production and its relationship with nitrogen loading and phytoplankton biomass.

Hypoxia

Previous reports described a strong positive relationship between river flow and annual hypoxia (hypoxic volume-days). Box model-generated bottom layer oxygen demand estimates showed that the relative role of stratification effects associated with river flow and oxygen demand effects associated with nutrient and organic matter loading created the positive

relationship that was observed. Moreover, the functional form of the hypoxia vs. river flow relationship was reevaluated (Hagy 1996; Chapter 3).

During 1985-1992, annual hypoxia (the annual integral of hypoxic volume) varied between 1,497 10^6 m^3 d y^{-1} in 1986 and 6,923 10^6 m^3 d y^{-1} in 1987. To put these values in perspective, we estimated that maximum likely value that would be expected, based on assumptions determined from experience with the Chesapeake Bay Water Quality Monitoring Program Data, and called it the "maximum likely hypoxia." These assumptions were that: (1) hypoxia was not likely to occur when water temperatures were too cold for rapid metabolism to occur or when the water column was not well stratified; (2) with limited exceptions, only waters below the pycnocline would be persistently hypoxic or anoxic, thereby providing a maximum volume; and (3) hypoxia would not affect the entire maximum volume immediately, but would increase in extent steadily to the maximum, then decrease. The first decrease in dissolved oxygen concentrations from saturation levels were usually observed in May. Thus, significant hypoxia would not be expected prior to June 1. Because a breakdown of stratification usually occurred toward the end of August, hypoxia would be expected to persist only rarely beyond August 31. Assuming a sinusoidal increase to the maximum hypoxic volume beginning June 1, then a similar decline concluding on September 1, the maximum likely hypoxia for Patuxent River would be 9,869 10^6 m^3 d y^{-1}. The maximum observed annual hypoxia during 1985-1992 was 70% of this maximum. Thus, hypoxia in Patuxent River, in the worst years, was severe but could have been worse.

Calculating "maximum likely hypoxia" indicated that the relationship between nutrient loading and hypoxia could not be linear unless it was assumed that the relationship broke down at high levels of nutrient loading. Although the relationship between river flow and annual hypoxia had a linear component, the best relationship was obtained using a hyperbolic functional form (Figure 5).

The best-fit hyperbola (r^2=0.92) was:

$$Hypoxia = 9562 - \frac{50241}{Flow} \qquad (4)$$

where *Hypoxia* = annual hypoxia (10^3 m^3 d y^{-1}) and *Flow* = water-year mean fall line river flow (m^3 s^{-1}). The estimated asymptotic value of the equation (9,562 10^3 m^3 d y^{-1}) was very close to the estimated maximum likely annual hypoxia (9,869 10^3 m^3 d y^{-1}). The flow level at which no hypoxia would be expected was 5.25 m^3 s^{-1}, barely lower than the average flow that occurred in 1986. To investigate the relative role of water column stratification and bottom layer oxygen demand in generating the above relationship, both factors were individually related to river flow. There was no significant relationship between hypoxia and river flow averaged over any period and stratification. However, bottom layer oxygen demand increased with river flow and approached an asymptotic value (Figure 6). The relationship (r^2=0.88) was:

$$OD = 1492 - \frac{5178}{Flow} \qquad (5)$$

where OD = annual bottom layer oxygen demand (g O_2 m^{-2} y^{-1}) in equation 4 and $Flow$ = water-year mean fall line river flow (m^3 s^{-1}). The proper functional form for the relationship between bottom layer dissolved oxygen demand and annual hypoxia was not statistically clear from the data. However, only the linear relationship had conceptually valid predicted values. The best fit linear line relating oxygen demand to hypoxia was:

$$Hypoxia = -4394 + 9.48(OD) \quad (6)$$

where the terms of the equation are as described above. The composite function obtained by combining eq. (5) and eq. (6) was similar to eq. (4). These results indicated that, in Patuxent River, oxygen demand was related to river flow and appeared to drive the formation of hypoxia. Because there was no direct conceptual link between river flow and oxygen demand, the nutrient and organic matter loading associated with river flow must drive the oxygen demand. Therefore, a relationship between nutrient loading and organic carbon production in the estuary was expected. The interannual variability was significant in terms of its capacity to generate hypoxia in Patuxent River.

Phytoplankton Biomass and Net Production

In previous reports, a series of regression models related chlorophyll a concentrations to fall line nutrient loading and river flow (Brandt *et al.* 1995; Kemp *et al.* 1992). A negative relationship between river flow and chlorophyll a was noted in the upper estuary and a positive relationship in the middle estuary. It was hypothesized that the upper estuary relationship was primarily driven by the dilution-effects of river flow; whereas, the middle estuary relationship was driven by nutrient enrichment. To test this hypothesis, the regional difference in the effect of Patuxent River discharge rate on residence times was quantified. The results did not contradict the hypothesis.

To further examine the hypothesis, net phytoplankton production was estimated for the upper estuary and middle estuary using the box models. The new series of box models used individual cruises as observations, rather than annual means used by the early regression models, and a non-parametric approach as opposed to regression. In general, the results from the box models were much more conclusive and the statistical approach more robust (Hagy 1996).

The box models confirmed earlier conclusions from the regression models. Phytoplankton biomass decreased in the upper estuary as river flow increased (Figure 7). Conversely, phytoplankton biomass was highest when river flow and nutrient loading was lowest, contradicting conventional nutrient enrichment concepts.. During much of the year, and especially the winter months, all nutrient concentrations were many times greater than limiting concentrations, eliminating nutrient limitation as an important factor. Given the high turbidity at all times of the year, light limitation was likely to occur and self-shading was probably important. Thus, the dilution effects related to high flow would be expected to both decrease phytoplankton biomass and increase net phytoplankton production in the upper estuary. This is exactly the result that was obtained by the model (Figure 8). Net phytoplankton production, especially during summer, increased with river flow. From a management perspective, these results may be disconcerting. In dry years when nature offers a temporary reprieve from some diffuse source nutrient loading, water quality tends to degrade rather than improve. However, limiting nutrient

concentrations are occasionally observed during summer, and nutrient loading reductions will likely increase the frequency of these occurrences.

Although patterns of phytoplankton biomass and net production in the upper estuary did not conform to the "agricultural paradigm," middle estuary phytoplankton biomass and production did conform. Phytoplankton biomass tended to increase with nutrient loading (Figure 9) and the increase was related to *in situ* phytoplankton production (Figure 10), rather than advection of phytoplankton from the upper estuary into the middle estuary. Because nitrogen concentrations in the middle estuary were frequently below limiting concentrations during summer and there was no discernible residence time effect of river flow, the causal chain of high nutrient load → nutrient enrichment → increased phytoplankton production → increased phytoplankton biomass was plausible for the middle estuary. However, a notable effect of increased nutrient loading to the middle estuary was to increase the variability in phytoplankton biomass in addition to the mean biomass.

Mainstem Box Models

The larger focus of the Chesapeake Bay Program modeling efforts dictated moving the focus of analysis from Patuxent River into the mainstem Chesapeake Bay. This required developing a box model for the mainstem Bay. The main goals of this effort are similar to those for Patuxent River; however, the possibilities for synthesis of research approaches may be greater due to the larger number of studies conducted on Chesapeake Bay. The effort will be more difficult, however, because of the greater complexity of Chesapeake Bay.

The Chesapeake Bay box models are branched, two-dimensional, time-variable models. The only aspect of the models that is fundamentally different from the Patuxent box models is the branching. The mainstem box models simulate exchanges between the mainstem Bay and the James, York, Rappahannock, Potomac, Patuxent, and Choptank Rivers. The structure of the box models is shown in schematic form in Figure 11. At present the models results seem reasonable; however, the models are still at a developmental stage.

References

Brandt, S. B., W. R. Boynton, W. M. Kemp, R. Wetzel, R. Bartleson, J. D. Hagy, K. J. Hartman, J. Luo, C. J. Madden, M. Meyers, T. Rippetoe, D. D. Fugate, and R. Batiuk. 1995. Chesapeake Bay Ecosystem Modeling Program. 1993-94 Technical Synthesis Report to the Chesapeake Bay Programs's Living Resources Subcommittee and Modeling Subcommittee. Chesapeake Bay Program. Annapolis, MD.

Hagy, J.D. 1996. Residence times and net ecosystem processes in Patuxent River estuary. M. S. Thesis. University of Maryland at College Park.

Kemp, W. M., S. B. Brandt, W. R. Boynton, R. Bartleson, J. Hagy, J. Luo, and C. J. Madden. 1992. Ecosystem models of the Patuxent River estuary relating nutrient loading to production of selected fish populations. Final Report, Year 1. Maryland Department of Natural Resources. Tidewater Administration. Chesapeake Bay Research and Monitoring Division. Annapolis, MD.

Officer, C. B. 1980. Box models revisited. In P. Hamilton and R. B. Macdonald (eds.). *Estuarine and Wetland Processes.* Marine Sciences Series. Vol. 11. New York: Plenum Press.

Pritchard, D. W. 1969. Dispersion and flushing of pollutants in estuaries. American Society of Civil Engineers. *Journal of the Hydraulics Division.* 95(HYI): 115-124.

Taft, J. L., A. J. Elliott, and W. R. Taylor. 1978. Box model analysis of Chesapeake Bay ammonium and nitrate fluxes. pp. 115-130. In M. L. Wiley (ed). *Estuarine Interactions.* New York: Academic Press.

Twilley, R. R., W.M. Kemp, K.W. Staver, J.C. Stevenson, W.R. Boynton. 1985. Nutrient enrichment of estuarine submersed vascular plant communities. 1. Algal growth and effects on production of plants and associated communities. Mar. Ecol. Prog. Ser. 23: 179-191

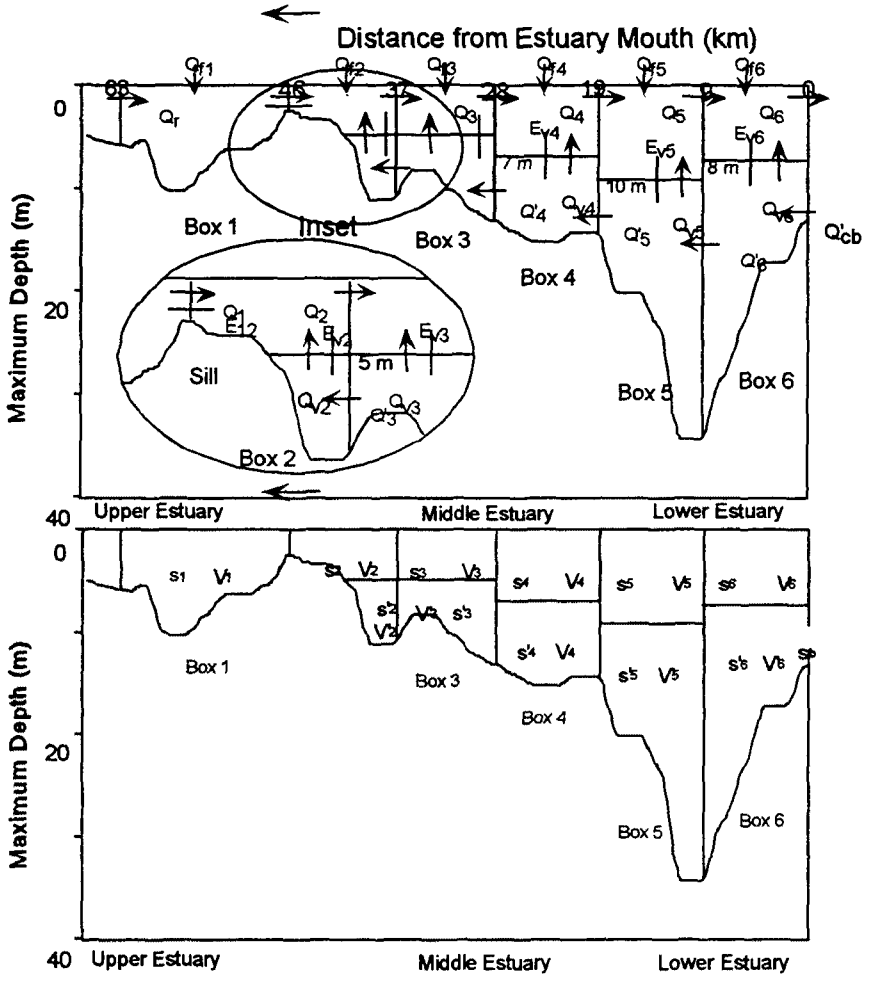

Figure 1. Schematic diagrams of the box model structure showing the box boundaries, the exchange coefficients that were estimated, and model input s. The estimated exchanges include seaward advection (Q_m) landward advection (Q'_m), vertical advection (Q_{vm}), vertical diffusive exchange (E_{vm}), and horizontal dispersion ($Q_{m,m+1}$). Inputs included the volume in each box (V_m and V'_m) concentration of salt for each box (S_m or S'_m), the input of freshwater to each box (Q_{fm}), and the salinity at the seaward boundary (S_{cb}). The sill noted at the boundary of box 1 and box 2 effectively terminates the landward flow in the bottom layer, forcing the water into the surface layer.

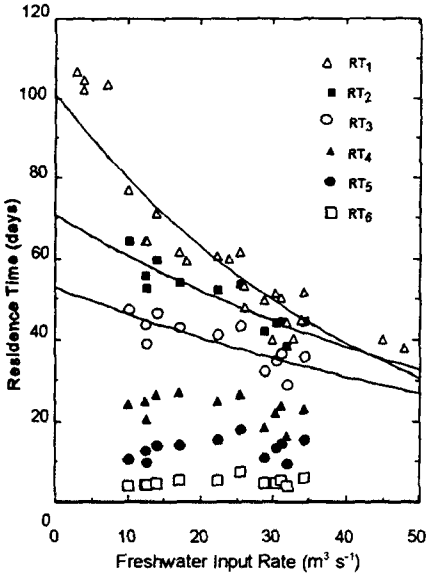

Figure 2. Residence times for surface layer boxes 1-6. This is the time required to flush from the estuary 63% of a material introduced to a single box in an instantaneous pulse. RT_i is equivalent to the residence time of freshwater. In addition to RT_i for the average year, RT_i for each February and August during 1985-1991. Exponential least-squares regression lines are shown for RT_1, RT_2 and RT_3.

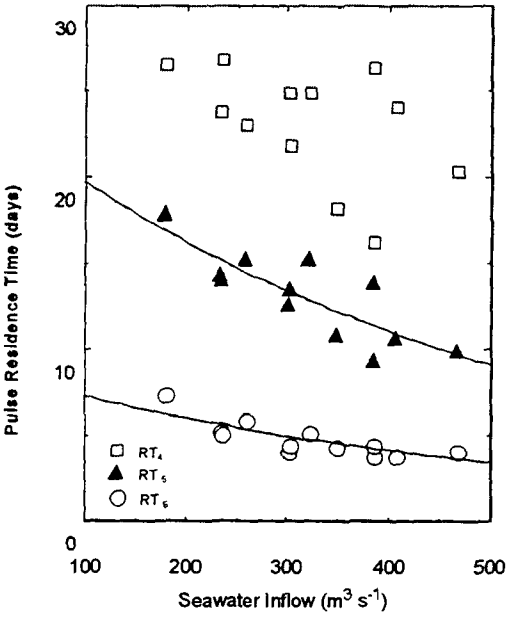

Figure 3. Residence times (RT) for surface layer boxes 4-6 related to seawater influx (Q'_{cb}). RT is defined as in Figure 2. Exponential regression lines are shown for RT_5 and RT_6, but not for RT_4.

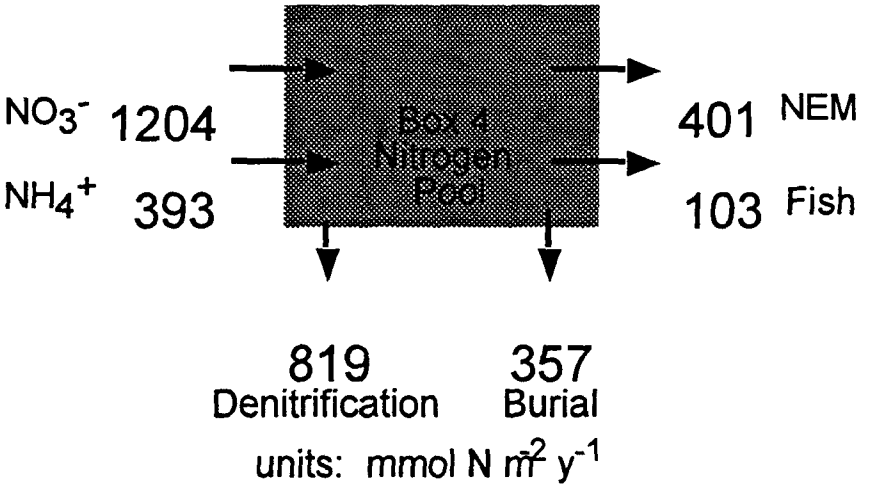

Figure 4. The balance of nitrogen for the middle Patuxent estuary (box 4). The inward arrows indicate the combined sources of inorganic nitrogen as determined by the box models. NEM is the nitrogen export associated with the net production or organic matter that is exported. Loss of nitrogen to fish is from Hagy (1996, p. 93), nitrogen burial is from Boynton et al. (1995), and denitrification is calculated by difference.

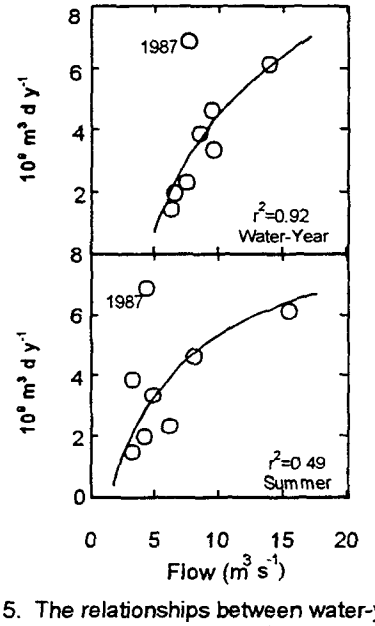

Figure 5. The relationships between water-year mean fall line river discharge and annual hypoxia (upper panel) and between summer (June-August) mean fall line river discharge and annual hypoxia (lower panel). Correlation coefficients were calculated without the 1987 observation, and the curves were hand drawn.

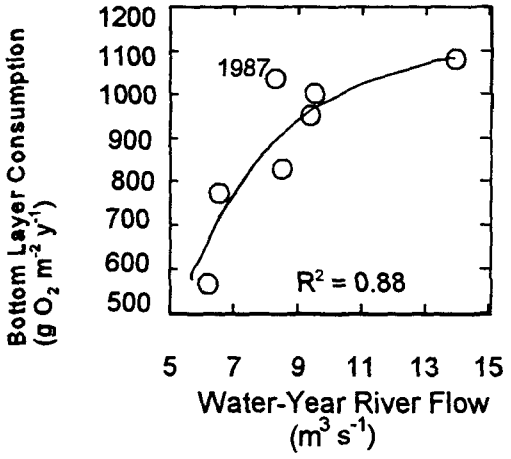

Figure 6. The relationship between water-year river flow and annual bottom layer oxygen consumption in the middle estuary for the period 1985-1991. The correlation coefficient was calculated without the 1987 observation. The curve is hand drawn to sho the functional form only.

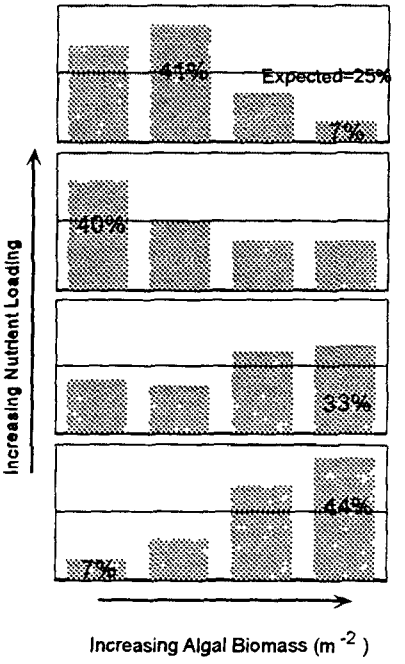

Figure 7 The relationship between phytoplankton biomass and nutrient loading in the upper Patuxent River estuary The nutrient loading and algal biomass observations were divided into quartiles by rank and the graph depicts the frequency in each of the 16 resulting cells of a contingency table The expected row percentage for each column is therefore 25% and departures from this value represent non-random association

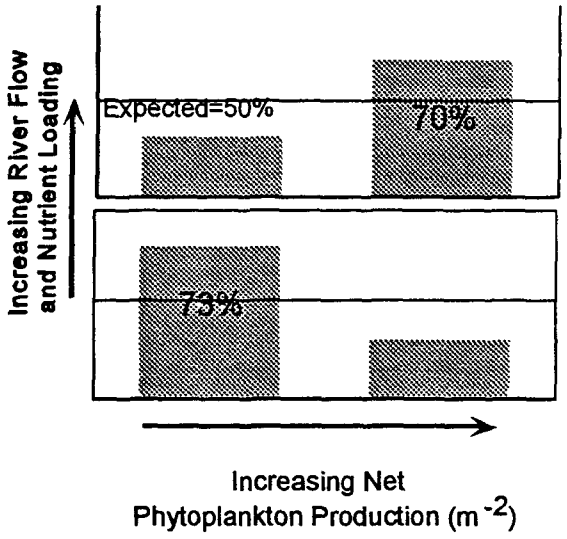

Figure 8. Upper estuary net phytoplankton production vs. river flow and nutrient loading. The ranked nutrient loadin and net phytoplankton production observations were divided into two groups at the median and the graph depicts the frequency in each of the four resulting cells of contingency table. The expected row percentage for each column is therefore 50% and departures from this value represent non-random association.

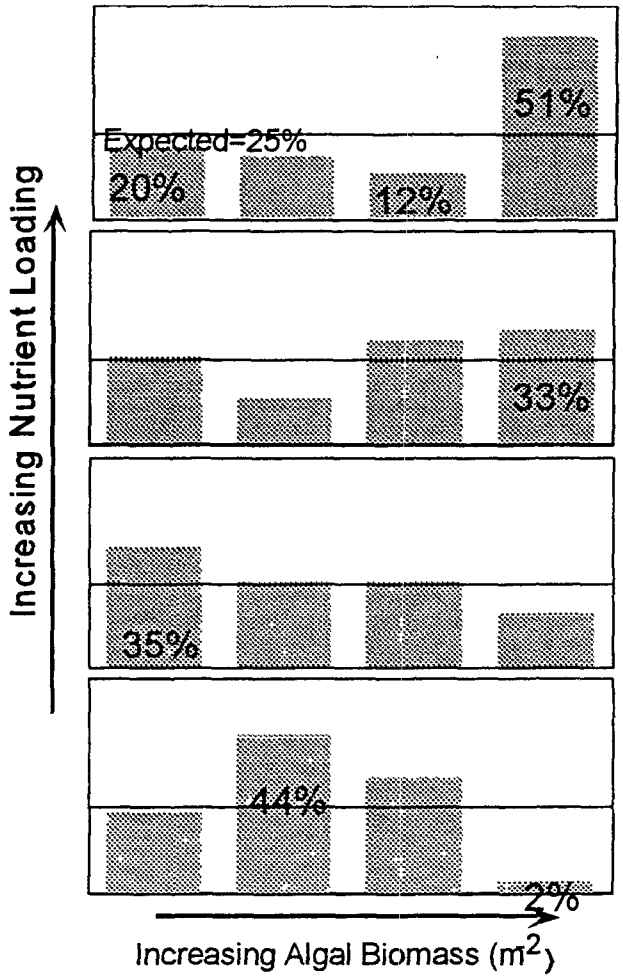

Figure 9. The relationship between middle Patuxent estuary phytoplankton biomass and nutrient loading. The nutrient loading and algal biomass observations were divided into quartiles by rank and the graph depicts the frequency in each of the 16 resulting cells of a contingency table. The expected row percentage for each column is therefore 25% and departures from this value represent non-random association.

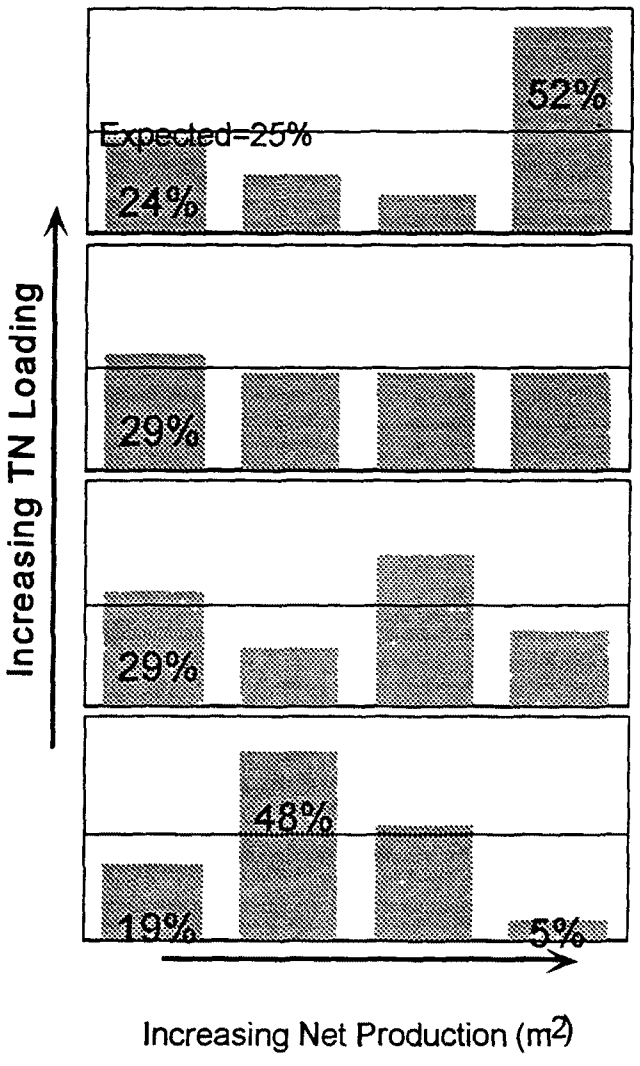

Figure 10. The relationship between middle Patuxent estuary net phytoplankton production and total nitrogen (TN) loading. The nutrient loading and net production observations were divided into quartiles by rank and the graph depicts the frequency in each of the 16 resulting cells of a contingency table. The expected row percentage for each column is therefore 25% and departures from this value represent non-random association.

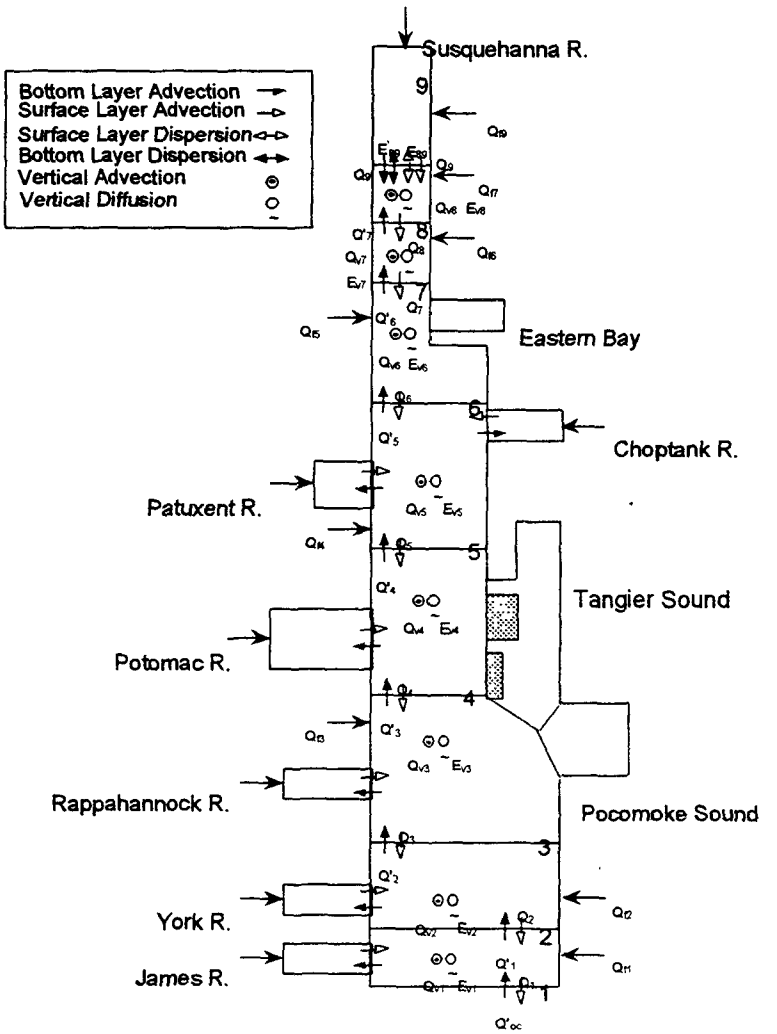

Figure 11. A schematic diagram of the box model being developed for Chesapeake Bay. The arrows pointing toward the outside of the model boxes indicate estimated freshwater inputs which are inputs to the box model calculation. The model has 9 segments in the mainstem Bay, of which 8 are divided into a surface and bottom layers. The mainstem segments exchange with the James, York, Rappahannock, Potomac, Patuxent, and Choptank Rivers. Pocomoke Sound, Tangier Sound, and Eastern Bay are included in the time-variable salinity calculations, but exchanges with the mainstem are not estimated by the models.

Modeling the Lower Chesapeake Bay Littoral Zone & Fringing Wetlands: Ecosystem Processes and Habitat Linkages

Christopher P. Buzzelli, Richard L. Wetzel and Mark B. Meyers

School of Marine Science / Virginia Institute of Marine Science
College of William & Mary
Gloucester Point, VA

Background

The estuarine littoral zone is a mosaic of different habitat types which are connected by the dynamic exchange of primary production, particulate and dissolved substances, and animal populations (Correll *et al.* 1992; Childers *et al.* 1993; Kneib and Wagner 1994; Rozas 1995). A number of coastal studies have focused on subsystem interactions within coastal marsh and shallow near-shore ecosystems (Wolaver *et al.* 1983; Stevenson *et al.* 1988; Dame *et al.* 1991; Correll *et al.* 1992; Vorosmarty and Loder 1994). These studies quantified material production and exchange in habitats fringing channel and upland environments. Although approximately 40% of the subtidal area of Chesapeake Bay is ≤ 2.0 m below mean low water (MLW), littoral zone ecosystems have not been included in efforts to simulate baywide environmental processes (Kuo and Park 1995; Spinner 1969). Biogeochemical processes in the fringing environments differ from those of the adjacent channel, but the two estuarine zones are linked on daily, seasonal, and annual time-scales (Malone *et al.* 1986; Kuo and Park 1995). Watershed factors, such as river discharge and nutrient runoff, can influence the annual patterns of production and nutrient cycling in the estuarine littoral zone (Correll *et al.* 1992). Understanding of the ecosystem processes and habitat patterns that occur within these fringing estuarine environments will help assess the role of wetlands and the littoral zone in Chesapeake Bay ecosystem dynamics.

The littoral zone environments of Chesapeake Bay exhibit patterns of aquatic productivity, sediment processes, and biogeochemical cycling distinct from those of adjacent channel environments (Kuo and Park 1995; Malone *et al.* 1986). Few published studies have employed mechanistic models to analyze habitat interactions among coastal ecosystem components to identify the probable linkages to other areas of the landscape (Boumans and Sklar 1990; Childers 1992; Costanza 1990). Understanding the synergistic interactions among littoral zone habitats would provide an essential link between the preservation of environmental quality and the protection of living resources, such as plant communities and fishery species (Dennison *et al.* 1993; Heck and Thoman 1984; Kneib and Wagner 1994). Mechanistic models can help address issues related to environmental change in coastal environments (Costanza *et al.* 1990; Wetzel and Hopkinson 1990).

Each of the different littoral zone habitats have a suite of primary producers including water-column phytoplankton, sediment microalgae, submerged aquatic vegetation (SAV) with attached epiphytic communities, and marsh grasses. Submarine irradiance, along with other meteorologic (seasonality in temperature and rainfall) and hydrodynamic factors (nutrient runoff and river flow), influence estuarine phytoplankton processes (Mallin 1994). Sediment microalgae significantly contribute to primary production in nonvegetated and vegetated subtidal

environments in many ecosystems, including those in Massachusetts (Gould and Gallagher 1990), South Carolina (Pinckney and Zingmark 1993a; 1993b) Mississippi (Moncreiff *et al.* 1992; Sullivan and Moncreiff 1988), and Denmark (de Jonge and Colijn 1994; Sand-Jensen and Borum 1991). Sediment microalgae also play an important role in the fluxes of oxygen and nutrients across the sediment-water interface (Rizzo *et al.* 1992; Sundback and Graneli 1988). SAV meadows are complex and productive littoral zone ecosystem components (Moncreiff *et al.* 1992; Murray and Wetzel 1987; Roman *et al.* 1990; Sand-Jensen and Borum 1991). SAV meadows can serve as indicators of water quality because the plants and attached epiphytes are sensitive to submarine light attenuation and the concentrations of chlorophyll a, suspended sediments, and inorganic nutrients (Bach 1993; Dennison *et al.* 1993; Wetzel and Neckles 1986).

Salt marshes are areas of increased rates of productivity and nutrient cycling (Childers *et al.* 1993; Dame and Kenny 1986; Pinckney and Zingmark 1993a). Few studies, however, have focused on the estuarine fringing wetlands of Chesapeake Bay (Drake and Read 1981; Gross *et al.* 1991; Wolaver *et al.* 1983). Ecosystem modeling offers the opportunity to include all of the principal autotrophs in an analysis of primary production and water quality over multiple habitats in the littoral zone.

Previous work focused on the development and simulation analysis of SAV models and conceptual modeling of emergent intertidal marsh communities. The SAV models clearly showed the importance of environmental factors (submarine light, temperature) and biological factors (epiphytic fouling, grazing) for controlling SAV growth, distribution, and long-term population survival (Wetzel and Neckles 1986). The SAV stand-alone model proved an accurate predictor of water quality-SAV response and habitat criteria for SAV survival (Wetzel and Meyers 1994). Over this past year, the SAV model was revised and expanded to include other components of the littoral zone. This effort will make it easier to relate littoral processes – which includes the benthos, SAV, and pelagic habitats – to models of hydrodynamics and water quality extant for Chesapeake Bay and its major tributaries.

The Lower Chesapeake Bay Littoral and Fringing Wetlands Model was developed, calibrated, and validated for habitats characteristic of mesohaline and polyhaline regions of the Bay. Simulation analyses of these ecosystem process models was conducted for specific, highly-distributed components of the estuary which emphasized intertidal wetlands, SAV habitats, and other principal components of the littoral zone. The conceptual models of the principal habitats of the littoral zone were refined and implemented into numerical simulation models. Incorporating spatially varying information such as salinity, nutrient concentration, and bathymetry as forcing functions can suggest how SAV-driven, phytoplankton-driven, and detrital and benthic microflora-driven food webs function along the tributaries and Chesapeake Bay. One of the goals was to formulate both spatially and temporally varying forcings in ways that will enable the incorporation of biological productivity and biologically driven elemental cycling (*e.g.*, for carbon, oxygen, and nitrogen) into large-scale, water quality and hydrodynamic models.

Model Description

Reference Site Description

Data for model development, calibration and verification were taken from the literature and to the extent possible from a single reference site in the lower Bay: the Goodwin Islands National Estuarine Research Reserve (GI NERR). The GI NERR is an 800 hectare (ha) littoral

zone ecosystem at the mouth of York River, Virginia, in the lower Chesapeake Bay (37° 12' 46" N, 76° 23' 46" W). The islands are owned by the College of William and Mary and are managed by the Chesapeake Bay National Estuarine Research Reserve System in Virginia (CBNERRS-VA) of the National Oceanic and Atmospheric Administration (NOAA). The research reserve includes the islands and a buffer zone that extends seaward to the -2.0 m depth contour (MLW). The -2 m depth contour is operationally defined as the littoral zone depth limit and the corresponding lateral boundary condition for the tributary water quality-hydrodynamic model. The GI NERR is an oblong island system with a large subtidal shoal extending between the shoreline and the -2.0 m depth contour. Between -1.0 and -0.5 m (MLW) is approximately 120 hectares of subtidal SAV, mostly comprised of eelgrass (*Zostera marina* L). There is approximately 100 hectares of nonvegetated intertidal habitats, with fine sands and silty sediments that surround 90 hectares of intertidal marsh vegetated primarily by smooth cordgrass (*Spartina alterniflora*). Some marsh regions are also vegetated by meadow cordgrass (*Spartina patens*), spikegrass (*Distichlis spicata*) and needlerush (*Juncus roemerianus*). The intertidal marsh grades into a salt bush habitat that includes marsh elder (*Iva frutescens*) and groundselbush (*Baccharis halimifolia*). The largest island has a small amount of maritime forest and upland vegetated by loblolly pine (*Pinus taeda*) and several hardwood species. Intertidal and subtidal habitat patterns vary over time (seasonally, interannually) and space (10's to 100's ha). Historical aerial photography depicts long-term stability in the GI NERR eelgrass meadows, but overall erosion and some horizontal migration for intertidal marshes.

Conceptual Model Structure

Four, hydrodynamically linked submodels were developed to represent the principal littoral zone habitats: (1) nonvegetated subtidal habitats (NVST) composed primarily of coarse sand; (2) vegetated subtidal habitats (VST) dominated by eelgrass; (3) nonvegetated intertidal (NVIT) typical of sand and mudflats; and (4) vegetated intertidal (VIT) dominated by smooth cordgrass. These four habitats and, thus, the models were selected based on abiotic and biotic characteristics relative to the depth gradient along which they were located. Figure 1 depicts the conceptual model structures for the four littoral zone habitat models based on the four habitat types.

The global forcing functions were tidally varying water level, solar and submarine irradiance, and water temperature. The subtidal and intertidal nonvegetated models had seven state variables each, including: large and small phytoplankton size classes (diatoms and other plankton, respectively); labile and refractory particulate organic carbon (LPOC and RPOC); dissolved organic carbon (DOC); total dissolved inorganic nitrogen (TDIN); and sediment microalgae (SM). In addition to these seven state variables, the vegetated subtidal and intertidal habitat models included additional state variables representing epiphyte carbon (ZepiC), and shoot and root-rhizome carbon and nitrogen for eelgrass (ZSC, ZSN, ZRRC, ZRRN) and smooth cordgrass (SSC, SSN, SRRC, SRRN). Table 1 gives a list of the model state variables, their mathematical abbreviation and modeled units.

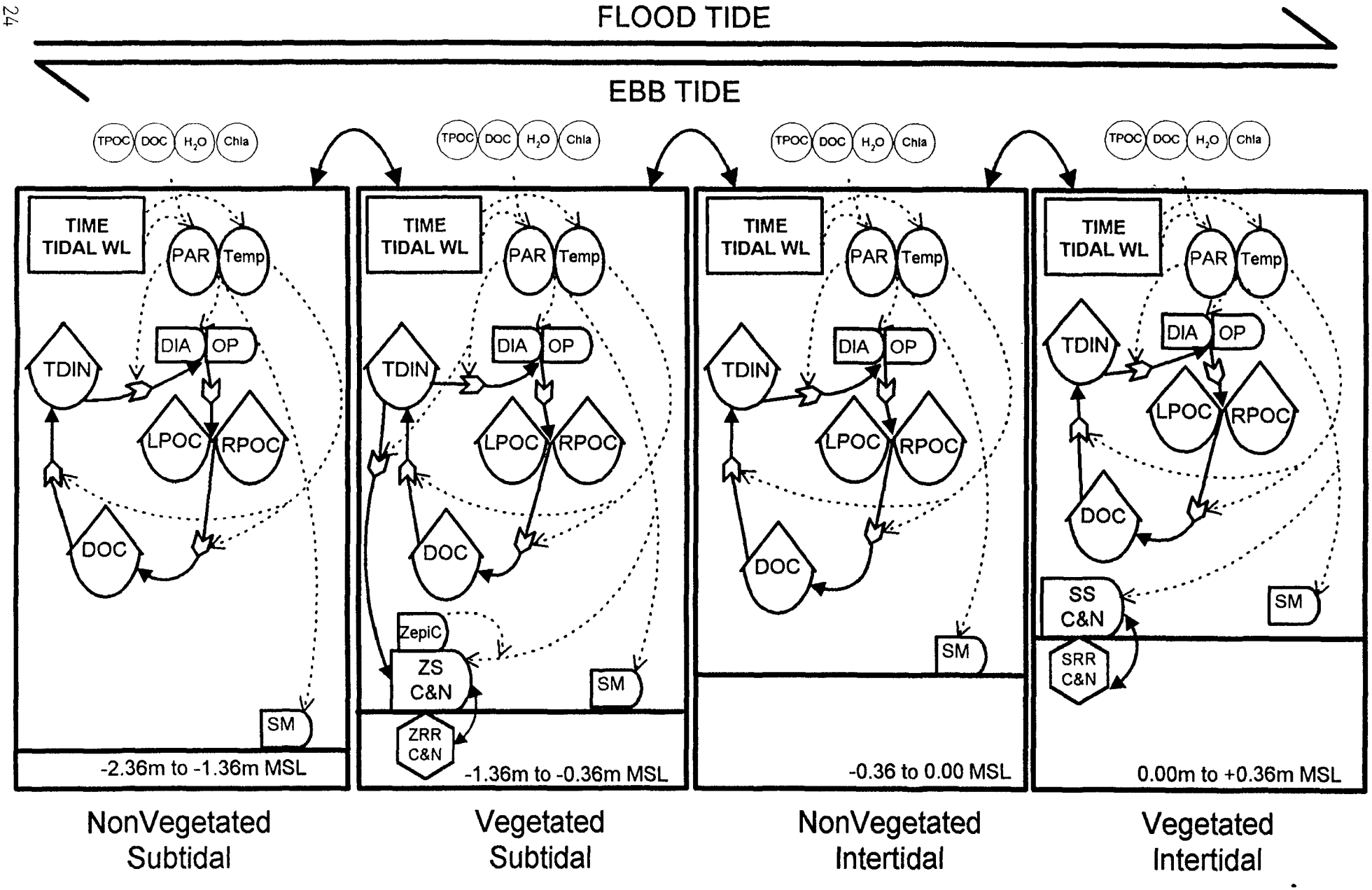
FLOOD TIDE
EBB TIDE
TPOC
DOC
H2O
Chla
TIME
TIDAL WL
PAR
Temp
DIA
OP
TDIN
LPOC
RPOC
DOC
SM
ZepiC
ZS
C&N
ZRR
C&N
SS
C&N
SRR
C&N
-2.36m to -1.36m MSL
-1.36m to -0.36m MSL
-0.36 to 0.00 MSL
0.00m to +0.36m MSL
NonVegetated
Subtidal
Vegetated
Subtidal
NonVegetated
Intertidal
Vegetated
Intertidal

Figure 1

Table 1. List of state variables for habitat models. Each habitat model includes the first 7 state variables listed. In addition to the basic seven the vegetated subtidal habitat model (VST) includes those related to *Zostera marina*; whereas, the vegetated intertidal habitat model (VIT) has those related to *Spartina alterniflora*.

ABBREV.	DESCRIPTION	UNITS
DIA	Diatom Carbon Mass	gC
OP	Other Plankton Carbon Mass	gC
LPOC	Labile Particulate Organic Carbon	gC
RPOC	Refractory Particulate Organic Carbon	gC
DOC	Dissolved Organic Carbon	gC
TDIN	Total Dissolved Inorganic Nitrogen	μM
SM	Sediment Microalgae	gC m^{-2}
ZSC	Zostera marina Shoot Carbon	gC m^{-2}
ZSN	Zostera marina Shoot Nitrogen	gN m^{-2}
ZRRC	Zostera marina Root-Rhizome Carbon	gC m^{-2}
ZRRN	Zostera marina Root-Rhizome Nitrogen	gN m^{-2}
ZepiC	Zostera marina Epiphytic Biomass	gC m^{-2}
SSC	Spartina alterniflora Shoot Carbon	gC m^{-2}
SSN	Spartina alterniflora Shoot Nitrogen	gN m^{-2}
SRRC	Spartina alterniflora Root-Rhizome Carbon	gC m^{-2}
SRRN	Spartina alterniflora Root-Rhizome Nitrogen	gN m^{-2}

Hydrodynamic Model Design

The four ecosystem process models were hydrodynamically linked by tidal exchange across the boundaries of a sequence of modeled cells representing the NVST, VST, NVIT, and VIT habitats. The cells filled and drained in sequence relative to the depth gradient, with the output from one cell providing the input for the next in the sequence dependent on tidal stage (i.e. ebb or flood periods). The nonvegetated subtidal habitat was bounded laterally by an infinite source/sink representing the offshore channel whereas the vegetated marsh was bordered by the upland with no exchange across the marsh-upland boundary. Watershed exchanges were assumed to be zero because the Goodwin Islands have little upland area and are isolated from the mainland. The cell (habitat) volume changed with each model time or integration interval (dt). Tidally driven exchanges for water column constituents (i.e. phytoplankton, DOC, LPOC, RPOC, and TDIN) were derived using finite difference solutions to equations for mass exchanges between a channel and an adjacent control volume in both flood and ebb directions (Kuo and Park 1995). This approach assumed no diffusion, no advection, and that the water within each cell was instantly mixed and homogeneous during each time-step. The change in tidal height with each time step was multiplied by habitat wet area to derive the changes in habitat volumes used in the simulation of water column processes. By definition, subtidal habitat wet areas were constant.

Intertidal habitat wet areas varied as a function of tidal inundation and were derived using a hypsometric relationship. Hypsometry was used because it provided a concise method for representing the cumulative characteristics of basin morphology (Friedrichs and Aubrey 1994; Strahler 1952). The area-height relationship of a hypsometric curve provided a better approximation for basin inundation regimes than did a linear 2-D profile, because it included the effects of shoreline curvature (Boon and Byrne 1981; Friedrichs and Aubrey 1994). Also, hypsometric determination of inundation can be useful in the analysis of wetland biogeochemical cycling (Childers *et al.* 1993; Eiser and Kjerve 1986).

The tidal exchange equation for a constituent *(e.g.*, chlorophyll a) of mass M_i where the subscript I = {1,..,4} represented each of four habitats is given in equation 1 below.

$$\frac{\Delta M_i}{\Delta t} = (\alpha m)\bullet M_i + \left[\frac{C_k \bullet \Delta h}{\Delta t} + b\right]\bullet A_i(t) \begin{cases} \Delta h>0(flood):k=i1 \\ \Delta h<0(ebb):k=i \end{cases} \quad (1)$$

Note that M_i is the total mass of a water borne constituent contained in the cell or habitat volume and can be calculated as C_i * h(t)* A(t), where C_i is the water column concentration, h(t) is time varying water depth and A(t) is the time varying wetted area of the habitat. A(t) was constant for the subtidal habitat, but variable for the intertidal habitats. The tidally varying water height, h, was referenced to mean sea level, and its change from one model time-step to the next was represented as Δh. Other processes affecting state variable masses were growth or biochemical production (α), losses from biological uptake or mortality and/or grazing (m); and exchanges with the benthos (b). In the present model, I=0 represented the channel boundary condition.

Ecosystem Processes Model Design

Ecological processes represented in the models for the various habitats included the principal factors controlling the uptake and loss of organic carbon and nitrogen as the primary limiting nutrient in these habitats. Detailed treatment of the mathematical structure, interaction coefficients and data sources for the governing equations are given in Buzzelli *et al.* (1995) and Buzzelli and Wetzel (1996) and are beyond the scope of this report. Given below is a general description of the ecological processes modeled and the state variables affected.

Primary production (gC m^{-2} or m^{-3} d^{-1}) was modeled using the rates of gross production, respiration, and loss through mortality or grazing. Phytoplankton (diatoms, DIA; and other plankton, OP) were also influenced by exudation, sedimentation, and transport to adjacent habitats. The mathematical representations of the basic metabolic rate processes in diatoms, other plankton, sediment microalgae, and *Spartina alterniflora* were all similar. Gross production was affected by temperature, irradiance, and dissolved inorganic nitrogen. Respiration followed an exponential relationship with temperature (Cerco and Cole 1994). Production and mortality were represented by Gaussian functions with temperature. Phytoplankton exudation and sedimentation were also modeled according to Cerco and Cole (1994). Sediment microalgae were lost through resuspension and grazing by higher trophic levels. The formulations for carbon productivity by *Zostera marina* and its epiphytes were taken from Wetzel and Neckles (1986) and Wetzel and Meyers (1994). Nitrogen uptake by the shoots and root-rhizomes of *Zostera marina* were modeled using Michaelis-Menten kinetics, limited by feedback functions based on the maximum and minimum nitrogen contents of the tissues. *Zostera marina* shoots and root-rhizomes maintained C:N ratios through the proportional nitrogen loss terms. Nitrogen was only translocated from root-rhizomes to shoots in order to meet shoot nitrogen demand. Nitrogen

translocation was also limited by feedback functions based on the maximum and minimum nitrogen contents of the tissues. The formulations for nitrogen state variables of *Spartina alterniflora* were similar to those of *Zostera marina,* except there was no shoot uptake of nitrogen in *Spartina alterniflora.*

Water column particulate organic carbon (POC; gC m^{-3}) was influenced by production, hydrolysis, settling, and exchange between adjacent habitats. POC was produced from phytoplankton and a fractional loss term added to that gained through resuspended sediment microalgae. POC was divided into labile and refractory fractions and rates of hydrolysis were calculated using an exponential relationship with temperature (Cerco and Cole 1994). LPOC and RPOC both settled from the water column and were exchanged laterally. DOC was influenced by production, remineralization, and exchange with adjacent habitats. Hydrolyzed POC provided the DOC production rate and the remineralization rate was controlled by a temperature function and the refractory DOC fraction (Cerco and Cole 1994). Water column TDIN (mmoles m^{-3}) was influenced by production, autotrophic uptake, sediment-water fluxes, and exchange with adjacent habitats. Production was calculated using the DOC remineralization rate and the C:N ratio of dissolved organic matter. TDIN was removed from the water column through uptake by phytoplankton in all habitat models and by *Zostera marina* in the vegetated subtidal habitat model. TDIN was exchanged vertically between the sediment and the overlying water column, based on rates determined from core incubations (Buzzelli 1996).

Model Simulation and Analysis

Sensitivity Analysis: A number of factors potentially influence the simulated behavior of the state variables (Buzzelli *et al.* 1995). The sensitivities of the model state variables to the integration interval (dt), integration routine (Euler vs Runge-Kutta), boundary conditions, and various parameters were investigated using a systematic series of model trial runs. The interval for Eulerian integration (dt) was initially set at 0.0625 day (1.5 hours). Analyses included determining variation in a particular state variable over successive years of the same model run, as well as the comparison of Year 2 results among a series of different sensitivity runs. The integration interval (dt) was halved during successive calibration runs to check the effects of dt on the water column concentrations in each habitat model. Euler and Runge-Kutta integration routines were compared at similar values of dt. Four to six individual parameters (i.e. rate coefficients) were selected based on their ecological significance for each state variable to analyze their effects on the model behavior. Year 2 simulations results were used in the analyses to avoid initial condition effects. Each parameter was varied by ±10% in separate model runs and the root mean square deviation (RMS) between the stable, nominal model case and the sensitivity run was calculated (Cerco 1993):

$$RMS = \sqrt{\frac{1}{n}\Sigma_{i=1}^{n}(P_i - O_i)^2} \qquad (2)$$

where P_i = model nominal run; O_i= sensitivity run; and n = number of dt in Year 2 simulation (n=5840). The RMS was compared with the average mean concentration of the nominal run. In

the cases of the carbon state variables of *Zostera marina* and *Spartina alterniflora*, the potential interactions among two or three varied parameters were investigated for Year 2 output.

Validation: Validation data specific to the Goodwin Islands reference site were available for only several model state variables. As for the sensitivity analysis, model validation was addressed by comparing Model Year 2 output of water column chlorophyll a, total particulate organic carbon (TPOC), and TDIN from the nonvegetated and vegetated subtidal habitat models with monitoring data available for the lower York River. Shoot, root-rhizome, and epiphyte carbon state variables of *Zostera marina* were compared with data collected at the Goodwin Islands by Moore *et al.* (1994). *Spartina alterniflora* shoot and root-rhizome carbon biomass were validated using data taken from the literature (including Mendelssohn 1973; Smith *et al.* 1979; Ornes and Kaplan 1989; Gross *et al.* 1991). There were no data available to validate model output for simulated patterns of littoral zone water column DOC, sediment microalgal production and biomass, and habitat-specific and inter-habitat variations in sediment-water and lateral (channel boundary condition) material exchanges.

Model Application

The modeled processes were integrated for Year 3 simulation results to derive annual rates for various, ecologically significant processes and to provide estimates for comparison with information derived through our own field-laboratory studies and the published literature. Processes included were: phototrophic net production, phototrophic nitrogen demand and uptake, and the exchanges of total phytoplankton, TPOC, DOC and TDIN. Annual carbon and nitrogen dynamics were compared among the autotrophs. Annual carbon production and nitrogen demand were compared among the four habitats. The annual material exchange that each habitat had with each of its two adjacent boundary habitats were then summed to derive an annual import or export estimate for the individual habitat. The annual net carbon production and suspended material budgets for the entire littoral zone of the Goodwin Islands NERR were then calculated using the summed process estimates for each habitat. These estimates were compared with those derived from studies on other mid-Atlantic coast marsh ecosystems.

Model Simulation Results

Model Sensitivity Analysis and Validation

The model was tested extensively for the effects of numerical integration routine and integration interval, initial conditions and rate coefficient values both singularly and in various logical combinations. Potential sources of error in simulation analyses and sensitive or controlling parameters that might require higher degrees of confidence in their estimation were identified. The results of these multiple runs were analyzed by sensitivity analysis and are discussed in detail in Buzzelli *et al.* (1995) and Buzzelli (1996). It is beyond the scope of this report to present these results but in summary the model was optimized for integration routine and interval. The most sensitive parameters with regard to effecting relatively large changes in model output (*i.e.* predictions of state variable behavior and concentrations) were rate coefficients associated with the primary producers and, in particular, those coefficients governing the interactions of light and photosynthesis, translocation and aboveground mortality. For the parameters identified as

sensitive, the values used for simulation were those derived from the best available data and values that resulted in model behavior consistent with field and/or laboratory observations.

Following these extensive model sensitivity tests, a model version was decided as the test case and validated against extant data available from a variety of sources. Model validation was carried out by comparing simulation output with observed seasonal behavior and concentrations of the principal state variables. Each is discussed separately below.

Subtidal Water Column Concentrations: The modeled concentrations of chlorophyll a, total POC (labile + refractory), and TDIN in the water column of the nonvegetated and vegetated subtidal habitats were validated using data collected during intensive field studies at the Goodwin Islands NERR (Fig. 2; Moore *et al.* 1994). The intensive field studies were conducted 7-17 June 1993. Figure 2A, 2B, and 2C depict the relationships between the field data and concentrations output from the VST model. VST model chlorophyll a was approximately 5 mg/m^3; whereas, the field data were varied and ranged

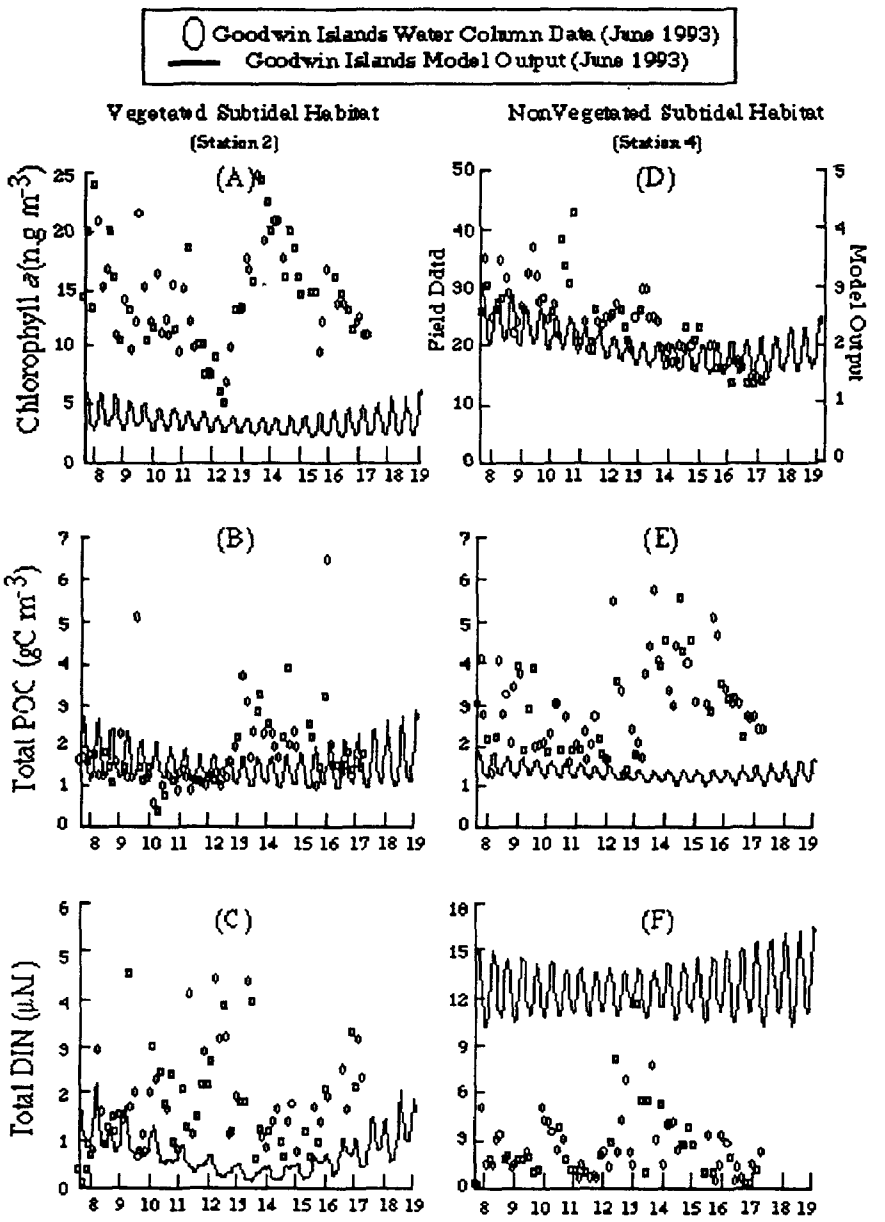

Figure 2

between 5 and 25 mg m^{-3} (Fig. 2A). Vegetated subtidal model concentrations of TPOC ranged between 1 and 3 gC m^{-3} and were within the range of values recorded in the field (Fig. 2B). Water column TDIN computed by the VST model were within the range of field data during the first few days of simulation, but declined to very low values beginning around 11 June (Fig. 2C). There was some variability in the concentrations measured in the field (0-5 μM). The comparisons between model output and field data for the nonvegetated subtidal habitat are shown in Figure 2D, 2E, and 2F. Model chlorophyll a was approximately an order of magnitude lower than field determinations (note different y-axis scales in Fig. 2D). NVST model chlorophyll a concentrations were slightly lower than those output from the VST model; whereas, concentrations measured at the Goodwin Islands were slightly increased in the offshore nonvegetated habitat (Fig. 2A and 2D). NVST model TPOC concentrations were slightly lower than those determined in the field (Fig. 2E); however, both model output and field data were similar among vegetated and nonvegetated habitats (Fig. 2B and 2E). NVST model TDIN concentrations ranged from 10-16 gC m^{-3} ; field observations ranged from 0 to 8 gC m^{-3} (Fig. 2F). The NVST model concentrations were considerably greater than those output from the VST model, although field concentrations between the two subtidal habitats were similar (Fig. 2C and 2D).

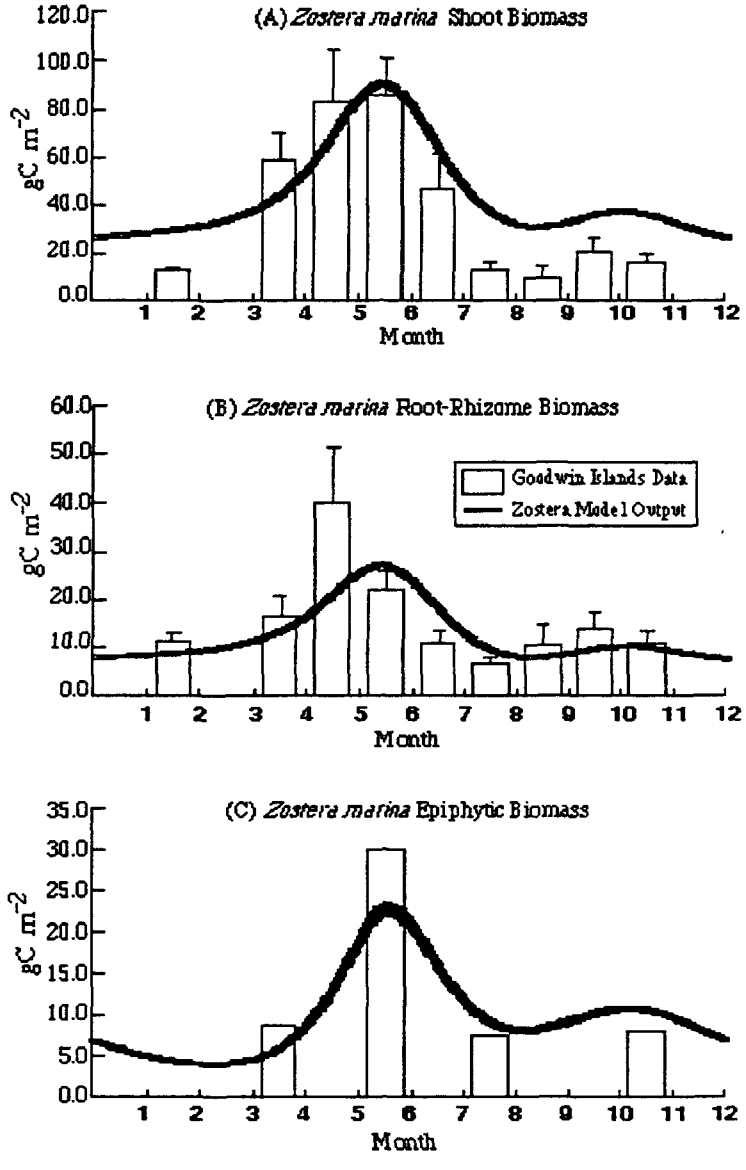

Figure 3

Zostera marina Biomass:

Comparison of modeled *Zostera marina* shoot, root-rhizome, and epiphytic biomass with field observations are shown in Figure 3. The validation data were collected at the Goodwin Islands NERR (Moore *et al.* 1994). The model sufficiently represented the annual patterns in the biomass of these three state variables. Although the model predicted summer shoot biomass of approximately 30 gC m^{-2}, actual shoot biomass was below 20 gC m^{-2} (Fig. 3A). Predicted root-rhizome biomass was consistent with field data, except for the large peak in

biomass recorded at the Goodwin Islands NERR in April 1993 (Fig.3B; Orth and Moore 1986). Although there were few data collected for epiphytic biomass at the Goodwin Islands NERR, model output was within the range reported and agree with other data collected in the York River, Virginia (Murray 1983; Neckles 1990).

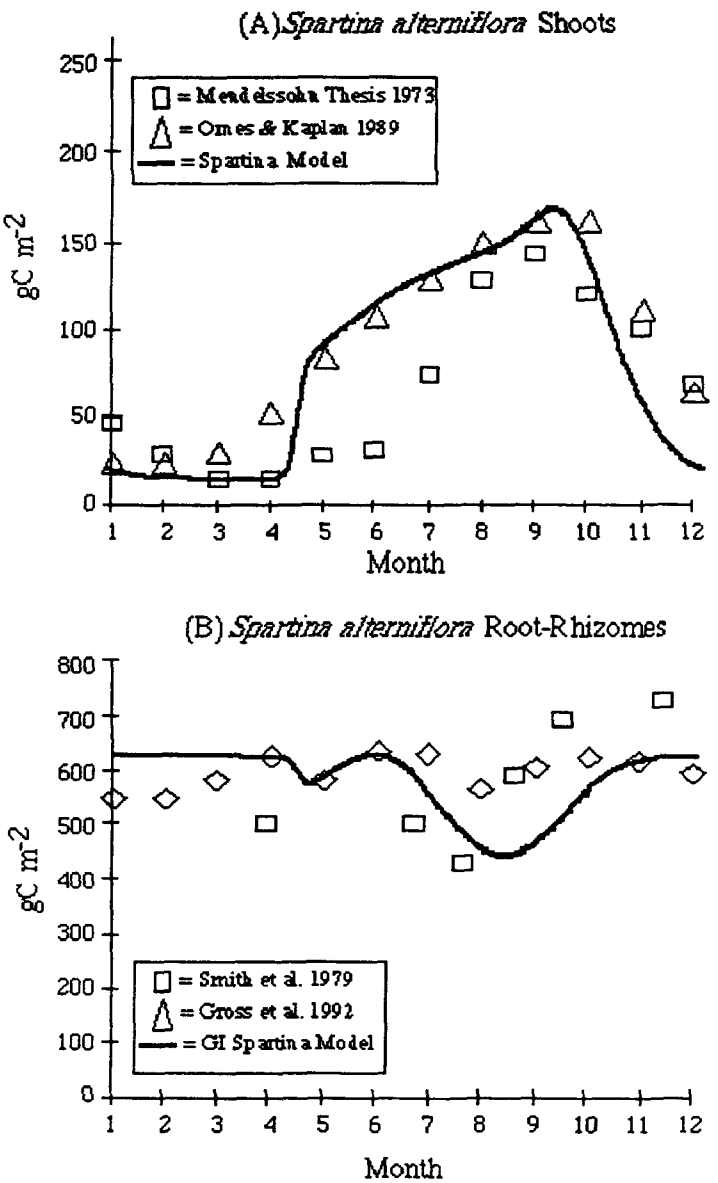

Figure 4

Spartina alterniflora Biomass: The model was calibrated using field data collected at the Goodwin Islands NERR. The annual patterns in shoot and root rhizome biomass of *Spartina alterniflora* generated by the model were validated with data assembled from the literature (Fig. 4). Shoot biomass was compared with data from the York River, Virginia, and from South Carolina (Mendelssohn 1973; Ornes and Kaplan 1989). The root-rhizome output was validated with data collected in New Jersey and Delaware (Smith *et al.* 1979; Gross *et al.* 1991). Shoot carbon biomass was initialized at 3 gC m^{-2} and stayed low until the spring pulse of carbon translocated from below-ground stocks (Fig. 4A). Root-rhizome carbon biomass was initialized at 635 gC m^{-2} and decreased in April due to the upward carbon translocation to shoots (Fig. 4B). Shoot and root-rhizome carbon biomass increased through May and June. Shoot biomass continued to increase, reaching a maximum of 160 gC m^{-2} by early September. The root-rhizome biomass declined during the summer due to increased below-ground respiration, which resulted from higher temperatures (Fig. 4). Shoot carbon biomass showed a precipitous decline in the fall, because carbon was translocated below-ground to the root-rhizome pool as both state variables returned to their initial values. Shoot carbon biomass predicted from the model agreed with field data from South Carolina (Ornes and Kaplan 1989). Root-rhizome carbon biomass was within the range of data reported for other marshes with latitudes similar to Chesapeake Bay (Smith *et al.* 1979; Gross *et al.* 1991).

Model Predictions of Littoral Zone Processes and Exchanges

Productivity: Annual production by phytoplankton state variables of the Goodwin Islands NERR habitat models was estimated at 66.0 gC m^{-2} (Table 2).

Table 2. Estimates of annual net production and contribution to ecosystem production in the littoral zone of the Goodwin Islands NERR using the four habitat models. Phytoplankton productivity was summed over all 4 habitats and intertidal habitat size used in this summation is the average areal inundation during model simulation time (m^2). The habitats are nonvegetated subtidal (NVST), vegetated subtidal (VST), nonvegetated intertidal (NVIT), and vegetated intertidal (VIT).

Photoautotrophic Component	Annual Net Production	Habitat Size	Annual Net Production	Percent of Total Ecosystem
	gC m-2 yr^{-1}	10^4 m^{-2}	10^6 gC yr^{-1}	%
Phytoplankton	66.0	671	442.7	15.8
Sed. Microalgae				
NVST	127.6	420	535.9	19.1
VST	101.2	120	121.4	4.3
NVIT	169.0	100	169.0	6.0
VIT	162.5	85	138.1	4.9
Zostera marina				
Epiphytes	55.9	120	67.1	2.3
Shoot	241.3	120	289.6	10.3
RR	54.2	120	65.0	2.3
Spartina alterniflora				
Shoot	830.8	85	706.2	25.2
RR	319.7	85	271.7	9.7
TOTAL			2806.7	99.9

The nonvegetated and vegetated subtidal areas were added to the average inundated area of each of the two intertidal habitats in order to calculate the total ecosystem size for phytoplankton production (671 m^2). Phytoplankton production rates are listed in Table 2.

The *Zostera marina* community included productivity from the shoots, attached epiphytes, and the root-rhizomes. *Zostera marina* epiphytes and root-rhizomes produced at a similar rate of approximately 55 gC m^{-2} yr^{-1} (Table 2). The *Zostera marina* community of the Goodwin Islands NERR produced approximately 421.7 x 10^6 gC yr^{-1}. The shoots of *Spartina alterniflora* had the greatest annual net productivity of any of the model autotrophs.

Nitrogen demand: Nitrogen demand of each phototroph was calculated using the net carbon production rate and the optimal C:N ratio. Nitrogen uptake was calculated for only the phytoplankton and the two plants, *Zostera marina* and *Spartina alterniflora*. Nitrogen uptake was calculated for the plants and phytoplankton state variables of each habitat model using Michaelis-Menten kinetics. There were no formulations to represent nitrogen uptake by sediment microalgae, although dissolved inorganic nitrogen was exchanged vertically within each habitat model, based on empirical data (Buzzelli 1996). Table 3 summarizes the annual nitrogen demand and uptake by each of the phototrophic components of the Goodwin Islands NERR habitat models. The annual carbon production and nitrogen demand of each of the autotrophs in the habitat models was calculated to compare the four different littoral zone habitats (Table 4).

Flux: The four habitat models were used to estimate the annual net material fluxes for each habitat as well as the entire littoral zone of the Goodwin Islands NERR (Table 5). The water column constituents included total phytoplankton (gC yr^{-1}), TPOC (gC yr^{-1}), DOC (gC yr^{-1}), and TDIN (mmoles N yr^{-1}). Net import was designated as a negative flux and net export was shown as a positive flux. Values are provided in Table 5. To assess the interactions between the Goodwin Islands littoral zone and the surrounding estuary, the annual total exchanges were summed among the habitats. The totals that were calculated using the four habitat models provided annual imports of phytoplankton C (-5.9×10^7 gC), TPOC (-2.7×10^8 gC), and TDIN (-1.4×10^9 mmoles N) and an annual export of DOC (1.5×10^8) for the littoral zone of the Goodwin Islands NERR.

Table 3. Estimates of annual nitrogen demand and uptake for estuarine autotrophs using the Goodwin Islands habitat models. Demand is calculated using the net carbon production and the optimal C:N ratio. Uptake is calculated using a Michaelis-Menten relationship based on external nitrogen concentration, a half-saturation value, and the maximum uptake rate. Phytoplankton nitrogen processes were summed over the four separate habitat models. The habitats are nonvegetated subtidal (NVST), vegetated subtidal (VST), nonvegetated intertidal (NVIT), and vegetated intertidal (VIT).

Photoautotrophic Component	Annual Nitrogen Demand $gN\ m^{-2}\ yr^{-1}$	Annual Nitrogen Uptake $gN\ m^{-2}\ yr^{-1}$
Phytoplankton	11.5	15.7
Sediment Microalgae		
NVST	22.4	na
VST	17.8	na
NVIT	29.6	na
VIT	28.5	na
Zostera marina		
shoots	15.1	2.09
root-rhizomes	0.89	3.86
total	16	5.95
Spartina alterniflora		
shoots	26	na
root-rhizomes	1.53	11.5
total	27.5	11.5

Table 4. Estimates of net annual carbon production and nitrogen demand of each of the four littoral zone habitats of the Goodwin Islands NERR using the four habitat simulation models. The habitats are nonvegetated subtidal (NVST), vegetated subtidal (VST), nonvegetated intertidal (NVIT), and vegetated intertidal (VIT). Each habitat model includes diatoms, other plankton, and sediment microalgae. In addition to algae the vegetated subtidal and intertidal habitat models include the net shoot and root-rhizome production by *Zostera marina* and *Spartina alterniflora*, respectively.

Habitat	Size (ha)	Percent of Total Size	Annual C Production gC	Percent of Total C Production	Annual N Demand gN	Percent of Total N Demand
NVST	420	51.9%	740×10^6	28.6%	130×10^6	51.7%
VST	120	18.5%	562×10^6	21.7%	44×10^6	17.4%
NVIT	100	12.3%	170×10^6	6.6%	30×10^6	11.9%
VIT	85	11.1%	1116×10^6	43.1%	47×10^6	19.0%

Table 5. Estimates of annual material exchanges for the four littoral zone habitats of the Goodwin Islands NERR using the four habitat simulation models. The habitats are nonvegetated subtidal (NVST), vegetated subtidal (VST), nonvegetated intertidal (NVIT), and vegetated intertidal (VIT). The exchanges of phytoplankton carbon, total particulate organic carbon (TPOC), dissolved organic carbon (DOC), and total dissolved inorganic nitrogen (TDIN) between a habitat and its two adjacent boundaries were integrated annually and summed to calculate net import (-) or export (+).

	Phytoplankton ($gC\ yr^{-1}$)	TPOC ($gC\ yr^{-1}$)	DOC ($gC\ yr^{-1}$)	TDIN ($mmoles\ N\ yr^{-1}$)
NVST	-3.9×10^7	-4.7×10^7	1.4×10^8	-1.1×10^9
VST	-1.4×10^7	-1.7×10^8	2.4×10^7	-2.2×10^8
NVIT	-4.5×10^6	-4.7×10^7	-1.0×10^7	-4.7×10^7
VIT	-1.4×10^6	-1.4×10^7	-1.0×10^7	-1.5×10^7
TOTALS	-5.9×10^7	-2.7×10^8	1.5×10^8	-1.4×10^9

Discussion

This ecosystem processes modeling approach was developed to simulate ecosystem dynamics of littoral zone habitats characteristic of mesohaline and polyhaline shallow water areas of the lower Chesapeake Bay (Buzzelli 1996). The hydrodynamically coupled models simulate primary production and water column processes, integrate field and geographic data, and link distinct aquatic habitats with water quality and living resources of the estuary. The models also provided a framework to assemble available data, identify missing information, estimate ecosystem and habitat productivity, and investigate the potential impacts of altered environmental factors on ecosystem dynamics in the Chesapeake Bay littoral zone.

Model Sensitivity and Validation

Although not presented here, the extensive sensitivity analyses were carried out with the littoral zone model (see Buzzelli *et al.* 1996; Buzzelli, 1996). Computed concentrations of the various water column constituents for the intertidal habitat models (VIT and NVIT) proved very sensitive to changes in the integration interval (dt) and were caused by the interactions between the choice of dt and tidal inundation (i.e. water volume exchange between adjacent habitats). Water column concentrations (gC or mmole N m^{-3}) were calculated using the change in volume that resulted from exchanges between adjacent habitats. Because the marsh was not inundated over the entire tidal cycle, a large dt caused very large and sudden changes in flooded area and tidal prism volume. The numerical effects were mitigated when dt was reduced to time scales consistent with those that regulated changes in tidal height (i.e. minutes). A small dt created smoother hypsometric and volume relationships used to calculate marsh inundation and tidal volume. Based on considerations of model complexity and output versus computation time, an integration interval of 11.25 minutes (0.0078125 d) was chosen as the time step for the intertidal habitat models.

The computed concentrations for diatoms, labile-POC, and sediment microalgae during Year 2 of simulation in the vegetated subtidal model were very robust with respect to 10% deviations in key controlling parameters. The majority of mathematical expressions governing these state variables have been calibrated and utilized for a number of years (Cerco and Cole 1994; Kuo and Park 1995). In most cases, the computed concentrations of water column chlorophyll a, TPOC, and TDIN by the nonvegetated and vegetated subtidal models were consistent with data recorded at the Goodwin Islands NERR (Moore *et al.* 1994) and are within the range of longer-term measurements made in the lower York River (Batuik *et al.* 1992). The primary exceptions were for predicted chlorophyll a concentrations. Model output was an order of magnitude less than field data for the nonvegetated subtidal habitat. The comparatively low values of chlorophyll a generated by the NVST model resulted from the very large volume used to calculate the concentrations. Model chlorophyll a concentrations were lower than those predicted for the surface waters of the mainstem Chesapeake Bay (10-20 mg m^{-3}; Cerco 1993). The mass of diatoms and other phytoplankton in each of the habitat models were greatly influenced by the inter-habitat exchanges, because the magnitudes of the exchange rates were much greater than those associated with the associated production and loss terms. The TPOC concentrations from the Goodwin Islands subtidal habitat models were similar to those reported in Cerco (1993). The TDIN concentrations computed by the subtidal models were within the range of the surface and bottom values given in Cerco (1993).

Model simulation of *Zostera marina* shoot, root-rhizome, and epiphytic biomasses were also fairly robust relative to sensitivity analysis, although epiphytic biomass could change by 40% if its basal metabolic rate was increased or decreased by 10%. The model replicated the annual changes in *Zostera marina* biomass and was used to estimate net annual primary production for eelgrass meadows of lower Chesapeake Bay. The equations that represented *Spartina alterniflora* were highly parameterized. The shoot and root-rhizome carbon biomass was sensitive to changes in shoot maximum photosynthetic rate (P_{max}), the root-rhizome basal respiration rate, and the carbon translocation potential. The connectivity between above- and below-ground carbon pools was demonstrated by the effects of these three parameters on both shoot and root-rhizome carbon state variables. Net production was translocated downward, a pulse of carbon was translocated upwards in the spring, and a large fraction of shoot carbon remaining in the fall was translocated to the root-rhizomes. P_{max} appeared to be the most sensitive

parameter. Values calculated from the literature varied with methods, geographic locations, and conversion units and ranged from 0.01-0.36 d^{-1}. The maximum rate of 0.15 d^{-1} used in this study was the average value calculated from the other studies of *Spartina alterniflora* primary production which are summarized in Table 6.

Table 6. Comparison of *Spartina alterniflora* maximum photosynthetic rates (d^{-1}) calculated from literature sources. The research method referenced in the literature source is provided. A 12-hour day was used to convert between hourly and daily rates.

METHOD	RATE (d^{-1})	SOURCE
Gas flux chambers	0.01[a]	Blum *et al.*, 1978
Gas flux chambers	0.13[b]	Giurgevich and Dunn, 1979
Gas flux chambers	0.04[c]	Drake and Read, 1981
Curve fit from growth study	0.26[d]	Morris, 1982
Gas flux chambers	0.36[e]	Morris *et al.*, 1984
Gas flux chambers	0.06[f]	Pezeshki *et al.*, 1987
Nitrogen uptake experiments	0.36[g]	Morris and Bradley, 1990
Goodwin Islands model	0.15[h]	This study

[a]Estimated using 0.4 gC gdw^{-1} and 1045 gdw m^{-2}.
[b]Estimated empirically from data provided.
[c]Estimated using 0.4 gC gdw^{-1} and 500 gdw m^{-2} for a *Spartina patens* community.
[d]Estimated assuming 30 °C
[e]Estimated using 0.43 gC gdw^{-1}
[f]Estimated using 0.4 gC gdw^{-1} and 900 gdw m^{-2}
[g]Estimated using 0.006 gN gdw^{-1} root-rhizome tissue
[h]Average calculated from other studies listed for use in Goodwin Islands model

Model Simulation of Littoral Zone Processes

Primary Production: One principal objective of this modeling exercise was to estimate the annual rates of net primary production by phytoplankton, sediment microalgae, *Zostera marina*, and *Spartina alterniflora* in the Goodwin Islands NERR (Table 2). The net annual rate of phytoplankton production (66.0 gC m^{-2} yr^{-1}) accounted for 15.8% of total annual ecosystem production (Fig. 5A) and was within the range of values reported in the literature (Table 7). The annual patterns of chlorophyll a biomass computed using the subtidal habitat models were similar to long-term patterns evident in data collected in the lower York River, Virginia (Batuik *et al.*

1992). For comparison, annual net productivity rates for other water bodies are given in Table 7.

The net annual productivity of sediment microalgae predicted by the four habitat models of the Goodwin Islands NERR ranged from 101-169 gC m^{-2} yr^{-1} (Table 2) and accounted for 34.3% of the total annual littoral zone production (Figure 5A). The rate in the nonvegetated intertidal habitat (NVIT) was greater than that of the other three habitats. This resulted from the combined effects of reduced light attenuation, due to the depth of the overlying water column in the NVST and VST habitats and sediment shading by the plant canopy in the VST and VIT habitats. Light attenuation due to overlying water was reduced in the NVIT habitat, because it was inundated only 46% of the time over a simulated annual cycle (21,505 of 46,720 time steps). The effects of canopy shading are particularly evident in the differences between the productivity in the deeper sand habitat (NVST; 127.6 gC m^{-2} yr^{-1}) relative to the shallower SAV habitat (VST; 101.2 gC m^{-2} yr^{-1}). Although sediment microalgal productivity estimates vary with geographic location and habitat, the rates estimated using the Goodwin Islands habitat models were in overall agreement with those calculated from the biomass data collected as well as literature values (Table 7).

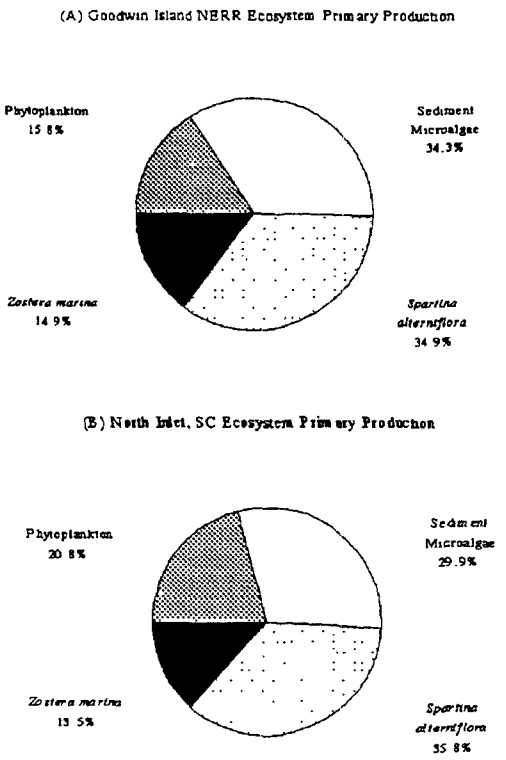

Figure 5

Zostera marina shoot net annual productivity predicted by the VST model was 241.3 gC m^{-2} yr^{-1}, approximately four times that computed for the epiphytes (55.9 gC m^{-2} yr^{-1}) or root-rhizomes (54.2 gC m^{-2} yr^{-1}; Table 2). *Zostera marina* community productivity accounted for about 15% of the total production in the littoral zone of the Goodwin Islands NERR (Figure 5A). The annual biomass curves for the three carbon state variables related to *Zostera marina* were similar to field data collected in the Goodwin Islands SAV meadow and were within the range of long-term data for the lower York River, Virginia (Orth and Moore 1986).

Spartina alterniflora annual shoot and root-rhizome biomass changes predicted using the model agreed with literature values. Model estimates of primary production were similar to those calculated using Goodwin Islands biomass data. *Spartina alterniflora* shoot and root-rhizome productivity were estimated at 830.8 and 319.7 gC m^{-2} yr^{-1}, respectively, and these rates were similar to the short form shoot and root-rhizome annual productivity predicted by Dai and Wiegert (in press) using a canopy model (749 and 397 gC m^{-2} yr^{-1}; Table 7). The similarities among the model of the Goodwin Islands *Spartina alterniflora* and those estimated for short form

Table 7. Summary of annual net production rates (gC m^{-2} yr^{-1}) taken from published literature. Estimated using linear regression equation provided, [2] Averaged from values provided. R/R in table denotes below ground production by roots and rhizomes.

Phototroph/Location		Annual Rate	Literature Source
Phytoplankton :	Chesapeake Bay	20.26[1]	Malone *et al.* 1986
	Narragansett Bay	101.61	Keller 1989
	Narragansett Bay	91.25[2]	Keller 1988
	Neuse River, NC	373.4	Boyer *et al.* 1993
	North Carolina Estuaries	52-500	Mallin 1994
	Goodwin Islands Models	66.0	This Study
Sediment Microalgae:	Mudflat in England	143.0	Joint 1978
	Subtidal in Denmark	89.0	Colijn and DeJong 1984
	Marsh in Mississippi	57.4	Sullivan and Moncreiff 1988
	Mudflat in Massachusetts	250.0	Gould and Gallagher 1990
	Seagrass Mississippi	339.0	Daehnick *et al.* 1992
	Marsh in South Carolina	55-234	Pinckney and Zingmark 1993
	Goodwin Islands Models	101-169	This Study
***Zostera marina* :**	Shoots in Massachusetts	155-345	Roman and Able 1988
	Shoots in Netherlands	160-412	van Lent and Verschuure 1994
	Modeled Shoots	241.3	This Study
	R/R in Netherlands	53-132	van Lent and Verschuure 1994
	R/R in North Carolina	55-102	Kenworthy and Thayer 1984
	Modeled R/R	54.2	This Study
***Spartina alterniflora* :**	Shoots in South Carolina	289-875	Dame and Kenny 1986
	Shoots in Georgia	749-1421	Dai and Wiegert in press
	Modeled Shoots	830.8	This Study
	R/R in South Carolina	945-2178	Dame and Kenny 1986
	R/R in Georgia	397-872	Dai and Wiegert in press
	R/R in Virginia	270-857	Blum 1993
	R/R in New Jersey	880.0	Smith *et al.* 1979
	Modeled R/R	319.7	This Study

Spartina alterniflora from Georgia (Dai and Wiegert, in press) resulted primarily from the inclusion of seasonal cycles of internal carbon translocation in both. *Spartina alterniflora* whole plant production accounted for almost 36% of the total ecosystem production in the Goodwin Islands littoral zone (Fig. 5A).

Nitrogen demand: The annual Goodwin Islands phytoplankton nitrogen demand was estimated to be 11.5 gN m^{-2}, based on a C:N weight ratio of 5.7 (Table 3). The annual phytoplankton nitrogen uptake rate was estimated to be in excess of nitrogen demand, at 15.7 gN

m^{-2}. This disparity resulted because, unlike *Zostera marina* and *Spartina alterniflora*, there were no mechanisms in the model that limited nitrogen uptake as a function of internal C:N ratio. This difference may reflect potential luxury nitrogen uptake by phytoplankton. The differences in the nitrogen requirement of sediment microalgae among the four habitat models resulted from the differences in the net annual carbon productivity (Tables 2 and 3). Although nitrogen uptake by sediment microalgae was not explicitly modeled, the models included a vertical exchange of TDIN between the water column and sediment, based on empirical data collected in subtidal and intertidal habitats (Neikirk 1996). These field studies measured sediment-water column exchanges only during the daytime. Other studies are being conducted to determine the diel variability of sediment-water biogeochemcial fluxes in littoral zone environments of lower Chesapeake Bay (K.A. Moore and I. C. Anderson, Virginia Institute of Marine Science, Blacksburg, VA).

Nitrogen was taken up from the water column by the shoots and from the sediments by the root-rhizomes of *Zostera marina*. Other studies determined that the sediment was the primary source of nitrogen for eelgrass (Iizumi and Hattori 1982; Short and McRoy 1984). Nitrogen was translocated from root-rhizomes to the shoots in order to meet the shoot nitrogen requirement for growth in the Goodwin Islands model (Buzzelli, 1991). Nitrogen uptake by the shoots and root-rhizomes was influenced both by the external concentration and by feedback limitation terms based on the maximum and minimum C:N ratios of the tissues. The difference between the annual nitrogen demand of *Zostera marina* (16.0 gN m^{-2} yr^{-1}) and the annual nitrogen uptake (5.95 gN m^{-2} yr^{-1}) was attributed to the role of translocation and internal recycling (Table 4). Based on the Goodwin Islands model, approximately 63% of the plant nitrogen requirement was met through internal recycling. This value was within the range of annual estimates made by Borum *et al.* (1989; 64%), but was approximately twice the short-term rates of translocation measured by Buzzelli (1991; 34%). Later refinements to this model will include bi-directional nitrogen translocation within individual plants, as well as carbon and nitrogen translocated from adjacent root-rhizomes connected below-ground.

Whole plant nitrogen demand and root-rhizome uptake of *Spartina alterniflora* was calculated using the vegetated intertidal marsh model. A similar approach to that used to model the nitrogen relationships of *Zostera marina* was adopted for the shoot and root-rhizome nitrogen state variables of *Spartina alterniflora*, except that there was no nitrogen uptake by the shoots . As for eelgrass, the whole-plant nitrogen requirement for growth of *Spartina alterniflora* (27.5 gN m^{-2} yr^{-1}) was in excess of nitrogen taken up by the plant (11.5 gN m^{-2} yr^{-1}; Table 3). Approximately 58% of the plant nitrogen requirement was met through internal recycling, which agrees with the 54% estimated from studies in a Georgia marsh (Hopkinson and Schubauer 1984). Further field and laboratory studies should include the determination of the actual short- and long-term rates of carbon and nitrogen uptake and translocation in *Spartina alterniflora*. A refinement to the model was the inclusion of bi-directional translocation of nitrogen to synchronize with seasonal carbon translocation.

Habitat Relationships: Despite the fact that the VIT was the smallest habitat, the annual production by phytoplankton, sediment microalgae, and *Spartina alterniflora* (1116 x 10^6 g C) accounted for 43.1% of total in the littoral zone of the Goodwin Islands NERR (Table 4). Over 80% of the intertidal primary production and 34.1% of the total for the littoral zone was attributable to *Spartina alterniflora*. This characteristic explained the comparatively low fraction

of the total ecosystem nitrogen demand required by the VIT (Table 4), because the C:N ratio of *Spartina alterniflora* shoots and root-rhizomes was 7-10 times that of the phytoplankton or sediment microalgae. Conversely, phytoplankton and sediment microalgae primary production in the NVST was only 28.6% of the total production in the littoral zone of the Goodwin Islands NERR, although it was the largest of the four habitats (Table 4). The NVST did require 51.7% of the total littoral zone nitrogen demand, due to the low C:N ratio, compared with the habitats that include plants. The annual C production by the vegetated subtidal habitat (VST; 562 x 10^6 gC) was approximately half that of the vegetated intertidal habitat (1116 x 10^6 gC), but the annual nitrogen demand and fraction of total ecosystem nitrogen requirement were similar (44 x 10^6 vs 47 x 10^6 gN). The nonvegetated intertidal habitat had the least influence on the annual ecosystem carbon production (6.6%) and nitrogen requirement (11.9%) of the four littoral zone habitats.

Figure 6 A-D depicts the annual net exchanges for each habitat and water column constituents. An arrow into the habitat denotes a net annual import into the habitat from the adjacent habitats; an arrow out of a habitat represents a net export of the constituent across its two boundaries. The nonvegetated and vegetated subtidal models (NVST and VST) both predicted net annual imports of phytoplankton, particulate organic carbon, and dissolved inorganic nitrogen; both predicted net annual exports of dissolved organic carbon (Table 5). The nonvegetated and vegetated intertidal models (NVIT and VIT) predicted net annual imports of all four water column constituents including dissolved organic carbon (Table 5). The subtidal net DOC production and export were caused by the increased exudation of the comparatively large phytoplankton population that was imported (Fig. 6A and 6C). The intertidal net DOC imports resulted from the decreased exudation and import of phytoplankton, compared with the subtidal habitat models (Fig. 6A and 6C). Over an annual cycle, the nonvegetated intertidal habitat was inundated 46% of the time; whereas, the vegetated intertidal habitat was inundated only 25% of the time. The decreased inundation time and phytoplankton import of the intertidal habitats, relative to the subtidal habitats, did not translate to decreased TPOC import into the intertidal habitats (Table 5 and Fig 6B). The vegetated subtidal habitat imported the greatest TPOC annually (-1.7 x 10^8 gC); the other three habitats were similar relative to TPOC import (Table 5 and Fig. 6B). All four habitats imported dissolved inorganic nitrogen and the annual TDIN imported was correlated to the annual phytoplankton mass imported as phytoplankton remove nitrogen from the water column (Fig. 6A and 6D).

Flux: The exchange of dissolved and particulate materials between coastal marshes and adjacent environments are governed by their historical geomorphology, basin configuration, and hydroperiod (Childers *et al.* 1993; Rozas 1995). The hydroperiod of an individual marsh is unique and has a significant influence on the horizontal and vertical material exchanges (Vorosmarty and Loder 1994). Despite the differences in geomorphology and hydroperiod among marshes, it is useful to compare and contrast the flux characteristics among marshes as a way to identify spatial or temporal patterns (Childers 1992). The material exchange estimates generated for the littoral zone of the Goodwin Islands NERR were compared to annual flux estimates derived from other studies (Table 8).

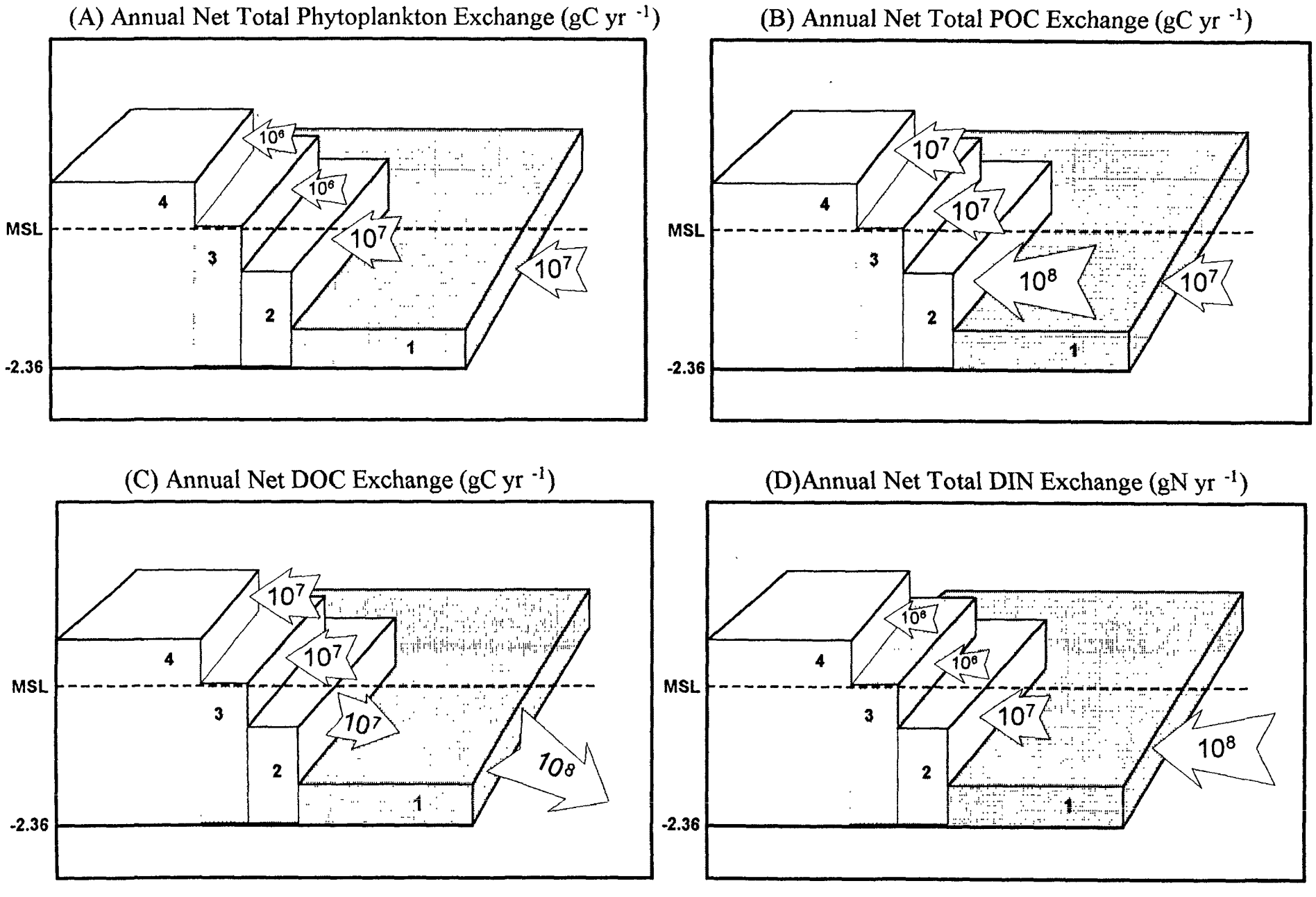
(A) Annual Net Total Phytoplankton Exchange (gC yr -1)
(B) Annual Net Total POC Exchange (gC yr -1)
(C) Annual Net DOC Exchange (gC yr -1)
(D)Annual Net Total DIN Exchange (gN yr -1)
MSL
-2.36
4
3
2
1
10^6
10^7
10^8

Figure 6

Table 8. Summary of marsh ecosystem flux estimates assembled from published literature. Negative flux (-) denotes net import to marsh, positive flux (+) denotes net export from marsh.

Location	Size (ha)	POC flux gC yr^{-1}	DOC flux gC yr^{-1}	DIN flux mmoleN yr^{-1}	Literature Source
Carter Creek, Virginia	10	1.17×10^7	-2.5×10^6	-2.6×10^7	Axelrad *et al.* 1976
Carter Creek, Virginia	10	na	na	-2.0×10^7	Wolaver *et al.* 1983
Rhode River, Maryland					
Low marsh	13	na	na	-8.6×10^6	Correll *et al.* 1992
Bly Creek, South Carolina					
Marsh	12	-2.1×10^7	1.8×10^7	-1.2×10^7	Dame *et al.* 1991
Goodwin Islands Marsh Model	85	-1.4×10^7	-1.0×10^7	-1.5×10^7	This Study

The Goodwin Islands marsh model predicted a net POC import to the marsh annually (Table 8). The difference between the POC export at Carter Creek and the POC import predicted using the Goodwin Islands model was attributed to the absence of an upland connection at the Goodwin Islands NERR and the proximity of the terrestrial boundary at Carter Creek (Axelrad *et al.* 1976). Like the Carter Creek marsh on the York River, Virginia, the Rhode River, Maryland marsh has an upland connection (Correll *et al.* 1992).

Conclusions

The Chesapeake Bay Littoral Zone and Wetlands Models employed a series of simulation models to calculate annual carbon production, nitrogen demand, and water column dynamics in the littoral zone of the lower Chesapeake Bay. These models also investigated potential change in habitat and ecosystem properties. Environmental problems that can be explored include: potential effects of changing water quality on productivity in the eelgrass community; the possible effects that significant changes in the distribution and abundance of eelgrass might have on primary production and nitrogen uptake in the subtidal habitats; and the potential effects of changes in mean sea level on intertidal productivity and material exchange properties.

The current models were designed to be coupled to coarser-scale models of water quality in the Chesapeake Bay watershed (Cerco 1993). Of course, many important physical and biogeochemical processes are currently not present in the models. The development of the sediment state variables and processes and linkages to the overlying water column must be included to better investigate production and material cycling in shallow and irregularly flooded littoral zone habitats. Phosphorus dynamics, the contribution of living and dead plants to DOC

production and exchange, and the nitrogen relationships of sediment microalgae would greatly improve the biogeochemical portions of the models. Secondary productivity within the different littoral zone habitats should be included as a vehicle to transfer energy and nutrients between the autotrophs and higher trophic levels. This would provide additional mechanisms to link the habitats in time and space, as well as better address other living resources issues facing the management community (*e.g.* higher trophic level dynamics and controls).

Data Needs

The dynamics of 37 different state variables can be represented by these four littoral zone habitat models (Figure 1). The output of only a few of these state variables was validated in this summary. Although one of the objectives of this modeling project was to organize data relevant to Chesapeake Bay littoral zone ecology, another was to identify information that was lacking. Additional data are required in several areas, including: the annual variation in the productivity and biomass of sediment microalgae in all habitats; the relationships between sediment microalgal production and the effects of plant canopy shading; the spatial and temporal dynamics of dissolved organic carbon in shoal waters of lower Chesapeake Bay; the processes of gross and net photosynthesis, nitrogen uptake, and internal carbon and nitrogen translocation in *Spartina alterniflora*; and the horizontal exchange of dissolved and particulate materials between the vegetated intertidal marsh and the surrounding habitats.

Management Implications and Future Directions

The Lower Chesapeake Bay Littoral Zone and Fringing Wetlands Ecosystem Model links water quality and living resource dynamics in the littoral zone habitats that are essential to the survival of important juvenile and adult fishes and invertebrates. This model can investigate the potential effects of habitat alteration, water quality conditions, relative sea level variation, or watershed practices on the ecology of the littoral zone. Specific questions that can be addressed within this modeling framework are:.

- What is the relationship between habitat area (*i.e.*, changes in area covered by SAV or marsh) and water quality or plant production?

- What is the impact of short-term, high frequency or seasonal pulses (of a water column constituent such as total suspended solids, chlorophyll, dissolved inorganic nitrogen, or of seasonally immigrating grazers and predators) on plant production within SAV and marsh habitats? Is there a difference in modeled outcome based on the frequency of pulsed events? Is there a critical time of year for water or habitat quality?

- What is the relationship between plant production and area of habitat to the potential trophic transfer to, or production of, invertebrates and fishes?

- How do predictions for littoral zone habitats from the large-scale Chesapeake Bay Program Water Quality model compare with a small-scale model of SAV production and littoral zone water quality? If they differ, why and what are the implications of this?

References

Axelrad, D. M., Moore, K. A., and Bender, M. E. 1976. Nitrogen, phosphorus, and carbon flux in Chesapeake Bay marshes (OWRT Project B-027-VA Bulletin 79). Blacksburg, Virginia: Virginia Institute of Marine Science.

Bach, H. K. 1993. A dynamic model describing the seasonal variations ingrowth and the distribution of eelgrass (*Zostera marina* L.) I. Model theory. Ecological Modeling 65:31-50.

Baird, D. and Ulanowicz, R. E. 1989. The seasonal dynamics of the Chesapeake Bay ecosystem. Ecological Monographs 59:329-364.

Batuik, R. A., Orth, R.J., Moore, K.A., Dennison, W.C., Stevenson, J.C., Staver, L.W., Carter, V., Rybicki, N.B., Hickman, R.E., Kollar, S., Bieber, S., and Heasly, P. 1992. Chesapeake Bay Submerged Aquatic Vegetation Habitat Requirements and Restoration Targets: A Technical Synthesis: U.S. EPA, Chesapeake Bay Program.

Blum, U., Seneca, E.D. and Stroud, L.M. 1978. Photosynthesis and respiration of *Spartina* and *Juncus* salt marshes in North Carolina: Some models. Estuaries 1:228-238.

Blum, L. K. 1993. *Spartina alterniflora* root dynamics in a Virginia marsh. Marine Ecology Progress Series 102:169-178.

Boon, J. D. and Byrne, R. J. 1981. On basin hypsometry and the morphodynamic response of coastal inlet systems. Marine Geology 40:27-48.

Boumans, R. M. J. and Sklar, F. H. 1990. A polygon-based spatial (PBS) model for simulating landscape change. Landscape Ecology 4:83-90.

Borum, J., Murray, L., and Kemp, W.M. 1989. Aspects of nitrogen acquisition and conservation in eelgrass plants. Aquatic Botany 35:289-300.

Boyer, J. N., Christian, R. R., and Stanley, D. W. 1993. Patterns of phytoplankton primary productivity in the Neuse River estuary, North Carolina, USA. Marine Ecology Progress Series 97:287-297.

Buzzelli, C. P. 1991. Sediment Inorganic Nitrogen Stocks and Root-Rhizome Ammonium Uptake by Eelgrass (*Zostera marina* L.) in the lower Chesapeake Bay: M.A. Thesis, School of Marine Science, College of William and Mary, Williamsburg, VA.

Buzzelli, C.P. 1996. Integrative Analysis of Ecosystem Processes and Habitat Patterns in the Chesapeake Bay Littoral Zone: A Modeling Study of the Goodwin Islands National Estuarine Research Reserve. PhD. Dissertation, School of Marine Science, College of William and Mary, Williamsburg, VA.

Buzzelli, C.P. and R.L. Wetzel. 1996. Modeling the Lower Chesapeake Bay Littoral Zones and Fringing Wetlands: Ecosystem Processes and Habitat Linkages. II. Model Sensitivity Analysis, Validation, and Estimates of Ecosystem Processes. Special Report No. 335 in Applied Marine Science and Ocean Engineering, Virginia Institute of Marine Science, Gloucester Point, VA.

Buzzelli, C.P., Wetzel, R.L., and Meyers, M.B. 1995. Modeling the lower Chesapeake Bay littoral zone and fringing wetlands: Ecosystem processes and habitat linkages. I. Simulation Model Development and Description. Special Report No. 334 in Applied Marine Science and Ocean Engineering. School of Marine Science-Virginia Institute of Marine Science, College of William and Mary.

Cerco, C.F. 1993. Three-dimensional eutrophication model of Chesapeake Bay. Journal of Environmental Engineering 119(6):1006-1025.

Cerco, C.F. and T. Cole. 1994. Three-dimensional eutrophication model of Chesapeake Bay: Volume 1, main report. Technical Report EL-94-4, United States Army Engineer Waterways Experiment Station, Vicksburg, Mississippi.

Childers, D. L. 1992. Fifteen years of marsh flumes-A review of marsh-water column interactions in Southeastern U.S. estuaries. INTECOL Fourth International Wetlands Conference, Elsevier Press.

Childers, D. L., H.N. McKellar, R.F. Dame, F.H. Sklar, and E.R. Blood. 1993. A dynamic nutrient budget of subsystem interactions in a salt marsh estuary. Estuarine Coastal and Shelf Science 36:105-131.

Colijn, F., and V.N. deJonge. 1984. Primary production of microphytobenthos in the Ems-Dollard estuary. Marine Ecology Progress Series 14:185-196.

Correll, D. L., T.E. Jordan and D.E. Weller. 1992. Nutrient flux in a landscape: Effects of coastal land use and terrestrial community mosaic on nutrient transport to coastal waters. Estuaries 15:431-442.

Costanza, R., F.H. Sklar, and M.L. White. 1990. Modeling coastal landscape dynamics. BioScience 40:91-107.

Daehnick, A. E., Sullivan, M. J., and Moncreiff, C. A. 1992. Primary production of the sand microflora in seagrass beds of Mississippi Sound. Botanica Marina 35:131-139.

Dai, T., and Wiegert, R. G. (in press). Estimation of the primary productivity of *Spartina alterniflora* using a canopy model. Ecography.

Dame, R. F., J.D. Spurrier, T.M. Williams, B. Kjerfve, R.G. Zingmark, T.G. Wolaver, T.H. Chrzanowski, H.N. McKellar, and F.J. Vernberg. 1991. Annual material processing by a salt marsh-estuarine basin in South Carolina, USA. Marine Ecology Progress. Series 72:153-166.

Dame, R. F. and P.D. Kenny. 1986. Variability of *Spartina alterniflora* primary production in the euhaline North Inlet estuary. Marine Ecology Progress Series 32:71-80.

de Jonge, V. N. and F. Colijn. 1994. Dynamics of microphytobenthos biomass in the Ems estuary. Marine Ecology Progress Series 104:185-196.

Dennison, W. C., R.J. Orth, K.A. Moore, J.C. Stevenson, V.C. Carter, S. Kollar, P.W. Bergstrom, and R.A. Batuik. 1993. Assessing water quality with submersed aquatic vegetation. Bioscience 43:86-94.

Drake, B. G. and M. Read. 1981. Carbon dioxide assimilation, photosynthetic efficiency, and respiration of a Chesapeake Bay salt marsh. Journal of Ecology 69:405-423.

Eiser, W. C. and B. Kjerve. 1986. Marsh topography and hypsometric characteristics of a South Carolina salt marsh basin. Estuarine Coastal and Shelf Science 23:595-605.

Friedrichs, C. T. and D. G. Aubrey. 1994. Uniform bottom shear stress and equilibrium hypsometry of intertidal flats. In *Mixing Processes in Estuaries and Coastal Seas* (ed. C. Pattiaratchi). Washington, D.C.: American Geophysical Union.

Giurgevich, J.R. and E.L. Dunn. 1979. Seasonal patterns of CO_2 and vapor exchange of the tall and short height forms of *Spartina alterniflora* Loisel. in a Georgia salt marsh. Oecologia 43:139-156.

Gould, D. M. and E.D. Gallagher. 1990. Field measurements of specific growth rate, biomass, and primary production of benthic diatoms of Savin Hill Cove, Boston. Limnology and Oceanography 35:1757-1770.

Gross, M. F., M.A. Hardisky, P.L. Wolf, and V. Klemas. 1991. Relationship between aboveground and belowground biomass of *Spartina alterniflora* (Smooth Cordgrass). Estuaries 14:180-191.

Heck, K. L. and T.A. Thoman. 1984. The nursery role of seagrass meadows in the upper and lower reaches of Chesapeake Bay. Estuaries 7:531-540.

Hopkinson, C. S. and J.P. Schubauer. 1984. Static and dynamic aspects of nitrogen cycling in the salt marsh graminoid *Spartina alterniflora*. Ecology 65:961-969.

Iizumi, H. and A. Hattori. 1982. Growth and organic production of eelgrass (*Zostera marina* L.) in temperate waters of the Pacific coast of Japan. III. The kinetics of nitrogen uptake. Aquatic Botany 12:245-256.

Joint, I. R. 1978. Microbial production of an estuarine mudflat: Estuarine Coastal and Shelf Science 7:185-195.

Keller, A. A. 1988. An empirical model of primary productivity (^{14}C) using mesocosm data along a nutrient gradient. Journal of Plankton Research 10(4):813-834.

Keller, A. A. 1989. Modeling the effects of temperature, light, and nutrients on primary productivity: An empirical and a mechanistic approach compared. Limnology and Oceanography 34:82-95.

Kenworthy, W. J. and G.W. Thayer. 1984. Production and decomposition of the roots and rhizome of seagrasses, *Zostera marina* and *Thalassia testudinum*, in temperate and subtropical marine ecosystems. Bulletin of Marine Science 35(3):364-379.

Kneib, R. T. and S.L. Wagner. 1994. Nekton use of vegetated marsh habitats at different stages of tidal inundation. Marine Ecology Progress Series 106:227-238.

Kuo, A. Y. and K. Park. 1995. A framework for coupling shoals and shallow embayments with main channels in numerical modeling of coastal plain estuaries. Estuaries 18:341-350.

Mallin, M. A. 1994. Phytoplankton ecology of North Carolina estuaries. Estuaries 17:561-574.

Malone, T. C., W.M. Kemp, H.W. Ducklow, W.R. Boynton, J.H. Tuttle, and R.B. Jonas. 1986. Lateral variation in the production and fate of phytoplankton in a partially stratified estuary. Marine Ecology Progress Series 32:149-160.

Mendelssohn, I. A. 1973. Angiosperm production of three Virginia marshes in various salinity and soil nutrient regimes. M.A. Thesis, School of Marine Science, College of William and Mary, Williamsburg, Virginia.

Moncreiff, C. A., M.J. Sullivan, and A.E. Daehnick. 1992. Primary production dynamics in seagrass beds of Mississippi Sound: the contributions of seagrass, epiphytic algae, sand microflora, and phytoplankton. Marine Ecology Progress Series 87:61-171.

Moore, K. A., J.L. Goodman, J.C. Stevenson., L. Murray, L. and K. Sundberg. 1994. Chesapeake Bay Nutrients, Light, and SAV: Relations Between Variable Water Quality and SAV in Field and Mesocosm Studies: U.S. EPA Chesapeake Bay Program.

Morris, J. T. 1982. A model of growth responses by *Spartina alterniflora* to nitrogen limitation. Journal of Ecology 70:25-42.

Morris, J. T., R.A. Houghton and D.B. Botkin. 1984. Theoretical limits of belowground

production by *Spartina alterniflora*: An analysis through modeling. Ecological Modelling 26:155-175.

Morris, J. T. and P. Bradley. 1990. Influence of oxygen and sulfide concentration on nitrogen uptake kinetics in *Spartina alterniflora*. Ecology 71:282-287.

Murray, L. 1983. Metabolic and Structural Studies of Several Temperate Seagrass Communities with Emphasis on Microalgal Components. Ph.D. Dissertation, School of Marine Science, College of William & Mary, Williamsburg, VA.

Murray, L. and R.L. Wetzel. 1987. Oxygen production and consumption associated with the major autotrophic components in two temperate seagrass communities. Marine Ecology Progress Series 38, 231-238.

Neckles, H. A. 1990. Relative Effects of Nutrient Enrichment and Grazing on Ephiphyton-Macrophyte (*Zostera marina* L.) Dynamics. Ph.D. Dissertation, School of Marine Science, College of William & Mary, Williamsburg, VA.

Neikirk, B.E.B. 1996. Exchanges of dissolved inorganic nitrogen and dissolved organic carbon between salt marsh sediments and overlying tidal water. M.A. Thesis, School of Marine Science, College of William and Mary, Williamsburg, VA.

Ornes, W. H. and D.I. Kaplan. 1989. Macronutrient status of tall and short forms of *Spartina alterniflora* in a South Carolina salt marsh. Marine Ecology Progress Series 55:63-72.

Orth, R. J. and K.A. Moore. 1986. Seasonal and year-to-year variations in the growth of *Zostera marina* L. (eelgrass) in the lower Chesapeake Bay. Aquatic Botany 24:335-341.

Pezeshki, S. R., R.D. DeLaune and W.H. Patrick. 1987. Gas exchange characteristics of Gulf of Mexico coastal marsh macrophytes. Journal of Experimental Marine Biology and Ecology 111:243-253.

Pinckney, J. and R. Zingmark. 1993a. Modeling the annual production of intertidal benthic microalgae in estuarine ecosystems. Journal of Phycology 29:396-407.

Pinckney, J. and R. Zingmark. 1993b. Biomass and production of benthic microalgal communities in estuarine sediments. Estuaries 16:887-897.

Rizzo, W. M., G.J. Lackey and R.R. Christian. 1992. Significance of euphotic, subtidal sediments to oxygen and nutrient cycling in a temperate estuary. Marine Ecology Progress Series 86:51-61.

Roman, C. T., and K.W. Able. 1988. Production ecology of eelgrass (*Zostera marina* L.) in a Cape Cod salt marsh-estuarine system, Massachusetts. Aquatic Botany 32:353-363.

Roman, C. T., K.W. Able, M.A. Lazzari and K.L. Heck. 1990. Primary productivity of angiosperm and macroalgae dominated habitats in a New England salt marsh: A comparative analysis. Estuarine Coastal and Shelf Science 30:35-46.

Rozas, L. 1995. Hydroperiod and its influence on nekton use of the salt marsh: A pulsing ecosystem. Estuaries 18(4):579-590.

Sand-Jensen, K. and J. Borum. 1991. Interactions among phytoplankton, periphyton, and macrophytes in temperate freshwaters and estuaries. Aquatic Botany 41:137-175.

Short, F. T. and C.P. McRoy. 1984. Nitrogen uptake by leaves and roots of the seagrass *Zostera marina* L. Botanica Marina, 27:547-555.

Smith, K. K., R.E. Good and N.F. Good. 1979. Production dynamics for above and belowground components of a New Jersey *Spartina alterniflora* tidal marsh. Estuarine.and Coastal Marine Science 9:189-201.

Spinner, G. P. 1969. Serial Atlas of the Marine Environment. In: The wildlife wetlands and shellfish areas of the Atlantic coastal zone, vol. Folio 18. New York City· American Geophysical Union.

Stevenson, J. C., L. G. Ward, and M. S. Kearney. 1988. Sediment transport and trapping in marsh systems: Implications of tidal flux studies. Marine Geology 80:37-59.

Strahler, A. N. 1952. Hypsometric (area-altitude) analysis of erosional topography. Bulletin of Geological Society of America 63:1117-1142.

Sullivan, M. J. and Moncreiff, C. A. 1988. Primary production of edaphic algal communities in a Mississippi salt marsh. Journal of Phycology 24:49-58.

Sundback, K. and Graneli, W. 1988. Influence of microphytobenthos on the nutrient flux between sediment and water: a laboratory study. Marine Ecology Progress Series 43:63-69.

van Lent, F. and J.M. Verschuure. 1994. Intraspecific variability of *Zostera marina* L. (eelgrass) in the estuaries and lagoons of the southwestern Netherlands. I. Population dynamics. Aquatic Botany 48:31-58.

Vorosmarty, C. J. and T.C. Loder. 1994. Spring-Neap tidal contrasts and nutrient dynamics in a marsh dominated estuary. Estuaries 17:537-551.

Wetzel, R. L. and C.S. Hopkinson. 1990. Coastal ecosystem models and the Chesapeake Bay Program: philosophy, background and status, pp7-23. IN: M. Haire and E.C. Krome (es.) Perspectives on the Chesapeake Bay 1990: Advances in Estuarine Sciences. CBP/TRS41/90, CRC, Inc., Gloucester Point, VA.

Wetzel, R.L. and M.B Meyers. 1994. Ecosystem process modeling of submerged aquatic vegetation in the lower Chesapeake Bay. Final report (1993) to USEPA Region III Chesapeake Bay Program Office.

Wetzel, R. L. and H.S. Neckles. 1986. A model of *Zostera marina* L. photosynthesis and growth: Simulated effects of selected physical-chemical variables and biological interactions. Aquatic Botany 26:307-323.

Wolaver, T. G., J.C. Zieman, R.L. Wetzel and K.L. Webb. 1983. Tidal exchange of nitrogen and phosphorus between a mesohaline vegetated marsh and the surrounding estuary in the lower Chesapeake Bay. Estuarine Coastal and Shelf Science 16:321-332.

Trophic Control of SAV Responses to Nutrient Enrichment: Simulation Modeling of Mesocosm Experiments

R. Bartleson, L. Murray, W. M. Kemp

Horn Point Environmental Laboratory
University of Maryland
Cambridge, MD

Background

Nutrient enrichment of coastal waters promotes growth of planktonic and epiphytic algae, which tend to inhibit production and survival of estuarine submerged aquatic vegetation (SAV) and Bay grasses (Kemp *et al.* 1983; Twilley *et al.* 1985; Coleman and Burkholder 1995; Duarte 1995; Short *et al.* 1995). In many shallow eutrophic habitats, epiphytic algal growth appears to be of primary importance for regulating abundance of SAV (Borum 1985; Duarte 1995). In some environments, invertebrate grazing can effectively reduce the effects of epiphytes on SAV. However, the relative effectiveness of herbivorous grazing control on epiphytes tends to vary with season, region, and feeding mode of the grazer populations (Howard 1982; Brönmark 1985; Neckles *et al.* 1993). In addition, significant changes in the mortality of these grazers, which may result from predation or altered environmental conditions (e.g., Lubbers *et al.* 1990), can regulate the ability of grazers to control epiphyte growth. Ultimately, differences in trophic structure of the community associated with submersed plants can radically alter the plant responses to changes in nutrient levels.

Relating SAV growth and survival to both *in situ* environmental conditions and habitat requirements (e.g., nutrient concentrations) and to the effects of nutrient load reduction strategies (e.g., 40 % reduction goals; Dennison *et al.* 1993) are of particular interest to environmental decision-makers. Although a variety of mesocosm experiments (*e.g.*, Twilley *et al.* 1985, Neudnorfer and Kemp 1990) have demonstrated the potential importance nutrient enrichment on Bay grass production, it is difficult to relate experimental nutrient loading rates and concentrations to conditions observed in the field. Size limitations for most mesocosm experiments preclude inclusion of full trophic structure as it occurs in nature. Current experiments in the Environmental Protection Agency (EPA) Multiscale Experimental Ecosystem Research Center (MEERC) program at the University of Maryland Center for Environmental and Estuarine Studies (UMCEES) are examining the effects of variations in trophic structure on susceptibility of SAV populations to stress from nutrient enrichment.

One way to relate results from mesocoms experiments to field conditions is with the aid of numerical ecosystem process models. Several models of SAV production have examined responses to nutrient enrichment and grazing regulation of epiphyte growth (Wetzel and Neckles 1986; Kemp *et al.* 1995; Madden and Kemp 1996). These models have not simulated dynamics of the grazers themselves and feedback interactions among grazers, epiphytes and SAV. In addition, no experiments or models have explicitly considered how herbivorous grazing may be controlled by resident predator populations. This model explores some of the consequences of interactions between fish and grazers at different nutrient concentrations. Results should improve understanding of how nutrient concentrations affect the survival of SAV.

Model Development

The current model has several modifications from the original SAV model (e.g., Kemp *et al.* 1995; Madden and Kemp 1996). The model equations were developed from empirical relationships based on laboratory and field data from mesohaline Chesapeake Bay, other estuaries, and theoretical functions. The model structure is shown in Figure 1. Because internal nutrient storage may affect competition between SAV and algae, plant nitrogen (N), including nonstructural nitrogen, was modeled separately from carbon (C). Nonstructural carbohydrate pools of SAV biomass were also included in the model to allow realistic C-allocation. The model was designed to track N, phosphorus (P), oxygen (O), and C through the system compartments. It has 19 state variables: SAV leaf C and N; SAV root C and N; SAV nonstructural C and N; epiphytic algae; benthic algae; phytoplankton; amphipods; fish; infauna; sediment labile organic carbon; sediment refractory organic carbon; water column dissolved inorganic N and P; sediment porewater dissolved inorganic N and P; and dissolved oxygen. Data from MEERC mesocosm experiments (*e.g.*, Sturgis and Murray 1997) were used to calibrate the model.

The model used a time step of 15 minutes to capture diel effects of light on nutrients, production and respiration. Integration was performed using fourth order Runga-Kutta numerical integration. The model was calibrated with field data and data collected from 1 m^2 mesocosms in a 1995 experiment (Figure 2). The model experiments examined the interacting effects of trophic complexity and nutrient enrichment (Figure 3). The model was run at three nutrient addition rates (1, 15, and 405 M l^{-1} d^{-1}) for each of three trophic complexity conditions: no grazers; with grazers; and with grazers and fish. Grazers (1.5 g C) were added at week 2, and fish (2.5 g C) were added at week 5 at densities in the mid-range (1-2 g C m^{-2}) reported from shallow-water systems (*e.g.* Virnstein *et al.* 1983, Kemp *et al.* 1983).

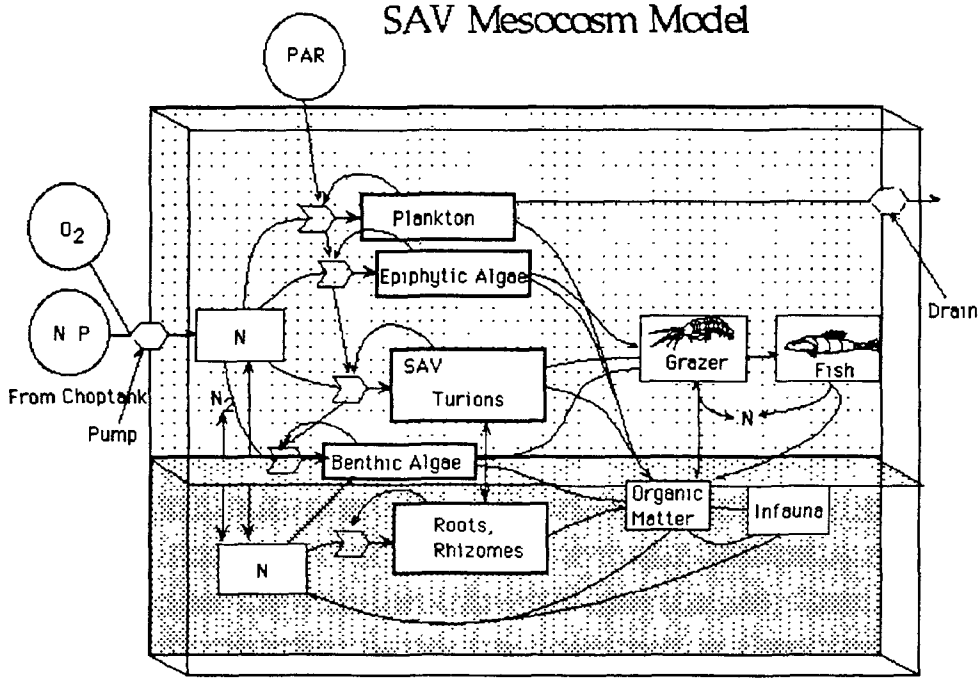

Figure 1. General structure of SAV model is shown. Some material flows are left out for simplicity. N is modeled in stoichiometry with C except in SAV where structural and nonstructural N and C are modeled separately.

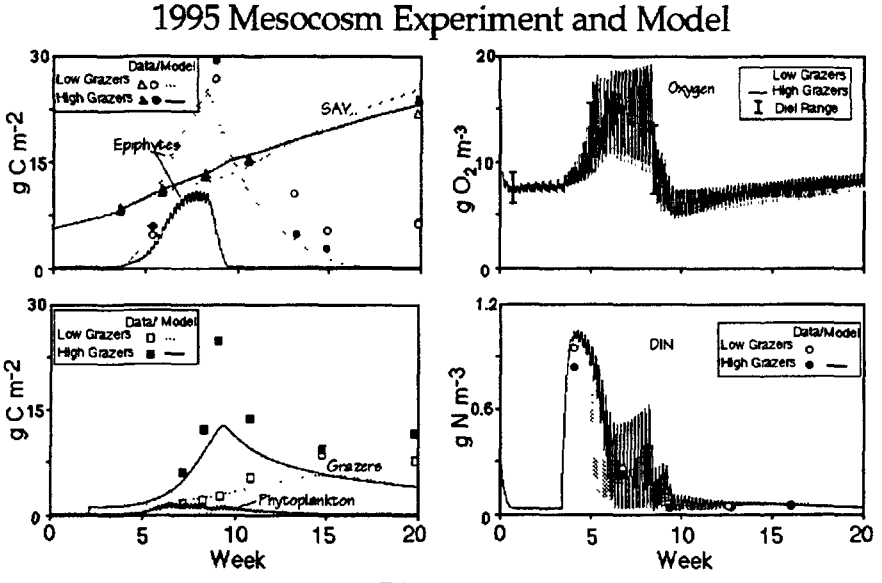

Figure 2

Results and Discussion

Baseline Experiment

The model output matched the oxygen and dissolved inorganic nitrogen data from the 1995 mesocosm experiments quite well (Fig. 2). Simulations of community production and respiration, as well as growth rate and SAV biomass measurements, were comparable with mesocosm experimental data, but biomass of epiphytes and grazers diverged from model results. The model predicted that grazers would control epiphyte biomass in the high-grazer treatment and that epiphyte biomass would be higher in the low-grazer treatment.

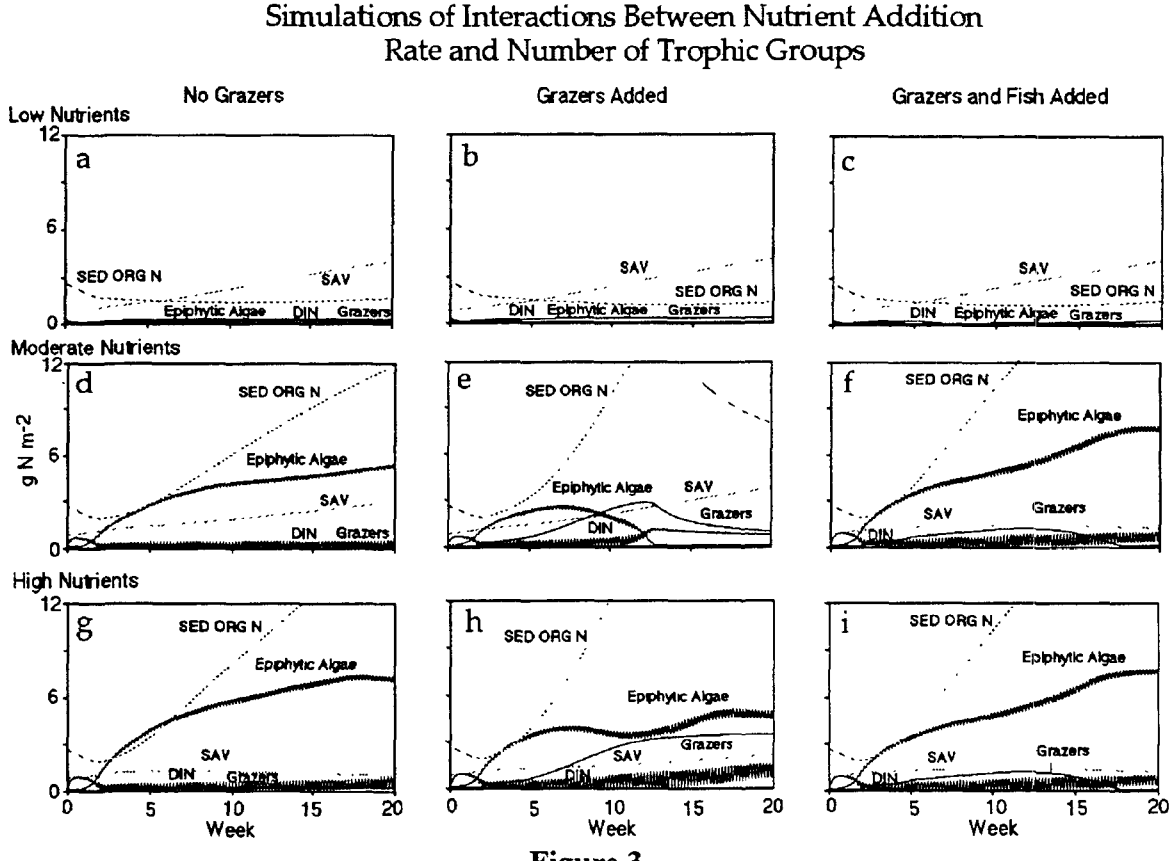

Figure 3

The measured epiphyte biomass, however, was not significantly different among treatments. This discrepancy could have resulted from an increased regeneration rate of P in the high-grazer treatment, which led to enhanced growth of N-fixing epiphytic blue-green algae. It appearred that these blue-greens were not effectively controlled by amphipod grazing. Phosphorus was not explicitly included in this model, but expeimental data revealed that P was quite low in the treatments and control, so regeneration rates would be important in controlling growth rates of the autotrophs. In another study, blue-green algae dominated the epiphytic algal community when amphipods and isopods were present in a nutrient enriched eelgrass microcosm (Neckles *et al.* 1994).

Trophic complexity experiment

Grazers can significantly increase or decrease nitrogen retention (Fig. 3, panels d and e) in an SAV mesocosm. This is due to the stimulating effect of grazers on primary production, through nutrient regeneration, and the negative effect of reducing epiphytic algal biomass to low levels. When producer biomass is sufficient, increased nitrogen cycling and production should reduce the rate of outflow. Adding fish, however, increased (fig. 3, panels e and f) nitrogen cycling with moderate nutrient additions and decreased (panels h and i) nitrogen cycling with high nutrient additions. Results were dependent on the coefficients picked for the model. For example, if a lower grazing rate was used in the moderatre nutrient,grazer added scenario (panel e), epiphyte biomass may have remained high, giving a model result more like the fish addition scenario (panel f). Sensitivity analysis will show the coefficients that have the most influence on model behavior.

Using the mesocosms to improve the model

The epiphytic algae did not decrease as expected in the amphipod treatments, because the filamentous blue-green algae were not noticeably grazed. In the next generation of the model, blue-green algae will be added as an explicit state variable. Since water-column P was found in more limiting concentrations than N, it was necessary to add P to the model. This will improve the model's ability to accurately predict rates of primary production. Fish will be added to the model to help determine the number that will reduce, but not eliminate the amphipods. In this way, the model may be used to improve the experiment.

References

Borum, J. 1985. Development of epiphytic communities on eelgrass, *Zostera marina,* along a nutrient gradient in a Danish estuary. Mar. Biol. 87: 233-241.

Brönmark, C. 1985. Interactions between macrophytes, epiphytes and herbivores: an experimental approach. Oikos 45: 26-30.

Coleman, V., and J. Burkholder. 1995. Response of microalgal epiphyte communities to nitrate enrichment in an eelgrass (*Zostera marina)* meadow. 31: 36-43

Dennison W.C., Orth R.J., Moore K.A., Stevenson J.C., Carter V., Kollar S., Bergstrom P.W., Batiuk R.A. 1993. Assessing water quality with submersed aquatic vegetation: habitat requirements as barometers of Chesapeake Bay health. Bioscience 43:86-94.

Duarte C.M. 1995. Submerged aquatic vegetation in relation to different nutrient regimes. Ophelia 41:87-112

Howard, R. K. 1982. Impact of feeding activities of epibenthic amphipods on surface-fouling of eelgrass leaves. Aquat. Bot. 14: 91-97

Kemp, W. M., W.R. Boynton, R.R. Twilley, J.C. Stevenson, J. C. Means. 1983. The decline of submerged vascular plants in upper Chesapeake Bay: Summary of results concerning possible causes. Mar. Technol. Soc. J. 17: 78-89

Kemp, W. M., W. R. Boynton, A. J. Hermann. 1995. Simulation models of an estuarine macrophyte ecosystem. pp. 262-278, In: B. Patten and S. E. Jørgensen (eds.) Complex ecology. Prentice Hall, Englewood Cliffs, NJ.

Lubbers, L., W. R. Boynton and W. M. Kemp. 1990. Variations in structure of estuarine fish communities in relation to abundance of submersed vascular plants. Mar. Ecol. Progr. Ser. 65: 1-14.

Madden, C. J. and W. M. Kemp. 1996. Ecosystem model of an estuarine seagrass community: Calibration and simulation of eutrophication responses. *Estuaries.* (In press).

Neckles, H. A., R.L. Wetzel, R.J. Orth. 1993. Relative effects of nutrient enrichment and grazing on epiphyte-macrophyte (*Zostera marina* L.) dynamics. Oecologia 93: 285-295

Neckles, H. A., E.T. Koepfler, L.W. Haas, R.L. Wetzel, R.J. Orth. 1994. Dynamics of epiphytic photoautotrophs and heterotrophs in *Zostera marina* (Eelgrass) microcosms: responses to nutrient enrichment and grazing. Estuaries 17: 597-605

Patten, S. E. Jorgensen and S. Auerbach (eds.) Complex ecology. Prentice Hall, Englewood Cliffs, NJ.

Short, F., D. Burdick and J. Kaldy. 1995. Mesocosm expeiments quantify the effects of eutrophication on eelgrass, *Zostera marina*. Limnol. Oceanogr. 40: 730-749.

Sturgis and Murray 1997. Scaling of nutrinet input to submersed macrophyte mesocosms. Submitted to Mar. Ecol. Progr. Ser.

Twilley, R. R., W.M. Kemp, K.W. Staver, J.C. Stevenson, W.R. Boynton. 1985. Nutrient enrichment of estuarine submersed vascular plant communities. 1. Algal growth and effects on production of plants and associated communities. Mar. Ecol. Prog. Ser. 23: 179-191

Wetzel, R. L. and H. Neckles. 1986. A model of *Zostera marina* L. photosynthesis and growth: Simulated effects of selected physical-chemical variables and biological interactions. Aquat. Bot. 26: 307-323.

A Simulation Model of Submersed Aquatic Vegetation (SAV) and Water Quality in Chesapeake Bay

Christopher J. Madden and W. Michael Kemp

Horn Point Environmental Laboratory
University of Maryland
Cambridge, MD

Background

A simulation model of the shallow littoral zone (<3 m) of the Patuxent River was created to investigate responses of submersed aquatic vegetation (SAV) to increased nutrient and sediment inputs. The objective of the modeling effort was to explore mechanisms responsible for the recent decline of SAV in Chesapeake Bay and to provide input to the management process about conditions required for habitat restoration. The model is currently calibrated to represent habitat dominated by *Potamogeton perfoliatus*, a well-studied grass formerly prevalent in the mesohaline estuary and found in abundance along the flanks and in many tributaries of the mainstem Bay. During the 1970s and 1980s, the distribution of *Potamogeton* and other submersed plants was severely reduced by a combination of environmental perturbations (Batiuk *et al.* 1992, Madden and Kemp 1996). Current management plans are directed at restoring SAV and increasing abundance and distribution of *Potamogeton* to former levels, using among other things, environmental benchmarks for several water quality characteristics which will hopefully lead to habitat improvement (Batiuk *et al.* 1992). The model described here was developed with assistance from the US Environmental Protection Agency and Chesapeake Bay Program Office, Annapolis, Maryland, to aid managers with refining restoration guidelines and facilitate the incorporation of littoral processes into other water quality models (Cerco and Cole 1993). This model is also being used by ecosystem researchers to test hypotheses and predict ecosystem responses to natural, anthropogenic, and management changes.

The model focuses on the relationship of light, nutrients and submersed vegetation. State variables for above-ground (leaves and stems) and below-ground (roots and rhizomes) plant biomass, phytoplankton, epiphytes, and particulate sediment carbon are included. The model has a time-step of 0.25 day and a simulation length of one to five years. The underwater light environment as influenced by sediment, phytoplankton, and epiphytes is strongly emphasized in model equation formulation, and four levels of PAR (photosynthetically active radiation) are calculated for each time-step: PAR at the surface, at 0.25% of total depth, at the average canopy depth, and at the SAV leaf surface. The model is used to examine how availability of nutrients and light control growth and productivity of SAV plants, phytoplankton and epiphytes in mesohaline Chesapeake Bay. Other environmental variables tracked by the model include suspended sediment concentration, total water column turbidity, phytoplankton chlorophyll concentration, and dissolved inorganic nitrogen concentration.

In previous model reports (Kemp *et al.* 1995, Madden and Kemp 1996), model results focused on the relationship between dissolved inorganic nitrogen (DIN) and SAV biomass. These results indicated that increases in DIN of 40% over baseline (1976) levels were sufficient to eliminate

SAV beds after three years. Increased DIN concentrations enhanced growth of algae, especially epiphytes attached to SAV leaves, which reduced light at the SAV leaf surface below the threshold required for net productivity in rooted aquatics. Reductions in water column nutrient concentrations (in the model) did not result in rapid restoration of SAV biomass during the first or even second year of simulated restored conditions. This lack of immediate response primarily was attributed to the lag time required to regenerate substantial below-ground root biomass. That is, the model showed that although water column light conditions may be favorable for SAV growth, if the below-ground structure required to regenerate above-ground shoots was not sufficient, appreciable growth rates would not be attained.

Model analysis also revealed a hysteresis in the relationship between ambient nutrient levels and the amount of SAV biomass present. This result indicated that despite a strong correlation between the amount of SAV biomass and ambient nutrient concentrations, levels of SAV productivity and biomass depended on whether recent nutrient concentrations were trending upward or downward. Previously higher nutrient concentrations stressed the SAV system and significant damage to habitat structure may limit growth of SAV, even under declining or acceptably "low" nutrient conditions. *P. perfoliatus*, with significant root/rhizome biomass, tended to integrate the history of plant health over a longer period in the below-ground structure than the above-ground structure. After periods of eutrophy resulting from high nutrient concentrations, the amount of below-ground biomass available was reduced compared with plants exposed to less eutrophic conditions. The model should quantify such interactions, predicting system responses based on current and previous conditions. It should also predict expected SAV recovery time under a variety of conditions.

New model experiments involved sediment and nitrogen feedbacks. Model experiments were performed to elucidate the nature of these feedbacks between SAV beds and the water column. Through such hypothesis testing, the efficacy of habitat criteria in restoring or protecting desirable submersed aquatic plants can be explored. Understanding these relationships is important to environmental resource managers because many environmental variables in question are used as habitat criteria that relate water quality improvements to SAV restoration.

Model Development

The SAV model was comprised of systems of simultaneous differential (finite-difference) equations, solved using a second-order Runge Kutta numerical integration scheme on a microcomputer platform. A time-step (dt) of 6 hours permitted resolution of diel light, photosynthesis and plant respiration patterns, and in the future, will permit the addition of tidal and organism movement signals. Rate equations for physiological processes were derived using relevant literature and empirical relationships from Patuxent River, Choptank River, or other Chesapeake Bay tributaries. The baseline condition of the model was established at 1968, when SAV was in significant abundance in the lower Patuxent River. Simulation experiments were performed to project light and nutrient conditions in the bed under a variety of nutrient loading rates. The model tracked biomass in units of organic carbon; phytoplankton, SAV, epiphyte, and detritus stocks were calculated in mg C m^{-2}. The Redfield atom ratio of 106:16:1 for C:N:P, and 106:16 for C:Si for diatoms, was assumed for plant tissue. This ratio was used to index nutrient uptake to carbon flow. N and P in the biota were also reported in mg m^{-2}. Initial model configuration simulated annual patterns for *Potamogeton perfoliatus*; the model is currently under

expansion to simulate additional species by varying rate coefficients, initial conditions and model equations.

The model was optimized for performing specific experiments on the subsurface light regime and SAV production. It describes a 1-3 m unstratified water column overlaying a benthic community with which the water column community interacted through sedimentation, diffusive fluxes, and nutrient translocation. Target variables included above-ground and below-ground *Potamogeton* biomass, epiphytic growth on plant leaves, two groups of phytoplankton, and organic material in sediments. Exchange between the grassbed in the model and the adjacent deep river channel occurred via lateral advective flow through the model boundary. Flows were regulated by a 10% mass water exchange flow and concentration gradients resulting from processes in the model. These gradients were primarily driven by photosynthetic production, metabolism, and the removal of epiphytes and phytoplankton by herbivorous grazers. Model forcing functions included temperature, PAR, inorganic nitrogen loading, and suspended particulates.

Growth in autotrophic compartments was controlled by maximum temperature-dependent photosynthetic rates and was reduced by turbidity from phytoplankton, suspended particulates, and epiphytes. Twilley *et al.* (1986) demonstrated that the attenuation of PAR at the leaf surface followed an exponential decline with increasing epiphyte biomass. The relationship between inorganic nutrient concentrations and photosynthesis followed Michaelis-Menton kinetics.

Zooplankton and herbivorous fish controlled grazing rate of phytoplankton and a community of composite herbivorous grazers consumed epiphytes. Predator grazing on epiphytes and two phytoplankton groups were described by separate Ivlev functions for each predator, which included a preference function when there was a choice of prey. There is no direct grazing of plant leaves in the model, as this loss for *Potamogeton* was generally deemed insignificant in natural systems (Stevenson 1988).

Light in the model was calculated in five stages, starting from daily incident PAR, supplied by forcing function. Number of daylight hours per day was determined using algorithms from Kirk (1983). Incident PAR (variable name=PAR_1) was partitioned into means for time intervals 0600-1000h, 1000-1400h, and 1400-1800h. PAR_1 was reduced 10% at the water surface by a mean scattering and reflection coefficient (PAR_2). Attenuation of light with depth was modeled with a Beers-Lambert function (Kirk 1983) resulting in exponential decay of PAR intensity with depth. The equation:

$$PAR_{(Z)} = PAR_2 * e^{(-K_D * Z)} \qquad (1)$$

yielded light intensity in $\mu Ein\ m^{-2}s^{-1}$ at any depth (Z), derived from PAR_2 at the surface. Down-welling attenuation (K_D) was the sum of component attenuation from phytoplankton (K_C), suspended particulates (K_S), and water itself (K_W) (Kirk, 1983). Equations of the form: $K_C = 0.054 * Chl^{0.667} + 0.0088 * Chl$ (Kremer and Nixon 1978); $K_S = 0.0396*SPM+0.39$ (Twilley *et al.* 1985); and $K_W = 0.03$ (Kirk 1983) determined components of attenuation in units of m^{-1} for K, $\mu g\ L^{-1}$ for Chl, and $mg\ L^{-1}$ for suspended particulate material (SPM). Active chlorophyll concentrations were based on chl:c ratios for diatoms of 1:50 and for other phytoplankton, 1:90 (Vant 1991, McBride *et al.* 1993).

PAR intensity at 30 cm (PAR_3) represents integrated mean quantum irradiance for the 1 m water column and for calculations of phytoplankton photosynthesis rates. Measurements by Goldsborough and Kemp (1988), indicate mean leaf length for *P. perfoliatus* of 0.25 m, setting

the depth of the plant canopy (Z_p) in the model at a constant 0.75 m for calculating irradiance at canopy depth (PAR_4) and photosynthesis rates for epiphytes. Light reaching submersed plant leaves (PAR_5) is used to calculate photosynthetic rates for submersed plants. was attenuated through the epiphyte layer, based on epiphyte density on leaf surfaces as in Twilley *et al.* (1985):

$$PAR_5 = PAR_4 * e^{(0.32-(0.42*2.5AE))} \quad (2)$$

The quantity 2.5*AE = the density of epiphytes per unit plant surface area (mg cm^{-2}), based on a carbon to dry weight ratio of 1:2.5.

Difference equations for autotrophic compartments (Table 1; end of this article) incorporated inputs of photosynthetic production; advective import; and in the case of rooted plants, growth of regenerative shoots. Loss terms included mortality; advective export; respiration; exudation; and in the case of rooted plants, translocation of carbon to roots and rhizomes. Biomass-specific photosynthesis (Ps) for autotrophs was a function of maximum specific growth rate P_{max}, related to temperature by an Arrhenius function (Odum 1983), adjusted by nutrient (N) and light (L) limitation function:

$$Ps = P_{max} * f(N, L) \quad (3)$$

where Ps and μ are in units of mg C (g C $d)^{-1}$; and f(N, L) ranges from 0-1, determined by nutrient and light availability.

For submersed plant production, an exponential growth function with Q_{10} of 2.15 was used:

$$P_{AG}=D_{AG} * 0.25 *(e^{(0.0633 * T-Gcrit)}-1) \quad (4)$$

where T = water temperature; G_{crit}, the critical temperature coefficient, was set at 12° C, calibrated to match the rate and timing of growth initiation of *P. perfoliatus* in Chesapeake Bay tributaries (Stevenson *et al.* 1993). Such a temperature coefficient has been used in various plant models (*cf.* Verhagen and Nienhuis 1983) to calibrate seasonal growth patterns. The self-limitation term D_{AG} is a density-dependent function determined by calibration calculated to apply the effect of crowding and self-shading in the canopy:

$$D_{AG}=1-(AG/d_{maxAG})^2 \quad (5)$$

AG is above-ground submersed plant biomass in g m^{-2} and d_{maxAG} a constant = 200 g C m^{-2}. A similar density-limited growth expression was used in the epiphyte production function:

$$D_{AE} = d_{AE}*0.17 * e^{(0.02 * T)} \quad (6)$$

where the density dependent self-limiting effect for algae is proportional to carbon density on plant leaves (mg C cm^{-2} of plant) as follows:

$$D_{AE}=1-(D_{ESA}/d_{maxAE})^2 \quad (7)$$

D_{ESA} = density of epiphytes on host leaves and d_{maxAE} is a constant = 20 mg C cm^{-2}. Maximum densities for both submersed plant and epiphyte were derived by inspection of values attained

under nutrient and light saturating conditions in field and laboratory studies (Staver 1984, Twilley *et al.* 1985).

The phytoplankton maximum growth function is defined by a temperature-dependent formulation similar to that employed by Kremer and Nixon (1978) in a model of Narragansett Bay phytoplankton:

$$G_P = 0.59\, e^{(0.0633 * (T - Gcrit))} \qquad (8)$$

where Gp is maximum photosynthetic rate in mg C mg C^{-1} d^{-1}, and T is Celsius temperature; growth is modified by addition of a specific temperature coefficient, where $G_{crit} = 1°$ C for diatoms and 8° C for other (summer) phytoplankton. The higher temperature coefficient for summer plankton delays growth and formation of peak biomass until early June; diatoms, with lower temperature optima, peak in March. Self-shading in phytoplankton was modeled implicitly via the plankton chlorophyll contribution (K_C) to total water column attenuation (K_D) (Huisman and Weissing 1994).

For all autotrophs, maximum temperature-based photosynthetic rates were downward-adjusted by limitation terms describing instantaneous nutrient and light-based carbon uptake. Carbon fixation rates for epiphytes and phytoplankton were modeled as functions of water column nutrient concentrations following Michaelis-Menton kinetics. Photosynthesis related to irradiance by rectangular hyperbola (*e.g.* Dennison and Alberte 1986) using different photosynthetic parameters (P_{max} and alpha) for each producer group to generate characteristic P vs I relationships. The minimum of all potential rates (nutrient and light) acted as the limiting effect on growth.

$$F(N, L) = MIN\left(\frac{N}{N+K_n}, \frac{P}{P+K_p}, \frac{Si}{Si+K_{si}}, \frac{PAR_5}{PAR_5+I_k}\right) \qquad (9)$$

This minimum value formulation selected a single limiting rate (either nutrient or light) by comparison of availability versus requirement for all four resources, (Kremer and Nixon 1978), and assumed no multiplicative limitation through nutrient interaction (*cf.* DiToro *et al.* 1971).

For nutrient uptake kinetics by submersed plants, the standard Monod (1942) formulation was modified to account for dual sources of nutrients: rooted plants, with access to pools in sediment pore waters as well as water column, incorporate both root and leaf uptake pathways (Kemp *et al.* 1995) as follows:

$$U = \frac{N_w + k'N_s}{K + (N_w + k'N_s)} \qquad (10)$$

where U (relative nutrient uptake rate) represents total uptake potential from both the sediment and water column pools. N_w and N_s represent water column and pore-water nutrient concentrations, respectively; K is the half-saturation constant for uptake of N_w; and (k'/K) is the reciprocal of the half-saturation for N_s (Kemp *et al.* 1995). It can be seen that when the water column concentration (N_w) is zero, the equation reduces to the simple Michaelis-Menton equation for uptake through roots. When the sediment pool concentration is equal to zero, the equation becomes which describes uptake kinetics through leaves alone. Intermediate conditions between these extremes produced an aggregate uptake rate based on

the relative proportions of half-saturation concentrations represented by pool concentrations. This formulation, therefore, simultaneously calculated uptake via both pathways, based on the relative proportion of demand satisfied by each pool, and the model inputs that combined proportion (0-1) to individual equations for N, P, and Si. The minimum function (eq 9) selected the term limiting to photosynthesis, as for the phytoplankton nutrient kinetics described above. Kinetic coefficients were chosen from literature values from controlled experiments by Izumi and Hattori (1982) and Thursby and Harlin (1982). Model runs produced patterns of DIN uptake by leaves and roots similar to experimental observations of Thursby and Harlin (1982) for *Potamogeton* sp.

Results and Discussion

Calibration

Above- and below-ground SAV biomass patterns generated by model baseline runs calibrated well with available data from Chesapeake Bay and were representative of SAV dynamics in mesohaline estuaries such as the Patuxent and Choptank Rivers (Kemp *et al.* 1984, Twilley *et al.* 1985, Lubbers *et al.* 1990). The model exhibited stable behavior under a variety of initial and forcing conditions, producing simulations closely replicating plant growth patterns measured in laboratory studies using Chesapeake Bay plants (Staver 1984, Neundorfer and Kemp 1993), as well as in field studies from sites around the world (Cambridge *et al.* 1986, Izumi and Hattori 1982, Huisman and Weissing, 1994, Burkholder *et al.* 1994). The model was robust over long simulation times of up to five years, although it was strongly responsive to small changes in key variables such as DIN concentrations and epiphyte growth rate. Monte Carlo analysis is being conducted to assess model sensitivity to each variable in a systematic manner. Because the model operates in a spatially averaged mode, and does not have a spatial component, the expansion or contraction of SAV distribution zones cannot be explicitly produced by the model in its current form. However, spatial information can be inferred from predictions of success or failure of submersed vegetation in the 1 m^2 spatial unit.

Experiments

The model was used to assess ecosystem relationships that would be relevant to management activities, including the development of habitat criteria for increasing baygrass distributions and densities. The response of model state variables to elevated nutrient concentrations simulated the effects of eutrophication, including higher phytoplankton and epiphyte growth and biomass, and the decline in SAV productivity as observed in Chesapeake Bay. When comparing nutrient concentrations required to elicit reductions in growth response or elimination of SAV in the model with those in the real system, model output was found to parallel observations in the Patuxent and Choptank Rivers, as well in various mesocosm and pond experiments (Kemp *et al.* 1984, Lubbers *et al.* 1990, Neundorfer and Kemp 1995, Twilley *et al.* 1986). Elevated DIN concentrations of 40% above baseline led to extremely low *P. perfoliatus* density and eventual loss of SAV.

Simulation experiments were conducted to examine critical feedback relationships in the SAV habitat. Two are reported here, including the effect of SAV on water column nutrient levels and the effect of SAV on water column turbidity. The nutrient experiment was

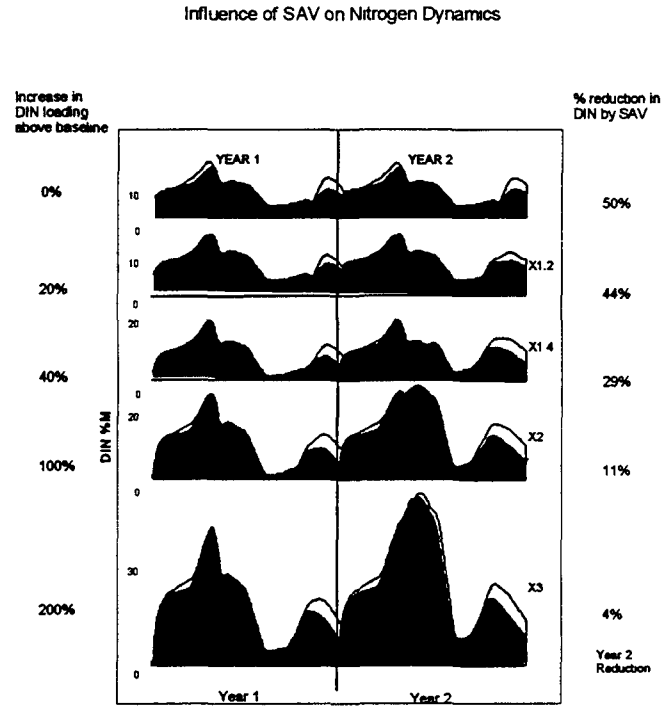

Figure 1

performed by subjecting the baseline SAV model system to increasing nutrient inputs and comparing the resulting SAV levels and dissolved nutrient concentrations with those in a similarly treated, but unvegetated site. Except for the absence of above-ground SAV leaves, the modeled "bare" site was identical in all respects to the vegetated site, including phytoplankton concentrations, sediment nutrient levels, potential for epiphyte colonization, etc. Initially, SAV plants were set at densities of 0 g m^{-2} leaf biomass and 45 g m^{-2} root/rhizome biomass in both "vegetated" and "unvegetated" sites, but unvegetated sites were not allowed to initiate above ground growth. Both habitats were exposed to nutrient loads of 0%, 20%, 40%, 100%, and 200% above baseline. The effect of SAV on water column nutrient levels was evaluated by determining mean nutrient concentrations predicted by the model in vegetated sites during the growing season (May-November) and comparing them with nutrient levels in unvegetated sites during the same period. The experimental simulation was carried out for a period of two years, ensuring model stability and reducing treatment sensitivity to initial conditions (Figure 1).

Results showed a number of interesting behaviors related to the way in which nutrients were processed by the SAV community. Vegetation significantly affected the nutrient levels in the beds. When present, SAV significantly reduced DIN concentrations during summer, even under the highest nutrient loading treatments. During Year 1, at all nutrient levels, DIN concentrations were about 50% lower in the waters overlying SAV beds, compared with unvegetated sites, indicating that after a certain lag time, most of the available new nutrient inputs were being taken up by plants. During Year 1, SAV began to decline during late summer in higher nutrient treatments and in Year 2, SAV biomass continued a progressive downward trend until the bed was essentially eliminated in the highest nutrient treatments. With reductions of SAV in Year 2, DIN concentrations progressively increased with additional DIN loading and the difference in DIN concentration over bare and vegetated sites diminished. In the +200% treatment, the difference between sites was insignificant.

Because the SAV root/rhizome component was impacted on a longer time scale than the above-ground component, loss of below-ground material in some cases was not evident until

the second year. In Year 1, high initial SAV biomass growth potential skewed the comparison of vegetated and unvegetated treatments because calculations of average nutrient concentrations included the spring growth phase, during which epiphytes did not have a chance to affect biomass production. In Year 1, due to healthy below-ground biomass, SAV grew strongly in spring even under high nutrient treatments and was able to take up significant water column nitrogen. In Year 2, the long-term effects of DIN loading were more apparent, and spring growth of SAV was affected by the previous year's poor growth and low below ground reserves. Running the model through Year 2 was thus essential to reduce the influence of initial conditions (i.e. the high potential for SAV growth) from results.

In all treatments with SAV present, there was a significant regeneration of DIN in fall and winter due to senescence. During fall and winter, DIN concentrations in water overlying vegetated sites exceeded that in unvegetated sites, a pattern which was most marked in the highest loading treatments. This suggested that below-ground decomposition and recycling contribute to nutrient pools, while at the same time, SAV was not present to intercept the sediment nutrients as they were released to the water column.

A second experiment involved the effect of SAV on suspended sediment concentrations in the bed. Ward *et al.* (1985) showed that SAV leaves could significantly reduce water current speeds within SAV beds, permitting sediments to fall out of suspension. Roots and rhizomes reduced the tendency for water motion to resuspend bottom sediments. Using empirical data on concentrations of suspended particulate material (SPM) in Choptank River *Potamogeton* beds of different leaf densities, a relationship was developed which represented the reduction of SPM in waters overlying the grassbed:

$$SPM = SPMa * 1-(0.1*e^{(SAV\#shoots*.0004)}) \quad (11)$$

where the SPM mg L^{-1} inside the bed equals the ambient SPM concentration, SPMa, reduced exponentially by a factor based on the number of shoots in the spatial unit (leaf density). Simulations produced a nearly linear reduction in SPM with increasing biomass (upper panel, Figure 2). Naturally, this relationship would approach an asymptote at some level less than 100% reduction. When the model was executed using different nutrient load factors (bottom panel, Figure 2), the reduction in SPM became nonlinear, with a discontinuity occurring at baseline +100% DIN addition. This trajectory demonstrated how the loss of SAV, which was nonlinearly related to increasing nutrient levels, secondarily affected sediment-trapping processes in the habitat, accelerating water quality deterioration. As SAV growth became impaired by increased nutrient loading, the clearing of sediments from the water column also became less effective. Lower sediment clearing resulted in a lower light environment and poorer conditions than would occur from increased nutrient levels alone.

Management Implications

Results of current and previous SAV model studies showed that increases of DIN loading significantly reduced biomass in a healthy SAV bed, shifting biomass peaks earlier in the growing season and reducing root/rhizome biomass. Model results indicated that habitat criteria targets for nitrogen appear to appropriately set to effect significant improvement in water quality. When target nutrient levels proposed as Tier 1 criteria (Stevenson *et al.* 1993, Batiuk *et al.* 1992) were used to drive the model, simulations showed vigorous growth of SAV and even supported successful re-establishment of SAV transplants in unvegetated areas.

Interestingly, applying proposed habitat criteria for nitrogen in the model automatically generated levels for other variables that approximated habitat criteria levels: the model predicted that chlorophyll a and K_D would reduce to 15 mg m^{-3} and 1.5 m^{-1} respectively if water column nitrogen concentration were reduced to to 10 μM, as called for in Tier 1 restoration criteria. Based on model predictions, Tier I habitat criteria should be appropriate for achieving goals established for SAV in the mesohaline Bay and may enable regrowth of *P. perfoliatus* in distributions observed in the lower Patuxent and Choptank Rivers during the 1960-1970s. As demonstrated, however, complexities in several feedback relationships, such as loss of sediment trapping ability of SAV, may make synergistic impacts more intractable than anticipated. Ongoing model studies will contribute to further understanding of these relationships and assist in refining critical thresholds for habitat quality.

Table 1. Difference equations and initial conditions for state variables in submersed plant model.

Diatom Biomass

$$PD(t) = PD(t - dt) + (Ps_{PD} + Ai_{PD} - Gr_{ZPD} - Gr_{MPD} - Ex_{PD} - Re_{PD} - Mn_{PD} - Ao_{PD} - Sd_{PD}) * dt$$

Other Phytoplankton Biomass

$$PO(t) = PO(t - dt) + (Ps_{PO} + Ai_{PO} - Gr_{ZPO} - Gr_{MPO} - Ex_{PO} - Re_{PO} - Mn_{PO} - Ao_{PO} - Sd_{PO}) * dt$$

Algal Epiphyte Biomass

$$AE(t) = AE(t - dt) + (Ps_{AE} + Ai_{AE} - Gr_{AE} - Re_{AE} - Mn_{AE} - Sb_{AE}) * dt$$

Plant Leaf/Stem Biomass (Above Ground)

$$AG(t) = AG(t - dt) + (Ps_{AG} + Tu - Re_{AG} - Td - Ts - Mn_{AG}) * dt$$

Plant Root/Rhizome Biomass (Below Ground)

$$BG(t) = BG(t - dt) + (Td + Ts - Re_{BG} - Mn_{BG} - Tu_{AG}) * dt$$

Sediment Carbon

$$CL(t) = CL(t - dt) + (Sd_{CL} - Re_{CL}) * dt$$

Ps= photosynthetic production; Ai= advective input; Tu= upward translocation (root to leaf); Td= downward translocation (leaf to root); Ts= seasonal root storage (leafto root); Gr= grazing loss (zooplankton, menhaden, or epiphytic grazers); Ex=exudation; Re= respiration; Mn= mortality (natural); Ao= advective output; Sd=sedimentation; and Sb= leaf substrate loss.

SYMBOL	DESCRIPTION	INIT QUANTITY	UNITS
PD	Biomass of Diatoms	450	mg C/m^2
PO	Biomass of Other phytoplankton	150	mg C/m^2
AE	Biomass of Algal Epiphytes	0	mg C/m^2

AG	Biomass of Plants above ground	0	mg C/m^2
BG	Biomass of Plants below ground	40000	mg C/m^2
CL	Sediment organic carbon-labile	20000	mg C/m^2

References

Batiuk, R. A, R. J. Orth, K. A. Moore, W. C. Dennison, J. C. Stevenson, L. W. Staver, V. Carter, N. B. Rybicki, R. E. Hickman, S. Kollar, S. Bieber, and P. Heasly. 1992. Submerged aquatic vegetation habitat requirements and restoration targets: A technical synthesis. CBP/TRS 83/92. Annapolis, MD 186 pp.

Burkholder, J. M., H.B Glasgow and J. E. Cooke. 1994. Comparative effects of water column nitrate enrichment on eelgrass Zostera Marina, shoalgrass *Halodule wrightii*, and widgeongrass *Ruppia maritima*. Marine Ecology Progress Series 105:121-138.

Cambridge, J. L., A. W. Chiffings, C. Brittan, L. Moore, and A. J. McComb. 1986. The loss of seagrass in Cockburn Sound, Western Australia II: Possible causes of seagrass decline. Aquatic Botany 24:269-285.

Cerco, C., and Cole, T. 1993. Three-dimensional eutrophication model of Chesapeake Bay. Journal of Environmental Engineering 119(6):1006-1025

Dennison, W. C. and R. S. Alberte. 1986. Photoadaptation and growth of *Zostera marina* L. (eelgrass) transplants along a depth gradient. Journal of Experimental Marine Biology and Ecology 98:265-282.

DiToro, D. M., D. J. O'Connor, R. V. Thomann. 1971. A dynamic model of phytoplankton populations in the Sacramento-San Joaquin Delta. Advances in Chemistry Series 106. p 131-180.

Goldsborough, W. J., and W. M. Kemp. 1988. Light responses of a submersed macrophyte: Implications for survival in turbid waters. Ecology 69:1775-1786.

Huisman, J. and F. J. Weissing. 1994. Light-limited growth and competition for light in well-mixed aquatic environments: An elementary model. Ecology 75(2):507-520.

Izumi, H. and A. Hattori. 1982. Growth and organic production of eelgrass (*Zostera marina)* in temperate waters of the Pacific coast of Japan. III. The kinetics of nitrogen uptake. Aquatic Botany 12:245-256.

Kemp, W.M., W.R. Boynton, J.C. Stevenson, and L.G. Ward. 1984. Influence of submersed vascular plants on ecological processes in up Chesapeake Bay. In: V.S. Kennedy (ed.) The Estuary as a Filter. Academic Press. New York. Pp. 367-393.

Kemp, W. M., W. R. Boynton, and A. J. Hermann. 1995. Simulation models of an estuarine macrophyte ecosystem. In: B. C. Patten (ed.) Complex Ecology. Prentice Hall, Englewood Cliffs, NJ. p 262-277.

Kirk, J. T. O. 1983. Light and photosynthesis in aquatic ecosystems. Cambridge Univ. Press. Cambridge, UK. 401 pp.

Kremer, J. and S. W. Nixon. 1978. A Coastal Marine Ecosystem: Simulation and Analysis. Springer-Verlag, New York. 217 pp.

Lubbers, L., W. R. Boynton, and W. M. Kemp. 1990. Variations in structure of estuarine fish communities in relation to abundance of submersed vascular plants. Marine Ecology Progress Series 65: 1-14.

Madden, C. J. and W. M. Kemp. 1996. Ecosystem model of an estuarine plant community: Calibration and simulation of eutrophications responses. Estuaries 19(2B):457-474.

McBride, G. B, W. N. Vant, J. E. Cloern, J. B. Liley. 1993. Development of a model of phytoplankton blooms in Manukau Harbor. NIWA Ecosystems Publication No. 3. Hamilton, New Zealand.

Monod, J. 1942. Recherches sur la croissance des cultures bacteriennes. Paris: Herman et Cie. Neundorfer, J. V. and W. M. Kemp 1993. Nitrogen versus phosphrus enrichment of brackish waters: responses of the submersed plant *Potamogeton perfoliatus* and its associated algal community. Marine Ecology Progress Series 94:71-82.

Odum, H. T. 1983. Systems Ecology: An Introduction. Wiley and Sons. New York. 644 pp.

Staver, K. 1984. Responses of epiphytic algae to nitrogen and phosphorus enrichment and effects on productivity of the host plant, *Potamogeton perfoliatus* L. in estuarine waters. MS thesis, Univ. MD, College Park, MD.

Stevenson, J. C. 1988. Comparative ecology of submersed grass beds in freshwater, estuarine, and marine environments. Limnology and Oceanography 33:867-893.

Stevenson, J. C., L. W. Staver, K. W. Staver. 1993. Water quality associated with survival of submersed aquatic vegetation along an estuarine gradient. Estuaries. 16(2): 346-361.

Thursby, J. E. and M. M. Harlin 1982. Leaf-root interaction in the uptake of ammonium by *Zostera marina.* Marine Biology 72:109-112.

Twilley, R. R., W. M. Kemp, K. W. Staver, J. C. Stevenson, and W. R. Boynton. 1985. Nutrient enrichment of estuarine submersed vascular plant communities. 1. Algal growth and effects on production of plants and associated communities. Marine Ecology Progress Series 23:179-191.

Twilley, R. R., G. Ejdung, P. Romare, and W. M. Kemp. 1986. A comparative study of decomposition , oxygen consumption and nutrient release for selected aquatic plants occurring in an estuarine environment. Oikos 47:190-198.

Vant, W. N. 1991. Underwater light in the Northern Manukau Harbor, New Zealand. Estuarine, Coastal and Shelf Science. 33:291-307.

Verhagen, J. H. G, and P. H. Nienhuis. 1983. A simulation model of production, seasonal changes in biomass distribution of eelgrass (*Zostera marina)* in Lake Grevelingen. Marine Ecology Progress Series 10:187-195.

Ward, L. G., W. M. Kemp, and W. R. Boynton. 1985. The influence of waves and seagrass communities on suspended particulates in an estuarine environment. Mar. Geol. 59:85-103.

Simulation Model of Biogeochemical Processes in Marsh Mesocosms

Christopher J. Madden, Jennifer Zelenke, and J. Court Stevenson

Horn Point Environmental Laboratory
University of Maryland
Cambridge, MD

Background

The high degree of complexity and variability in coastal marshes makes the use of models an important means of synthesizing data and understanding the biogeochemistry of marsh systems. In mesocosms established at the Multiscale Experimental Exosystem Research Center (MEERC) facility at Horn Point Environmental Laboratory (HPEL), University of Maryland, a series of 12 artificial marshes containing sediments and several types of vegetation will be analyzed both experimentally and with modeling techniques. Research on these mesocosm communities will determine the effects of time and community complexity on system functioning. Experiments will involve the manipulation of groundwater nitrogen inputs, plant community diversity, hydroperiod and water depth to determine their effects on nutrient processing, marsh productivity and plant succession. Results will be extrapolated using numerical models to help understand natural marsh system functioning. The experiments will be conducted over a period of several years beginning in 1996.

The primary purpose of the modeling effort will be to synthesize, interpret and extend the results of the mesocosm experiments. The plan is to develop the model concurrently or in advance of experiments, giving researchers tools for testing hypotheses, predicting outcomes of experiments, and even aiding in designing treatments and methodologies. Because model and experimentation will be interactive, feedback from each should be of assistance with refining the other.

Hydrological, biological and chemical processes will be examined using the model and relationships of these processes will be interpreted across spatial scales. Results of mesocosm experiments will be continuously assimilated into the model and results of modeling experiments will be extrapolated to the Chesapeake Bay ecosystem. The model is in the early phase of development and will be described here in general terms, along with a presentation of preliminary results.

Model Development

A working six-compartment model of the MEERC marsh mesocosms has been developed and initial diagnostics are being run. Initial efforts focus on modeling a single plant species, creating hydrological and geochemical sectors around the biological structure of the well-known marsh cordgrass species, *Spartina alterniflora*. Subsequently, sectors describing additional plant species and, eventually, consumers will be incorporated. This scheme gives the advantage of simplifying early stages of modeling as the model framework (forcing functions, physical dimensions) and

sectors (hydrology, sediment chemistry) that will be common to all biological sectors are formalized.

Tidal and groundwater forcing functions in the mesocosms will have significant impact on both the actual mesocosm and the model processes, and special emphasis has been placed on accurately capturing hydrological parameters of the mesocosm. The marsh mesocosms are raised at one end to create a 5° slope, allowing partial inundation by an artificial tide entering at the lower end. We determined, in consultation with the experimental team, that a two-cell model (high marsh and low marsh) should be established to represent the non-flooded and flooded portions of the mesocosm. The model will use a floating boundary between cells, its position dependent on the physical extent of flooding in the mesocosms, which is determined by experimental treatment. Because flooding is a variable and dominant factor in sediment chemistry, plant productivity and animal response, it is of paramount importance to capture the spatial extent of the water coverage on each tidal cycle in the model.

The biological submodel consists of *Spartina alterniflora* above-ground and below-ground carbon, as well as associated leaf and root litter. Biological sectors will be expanded to include *Eleocharis* sp., *Spartina patens*, *Hibiscus* sp., and *Scirpus olneyi* plant populations. The difference equations for each of the plant species will be similar to the equations for S. alterniflora:

(1) SHOOT(t) =
SHOOT(t - dt) + (Sht_Prod + Up_trans - Sht_Graze - Sht_Mort - Sht_Rsp - H - Dn_trans) * dt

(2) ROOT(t) =
ROOT(t - dt) + (Dn_trans - Rt_Mort - Rt_Graze - Rt_Resp - Up_trans) * dt

where above-ground biomass SHOOT (g C m^{-2}) is the sum of shoot production by photosynthesis (Sht_Prod), upward translocation from roots (Up_trans), minus losses from direct grazing (Sht_Graze), mortality (Sht_Mort), respiration (Sht_Rsp), harvesting (H) for samples, and downward translocation to roots (Dn_trans). Root biomass, ROOT (g C m^{-2}), is the sum of downward transport of photosynthesis (Dn_trans), minus mortality (Rt_Mort), direct loss to grazing (Rt_Graze), root respiration (Rt_Resp) and translocation of stored carbon to shoots (Up_trans).

The geochemical submodel includes nitrogen, phosphorus, sulfur and oxygen dynamics. Hydrologic input via groundwater is forced using experimental design specifications. Sediment porosity, bulk density and diffusivity of mesocosm soils are being analyzed and will be incorporated into the model as data become available. Presently, groundwater functions are based on empirical measures of water transit time and groundwater export rates in selected MEERC mesocosms. Model parameters include a time unit of 1 day, a time-step (dt) of 0.25, a simulation length of 1 yr. The spatial unit of the model is m^{-2}, and forcing functions include air temperature, PAR (photosynthetically active radiation), groundwater input rates, and groundwater nitrate concentrations. Boundary conditions included opaque, impermeable walls containing two horizontal cells for high and low marsh. Two vertical layers consisted of sediments and overlying water. Mesocosms were open and exposed to natural sunlight, air and precipitation.

Results

Calibration

The model has initially been developed for a monospecific stand of *Spartina alterniflora*, calibrated to produce growth and biomass patterns characteristic of temperate US East coast marshes. Two datasets were used to calibrate the *Spartina* model (Figure 1): a South Carolina salt marsh (Morris and Haskin 1990) and an Eastern Shore, Maryland salt marsh in Monie Bay (Stribling and Cornwell 1995). The model generates reasonable values for above-ground biomass, showing growth initiation in early spring, reaching a peak in late summer at about 175 g C m^{-2} before dieoff occurs. Both model and field data indicate that a significant amount of standing stock (approx. 110 g C m^{-2}) remains in place at the end of the growing season and persists into winter. This material is assumed to be mostly highly refractory standing dead material. To reduce standing material to winter levels in the field (about 40 g C m^{-2}), a special function will be required in the model.

As yet, the forcing (e.g. wind, rains, floods) which actually removes this material in the field, and its schedule, is not determined. This does however, illuminate an interesting point observed when comparing model results to the mesocosm biomass patterns: at the end of the first growing season in the actual mesocosm marsh community, a large percentage of standing dead biomass persisted throughout the winter into spring. In other words, the mesocosm behaved more like the model than like the natural marsh, which generally has low standing biomass at the end of winter. Apparently, a physical forcing is absent in the mesocosms which is responsible for removing standing dead material in the field each year. Model-mesocosm analysis may provide information concerning this observation.

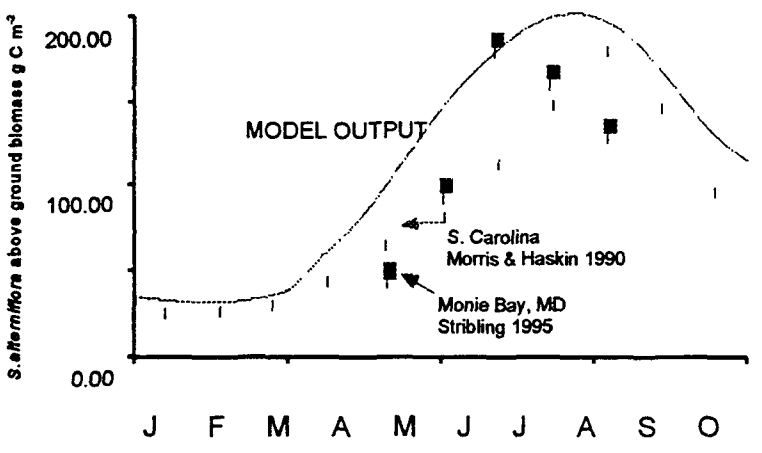

Figure 1. Calibration of plant biomass to literature values.

Biomass sampling

The marsh model has been used to aid design of mesocosm experiments *a priori* to predict effects of experimental treatments on marsh productivity. Initially, it was used to estimate the expected range of standing biomass in the area dominated by *S. alterniflora* in the mesocosms and to quantitatively assess appropriate scales and schedules for biomass sampling. The procedure by which productivity will be determined in the mesocosms is destructive biomass harvesting. This procedure introduces some error into the experiments. One objective of the modeling exercise was to determine the maximum rate of destructive sampling that *S. alterniflora* plantings could support, while sustaining minimal impact on plant growth. The model was run with different levels of biomass removal on a variety of schedules to observe the projected impact on standing stock. Experimenters intended to use the information to adjust sampling rates to optimize for plant biomass, replicating the nonharvested condition. Results indicated that monthly sampling of

approximately 5% of the above-ground biomass would not cause large deviations in standing stock from the unimpacted condition.

An important point needs to be raised concerning this experiment. Successful duplication of unimpacted patterns of biomass density does not necessarily mean that marsh processes are equivalent in both harvested and unharvested conditions. As revealed in the model, following each harvesting, a brief increase in plant productivity occurred, probably in response to increased light, reduced nutrient depletion, and lowered density-related inhibition. This resulted in a quick "filling in" of marsh standing stock, but the acceleration of processes (in the model) associated with the additional production caused changes in nutrient utilization, oxygenation of the root zone, and decomposition rates. Thus, although standing stocks in the mesocosm may be minimally impacted by a particular harvest schedule, other processes may in fact be strongly impacted. The model is currently being configured to analyze harvest impacts on all relevant geochemical processes and a suite of responses will be generated.

Nitrogen Transformations

Model experiments were performed to determine how processing of nitrogen may be affected by changes in the rate of gross primary production of *S. alterniflora* (Figure 2). Denitrification represents a permanent removal of nitrogen from the system via conversion of nitrate to the diatomic gaseous form (NO_3 to $N_{2(g)}$) and is an important term in the nutrient budgets of the mesocosms. Denitrification rates are dependent on sediment oxygen demand, temperature and nitrate concentrations. A series of experimental treatments using a range of *Spartina* biomass levels and productivity values was performed using the model. Simulated denitrification rates increased in the modeled system with increasing plant biomass and productivity. Because loss rates of nitrogen via denitrification often exceeded the supply of nitrate from groundwater inputs, other sources of nitrate (in addition to groundwater inputs) probably accounted for modeled denitrification rates. Much of the denitrification loss was apparently supported by decaying plant tissue which produced an increase in remineralized ammonium and was subsequently oxidized to NO_3 via nitrification (NH_4 to NO_3). Increases in primary productivity strengthened the coupling of the denitrification and nitrification processes by increasing ammonium supply to the oxidized upper sediments. The importance of this mechanism is currently quantitatively being investigated using the model. Both processes by which denitrification might increase (increased ammonium supply and reduced redox potential in the lower root zone) are dependent upon rates of vascular plant production. The interaction of biology and geochemistry has far-reaching management importance in marsh environments and the proper interpretation of the mesocosm experiments using modeling techniques will hopefully enable the extrapolation of experimental results to the natural system.

Discussion

The mesocosm model demonstrated reasonable behavior for U.S. temperate East Coast salt marshes and calibration of the model for the mesocosm system is currently underway. The model is useful as an interactive tool for designing experiments. Its utility with assisting experimental design was demonstrated; levels of manipulations and measurement techniques and expected impacts on the mesocosm system were calculated. In other experiments, results suggested that permanent nitrogen loss through denitrification was dependent on productivity of the marsh plants, but the importance of nitrogen removal versus nitrogen storage in plant biomass

has yet to be determined. The model should prove useful in examining these questions. Development will continue with linkage of the hydrologic submodel to biogeochemical components. As empirical data become available, incorporation into the model will enable better convergence of the two (experimental and model) systems and scaling of mesocosm processes to the natural system will follow.

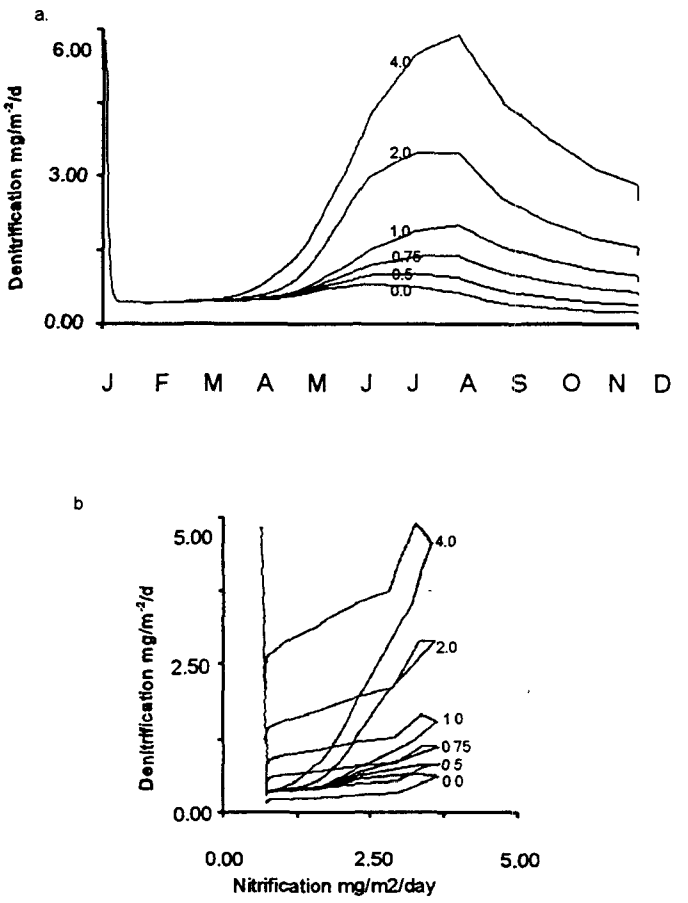

Figure 2. Modeled responses of denitrification to changes in *S. alterniflora* productivity. Gross production rate multiplier is indicated and was used to mimic relative ecosystem health. (a) ch denitrification in response to primary productivity (b) shifting of nitrification-denitrification in resp to primary production.

References

Kaplan, W, I. Valiela, and JM Teal. 1979. Denitrification in a saltmarsh ecosystem. L&O 24(4): 726-734.

Morris, JT, and B Haskin. 1990. A 5-year record of aerial primary production and stand characteristics of Spartina alterniflora. Ecology 71(6): 2209-2217.

Thompson, SP, HW Paerl, and MC Go. 1995. Seasonal patterns of nitrification and denitrification in a natural and a restored salt marsh. Estuaries 18(2): 399-408.

White, DS and BL Howes. 1994. Translocation, remineralization, and turnover of nitrogen in the roots of Spartina alterniflora (Gramineae). American Journal of Botany: 81(10): 1225-1234.

Zooplankton Process Model for Mesohaline Chesapeake Bay

Christopher J. Madden and W. Michael Kemp

Horn Point Environmental Laboratory
University of Maryland
Cambridge, MD

Background

Analysis of the role of zooplankton processes in trophic and nutrient cycling is an important component of the ecosystem process modeling strategy for Chesapeake Bay. *Acartia tonsa* and *Eurytemora affinis* are the two most abundant zooplankton species in the mesohaline reaches of the Bay mainstem, as well as in the lower parts of many Maryland tributaries, particularly the mesohaline Patuxent River. The two species differ in their responses to seasonal changes, resulting in winter-spring dominance by *Eurytemora* and summer dominance by *Acartia*.

Zooplankton represent a significant and variable source of predation to lower trophic levels, including herbivory of phytoplankton, consumption of microzooplankton and protozooplankton, and cannibalism of juvenile mesozooplankton. Resolution of grazer population cycles in Chesapeake Bay is important to understanding overall system functioning and is imperative for properly modeling the ecology of the system. Therefore, a stand-alone model of zooplankton interactions was developed which can be used to test the role of zooplankton in carbon and nutrient cycling in Chesapeake Bay.

This simple nutrient-phytoplankton-zooplankton (N-P-Z) model was conceptualized with zooplankton compartments aggregated into three state variables: *Eurytemora* sp., *Acartia* sp., and microzooplankton (Figure 1). These compartments dynamically interact with lower trophic levels. Predation from higher trophic levels (notably Anchovy) occurs in this model via seasonally variable forcing functions. The model will be used to examine phytoplankton-zooplankton interactions, simulate trophic carbon and nutrient transfers, interpret empirical observations of abundance and distribution, quantify effects of predation on zooplankton, and predict the response of zooplankton to water quality changes via bottom-up effects. Simulations will examine the functional role of zooplankton in nutrient regeneration, carbon transfer, anoxia and phytoplankton dynamics to assess the importance of zooplankton in the environment from a management perspective. This model will be linked to a series of similar models developed to examine aspects of zooplankton ecology and function in the mainstem Chesapeake Bay and reaches of the other tributaries.

A second model (See Madden *et al.*, A Stage-Structured Model..., this report) was created to examine factors influencing zooplankton community development. Environmental factors affect generation time, abundance-biomass relationships, organism condition, and size-dependent predator-prey relationships. Such a model requires stage-specific modeling of the zooplankton community and will be used to evaluate phytoplankton size relative to zooplankton size as a means of determining feeding behavior and top-down effects on primary production. This approach also yields a size-frequency spectrum of the zooplankton community, which is of relevance in their role as food items for planktivorous fish. (See Madden *et al.*, A Stage-

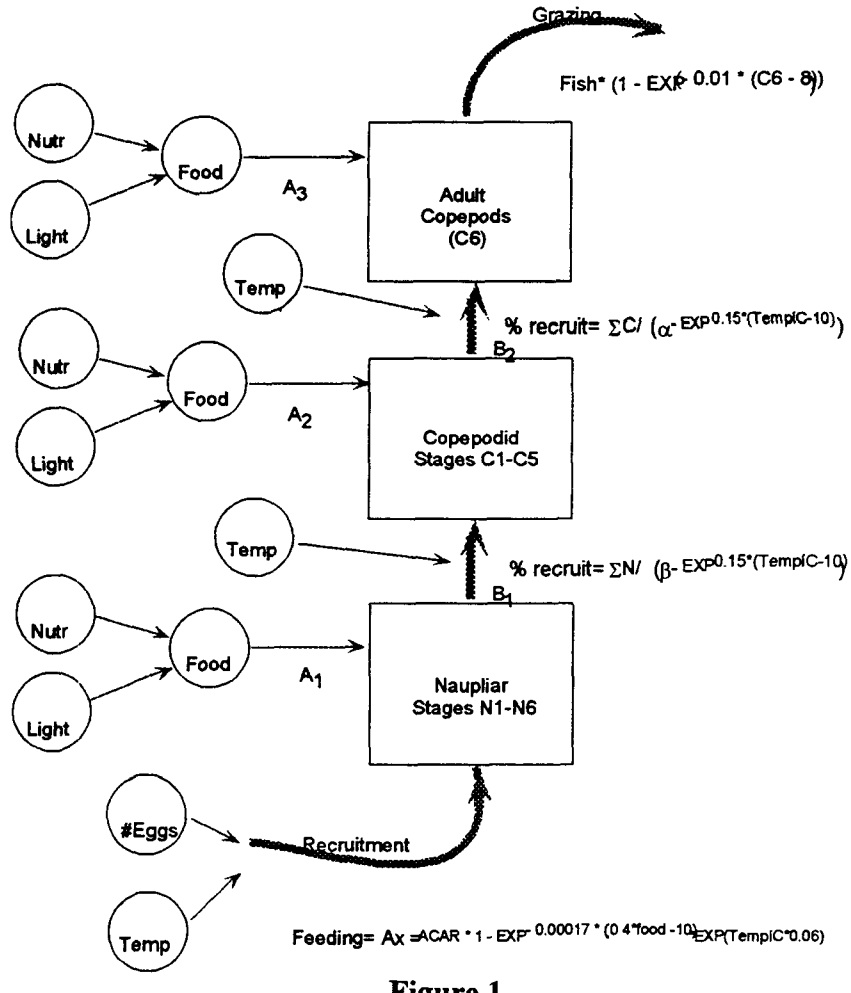

Figure 1

Structured Model..., this report.)

Together, the two modeling approaches synthesize Chesapeake Bay monitoring and modeling activities to assimilate and interpret new data. The models will help direct monitoring activities which will improve data collection efficiency and productivity. Model analysis can help determine sampling locations, as well as temporal and spatial scales for data collection. Ecosystem processes models can take information gained from small-scale sampling and extrapolate to large-scale processes.

Model Development

A simple numerical model of nutrient-phytoplankton-zooplankton interactions is being developed using the STELLA II simulation environment on a RISC-based microcomputer. The strategy for developing process models of Chesapeake Bay and tributaries is to calibrate separate models for representative segments of the habitats and then combine the models as confidence is gained in the calibration of each component. Model development is currently underway for tidal fresh, transitional, and mesohaline habitats in the Patuxent River. These models will be linked via hydrologic exchanges. The transitional and mesohaline segments will be represented by identical model structure, with variations in parameters, time constants, and hydrology, and the input functions specific to each area (*e.g.* nutrient loading). The tidal fresh version of the Patuxent River model includes additional freshwater species (*e.g. Bosmina* sp)

The mesohaline Patuxent River model represents a spatially averaged 1 m^2 area of water column and benthic sediment in the mesohaline open water region of the Patuxent River. The zooplankton process model described here divides zooplankton into two species groups (*Acartia* and *Eurytemora*), and a "microzooplankton" state variable which aggregates nauplii and

copepodid stages from both species, plus other small zooplankton and protozoa. The water column is treated as a single homogeneous layer in the littoral model. In the deep channel version, where there is two-layered structure, each state variable has upper and lower water-column components. Two versions of the mesohaline model were developed: one for the shallow, single-layered water column in the littoral zone and another for the deeper, channel region where stratification in the river results in formation of a two-layer water column structure. In the shallow model, the system is treated as vertically averaged over the 1-3 m water column. In the two-layer version, the upper layer is fixed at 6 m and the bottom at 10 m. For other reaches of the Patuxent River (transitional, tidal fresh) and other tributaries, the vertical dimensions of the model were adjusted to the mean bottom depth.

In the shallow littoral model, the water column is treated as a homogeneous parcel which exchanges nutrients and carbon with the benthos and sediments to a depth of 15 cm. In the two-layer model, the upper and lower water column exchange phytoplankton and particles by sinking; zooplankton via bidirectional migration; and nutrients via mixing across the pycnocline. As in the single layer model, the lower water column exchanges nutrients and carbon with the benthos and sediments to a depth of 15 cm.

Carbon transfer is tracked in units of mg C, with conversion of C to N using Redfield stoichiometry of 7.2:1. A time-step of 0.25 day, a base simulation length of 1 year, and a second-order Runge-Kutta integration scheme were used in the model. Simulation runs were conducted for single and multi-year periods.

The model consists of 12 state variables, each represented by a difference equation calculating total carbon biomass from summed inputs and outputs over each time-step. State variables include diatoms, flagellates and chlorophytes, *Acartia tonsa* and *Eurytemora affinis*, microzooplankton, benthic filter feeders, dissolved inorganic nitrogen (DIN), and oxygen. Modeling of the dominant zooplankton functional groups allows a distinction based on differences in food supply and temperature response resulting in a cold weather dominance of *Eurytemora* and a warm weather dominance of *Acartia*. Phytoplankton were also modeled as two separate state variables, with functional distinction based on differences in nutrient and light response. Temperature, nitrogen concentration and underwater light intensity regulate specific photosynthesis rates. Phytoplankton growth rate is determined by a photosynthesis versus irradiance (P vs I) relationship and Michaelis-Menton nutrient kinetics, with N representing the limiting agent. Maximum growth rate for phytoplankton P_{max} was defined by a temperature-dependent formulation (Kremer and Nixon 1978):

$$P_{max} = 0.59\, e^{(0.0633 * (T - Gcrit))} \qquad (1)$$

where P_{max} is the maximum photosynthetic rate in mg C mg C^{-1} d^{-1}, T is Celsius temperature, G_{crit} is a critical temperature coefficient = 1° C for diatoms, and 8° for other (summer) phytoplankton. The higher temperature coefficient for summer phytoplankton has the effect of delaying growth and peak biomass formation until early June; whereas, diatoms peak in March. Actual net primary production was calculated by multiplying phytoplankton biomass, the specific production described above, and the minimum of nutrient and light limitation factors. Mean water column light was calculated by integrating light level at several depths following the Beers-Lambert relationship (Kirk 1983):

$$PAR_{(Z)} = PAR * e^{(-K_D Z)} \qquad (2)$$

where PAR= light intensity or photon flux density at any depth (Z) is derived from PAR_s, the incident light entering the water column. Downwelling attenuation (K_D) is summed from component attenuations of phytoplankton (K_C), suspended particulates (K_S), and water (K_W). Equations use the form: $K_C = 0.054 * Chl^{0.667} + 0.0088 * Chl$, $K_S = 0.0396*SPM+0.39$, and $K_W = 0.03$. K is in units of m^{-1}, Chl in micro-g L^{-1}, and suspended particulate material (SPM), mg L^{-1}. Self-shading effects on phytoplankton photosynthesis rates are accounted implicitly by the phytoplankton contribution (K_C) to total water column attenuation (K_D). Active chlorophyll concentrations are based on chl:c ratios for diatoms of 1:50 and for other phytoplankton, 1:90. Maximum temperature-based photosynthetic rates are downward-adjusted by limitation terms describing instantaneous nutrient and light-based carbon uptake. Carbon fixation rates for phytoplankton are modeled as functions of water-column nutrient concentrations following Michaelis-Menton kinetics for nitrogen (N), phosphate (P), and silica (Si), using half-saturation constants of 1.5, 0.9, and 1.5 M, respectively (Monod 1942). Photosynthesis by phytoplankton is related to irradiance (PAR_5, mean irradiance in the water column) by rectangular hyperbola P-I, with a light saturation onset parameter (I_K) of 90 Ein m^{-2} s^{-1}. The minimum of all nutrient and light - related rates was taken as the overall limiting rate for phytoplankton growth:

$$F(N, L) = MIN\left(\frac{N}{N+K_n}, \frac{P}{P+K_p}, \frac{Si}{Si+K_{si}}, \frac{PAR_5}{PAR_5+I_k}\right) \quad (3)$$

Growth in the zooplankton compartments is the sum of grazing inputs, modified by an assimilation coefficient minus losses to predation, respiration, sinking and mortality. Conversion of zooplankton biomass to abundance of adult individuals per m^3 used a conversion constant of 5 micro-g carbon per adult (Roman, pers. comm.). Grazing is characterized by an Ivlev function based on predator and prey abundances. A separate Ivlev formulation was used for each zooplankton species for grazing on phytoplankton, incorporating temperature and oxygen effects (example for *Acartia*):

$$Gap=ACAR*(1 - (e^{(-0.0010 * ((DIA + (k* OP)-10)} * Tf * (O2/ (1 + O2)) \quad (4)$$

where Gap is the ingestion rate by *Acartia* of phytoplankton, ACAR = the biomass of adult *Acartia*; 0.001 is the Ivlev coefficient; DIA = the biomass of diatoms and OP = the biomass of other phytoplankton (mg m^{-3}), k is a preference function based on the seasonal availability of each phytoplankton group, where DIA is 50% more likely to be consumed during spring-early summer (DAY<190) and 25% more likely to be consumed in late summer though winter; Tf = an Arrhenius temperature function with Q_{10} of approximately 2 and of the form:

$$Tf=SQRT(e^{(Temp*0.069)}*0.5) \quad (5)$$

and the final term is an oxygen relationship which inhibits feeding at low oxygen concentrations, having a 1 mg L^{-1} half-saturation coefficient. A similar grazing function was used to represent zooplankton predation on microzooplankton (including juveniles):

$$Gam=ACAR*0.075*(1 - (e^{(-0.117*(MZ-5))}))* Tf * (O2/ (1+O2)) \quad (6)$$

where Gam is the ingestion rate by *Acartia* of microzooplankton, MZ = the biomass of small zooplankton in mg m^{-3}. Mesozooplankton grazed on detrital material according to the following relationship:

$$Gad=ACAR*0.005*(SPOC/(1000+SPOC)) * Tf * (O2/ (1+O2)) \quad (7)$$

where Gad is the ingestion rate by*Acartia* of detritus, SPOC is suspended particulate organic carbon (mg m^{-3}).

The feeding relationships for *Eurytemora* were similar, using an Ivlev coefficient (0.007) and the temperature coefficient adjusted to suppress feeding by 50% after mid-year. This formulation has the effect of enhancing *Eurytemora* feeding and growth during the early part of the year and restraining it during mid-year when *Acartia* dominates.

Losses from the zooplankton compartments include respiratory expenditures, natural mortality, and grazing. Respiration includes a basal metabolic rate that is temperature-driven, plus an active respiration rate related to feeding rate, as 15% of the carbon ingested, of the form:

$$Rz=ACAR*0.055*Tf+0.15*I \quad (8)$$

where Tf is the above Arrhenius function and I= the ingestion rate (sum of grazing rates from eqs. 4, 6, 7). Losses of zooplankton carbon due to grazing by planktivorous fish (anchovy) are related to zooplankton abundance from the model calculations and fish abundance provided by forcing function following the familiar Ivlev formulation:

$$Gfz= F*R3*0.11*(1-e^{(-0.01*ACAR)}) \quad (9)$$

where Gfz is grazing rate of *Acartia* by anchovy, F = anchovy abundance; R3 = a randomizing term to impart a 25% variability around the forcing function; -0.01 is the literature value Ivlev coefficient, empirically determined and ACAR = prey abundance (mg m^{-3}).

Zooplankton egg production was related to feeding rate and temperature following the relation:

$$Egg= I * e^{-0.01 * (I)} * e^{T*0.084} \quad (10)$$

where Egg is the number of eggs produced per mg of zooplankton biomass, I is the ingestion rate of the zooplankton. Recruitment to naupliar, then copepodid and adult stages, are functions of a characteristic development time (maximum=24 d), modified by temperature and losses to natural mortality and grazing.

Results and Discussion

The model is currently in the mid-development phase and has undergone successful preliminary calibration. Initial results showed stable model behavior, reflecting appropriate seasonal dynamics and feeding relationships. Calibration datasets for zooplankton were taken from mesohaline and Patuxent River monitoring data from 1964 and 1985 (Flemer 1970, Heinle 1974, MDE 1988). Calibration data for phytoplankton were from several sources reporting

measurements in the Patuxent and Choptank Rivers in 1970 and the 1980s (Flemer 1970, Boynton *et al.* 1982, Flemer *et al.* 1983, MDE 1988, Magnien *et al.* 1991, Kemp *et al.* 1981, 1995).

Seasonal phytoplankton and zooplankton abundances in the single layer water column model reproduced the spring period of dominance by diatoms and *Eurytemora*, yielding to summer dominance by flagellates (other phytoplankton) and *Acartia*. Model output for *Eurytemora* and *Acartia* adults followed calibration data from 1964 reasonably well. A peak in *Acartia* abundance in April-May in three calibration datasets was reproduced by the model. A peak in August predicted by the model corresponded well with a small summer peak in the 1964 dataset for the mesohaline Patuxent. The biomass peak also coincided in timing, but not in magnitude, to the 1985 mesohaline and transitional Patuxent dataset.

These results showed the model to be stable and within the range for Chesapeake Bay zooplankton populations. Further model refinement will likely improve matching of the recent trend of higher zooplankton abundance in summer and fall. The annual pattern of *Eurytemora* abundance was captured by the model, with a strong peak in March, declining to about the level of *Acartia* abundance during summer and fall. *Eurytemora* does not appear to exhibit a secondary peak, as does *Acartia* during late summer.

Seasonal phytoplankton and zooplankton abundances show that during an annual cycle baseline run, phytoplankton components of the aggregated model in both the upper and lower water column exhibited similar seasonal patterns of diatom and flagellate dominance as in the shallow littoral model. Some significant differences in vertical distribution were noted. In both phytoplankton groups, upper water layer compartments were generally 10-25% higher in mean algal biomass.

In the stratified model, *Eurytemora* and *Acartia* biomass in upper and lower water columns also reflected similar patterns as in the shallow model. However it was noteworthy that the second *Acartia* peak, which developed in late summer, occurred only in the upper water column. Additional analysis is required, but preliminary assessment ruled out food limitation, because in late summer, the upper and lower phytoplankton compartments were almost equally abundant. Numerical abundance of *Acartia* naupliar and copepodid stages in the upper layer followed adult patterns of abundance, indicating that during times of increased food availability and adult growth, there was increased egg production. The sum of all naupliar stages was about an order of magnitude greater than the adult density, and the sum of copepodid stages about 40% of the nauplii. The order of magnitude of copepodid abundance agreed well with the 1964 calibration data from Patuxent for most of the year, although the summer peak exceeded calibration data by about a factor of four and the spring peak in the model precedes the data by about one month.

Model-based analysis enables quantification of cause-effect relationships and the examination of emergent properties in the data. The aggregated two-layer model was used to analyze top-down control of phytoplankton biomass by varying the amount of predation pressure from Anchovy on the adult zooplankton components. Anchovy predation (a forcing function) was varied by changing predator abundance in successive runs to equal 10, 40, 80, 100, 120% of the baseline (1988) case (Figure 2), while maintaining constant feeding pressure of fish on zooplankton. Increased predation pressure on zooplankton reduced grazing on phytoplankton. Approximately 10 mg C m^{-3} increase in phytoplankton biomass was realized per 10% increase in anchovy predation due to top-down control. A doubling of Anchovy biomass resulted in an

increase in mean spring phytoplankton biomass of 80%. Model analysis focusing on the relationships between turbidity and submerged aquatic vegetation (SAV) evaluated effects of increased phytoplankton abundance on the underwater light regime. Model results suggested that as phytoplankton chlorophyll a doubled, water column attenuation (K_D) increased from 1.1 m^{-1} to 1.5 m^{-1}. This is relevant to management of living resources, as subsurface light is a critical factor for SAV survival. According to the SAV model, by doubling water column chlorophyll, PAR at the plant canopy declined by about 50% (204 to 97 Ein m^{-2} s^{-1}). A halving of PAR would severely inhibit SAV growth. Thus, albiet using forced top predator data, the model demonstrates a strong trophic cascade effect from top-down control. Use of the model to explore the magnitude of these effects, and the relative dependence of phytoplankton concentration on top-down versus bottom-up control will yield information useful to management of the mesohaline Bay.

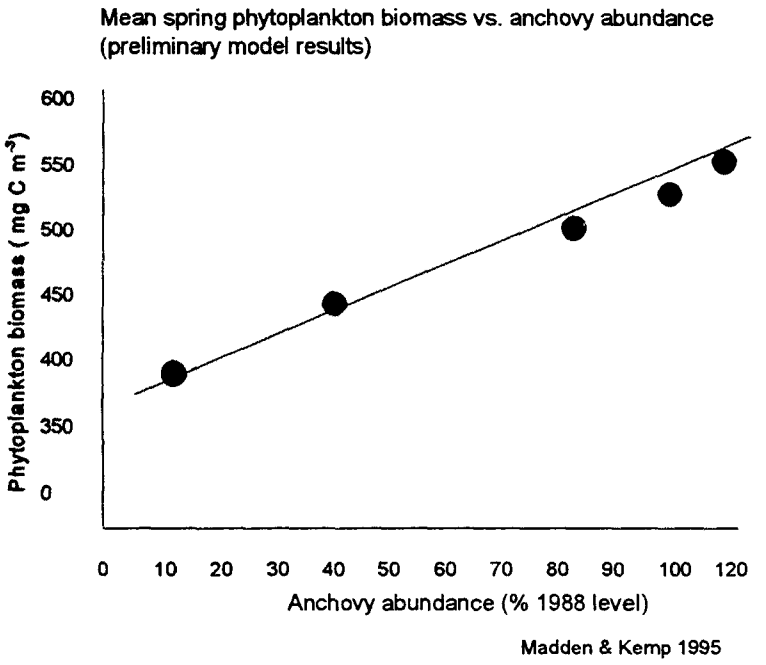

Figure 2

References

Boynton, W. R., W. M. Kemp, C. W. Keefe. 1982. A comparative analysis of nutrients and other factors influencing estuarine phytoplankton production. In: V. S. Kennedy (ed). Estuarine Comparisons. p 69-89.

Flemer, D. A. 1970. Primary productivity in the Chesapeake Bay. Chesapeake Science 11:117-129.

Flemer, D. A., MacKiernan, G., W. Nehlsen, and W. K. Tippie. 1983. Chesapeake Bay: A profile of environmental change. USEPA. 200 pp.

Heinle, D. R. 1974. An alternative grazing hypothesis for the Patuxent estuary. Chesapeake Science 15:146-150.

Kemp, W. M., A. Hermann, and W. R. Boynton. 1981. Resource dynamics and ecology of submerged aquatic vegetation in Chesapeake Bay: A modeling approach to demonstrate resource management concepts. Univ. MD Center Environ. Estuar. Stud. Red No. HPEL-81-214, Cambridge, MD.

Kemp, W. M., W. R. Boynton, and A. J. Hermann. 1995. Simulation models of an estuarine macrophyte ecosystem. In: B. Patten, (ed.) Complex Ecology. Prentice Hall.

Kirk, J. T. O. 1983. Light and photosynthesis in aquatic ecosystems. Cambridge Univ. Press. Cambridge, UK. 401 pp.

Kremer, J. and S. W. Nixon. 1978. A Coastal Marine Ecosystem: Simulation and Analysis. Springer-Verlag, New York. 217 pp.

Magnien, R. E, R. Eskin, R. Hoffman, and T. Parham. 1991. Water quality characterization report for the 1991 re-evaluation of the Chesapeake Bay nutrient reduction strategy. 107 pp.

MDE-Maryland Department of the Environment. 1988. Chesapeake Bay Water Quality Monitoring Program Mesozooplankton Component. Versar, Inc.

Monod, J. 1942. Recherches sur la croissance des cultures bacteriennes. Paris: Herman et Cie.

Roman, M. Personal communication. Horn Point Environmental Laboratory, Cambridge, MD.

A Stage-Structured Model of Zooplankton Dynamics in Chesapeake Bay

Christopher J. Madden, W. Michael Kemp, and Flemming Møhlenberg

Horn Point Environmental Laboratory
University of Maryland
Cambridge, MD

Background

A model of zooplankton-phytoplankton interactions was developed to investigate aspects of carbon flow and trophic transfer relationships in Chesapeake Bay. In estuarine systems, the zooplankton play an extremely important role in determining nutrient recycling rates, phytoplankton size, species composition, productivity, and rate of transfer of carbon to higher trophic levels. However, the zooplankton community is highly dynamic and the range of impacts can be highly variable, both seasonally and inter-annually. This zooplankton community dynamics model was developed as part of the Chesapeake Bay Ecosystem Process Model initiative as a means of studying and quantifying the impact of the zooplankton on lower trophic levels, nutrient cycling, and size-frequency distributions of their prey. The important feature of this model is the highly disaggregated zooplankton community, which is monitored by developmental stage. Generally, estuarine simulation models follow the zooplankton using one or two aggregated state variables, which follow juvenile and adult components. Madden *et al.*, Zooplankton Process Model..., this report, describes an aggregated, three-component model of the Chesapeake Bay zooplankton community which includes state variables for *Eurytemora affinis, Acartia tonsa,* and generalized microzooplankton.

This second zooplankton modeling effort was initiated to address specific questions about how zooplankton community development affects upper and lower trophic levels, and to provide guidance for monitoring efforts in Chesapeake Bay. It is expected that this model will also interface with bioenergetic models of Chesapeake Bay fish communities (Figure 1), allowing estimates of food availability and preferability for desirable fish species under a variety of environmental conditions. Ultimately this sort of model linkage could permit the prediction of potential fish production based on primary production rates. The current high-resolution zooplankton model will continue to be developed in parallel with the three-compartment model and both will be used in tandem to address different questions related to research and management.

The Chesapeake Bay zooplankton community is highly diverse in both function and size. Functionally, zooplankton community feeding rates vary depending on abundance and species composition of the zooplankton, water temperature, prey type and abundance. Size of the zooplankton community ranges from sub-mm for nauplia to several mm for adults of some species. The importance of predator-prey size relationships is emphasized in this model, as selective feeding will cause shifts in size and in species composition in prey. Tracking of zooplankton size distribution in the model is also important for zooplankton-fish trophic interactions. Fish gape size relative to prey size is critically important to year-class success (Cushing 1958). The match-mismatch hypothesis of Cushing has been borne out in numerous studies indicating the sensitivity of cohort success to coincidence of gape size and prey complex at

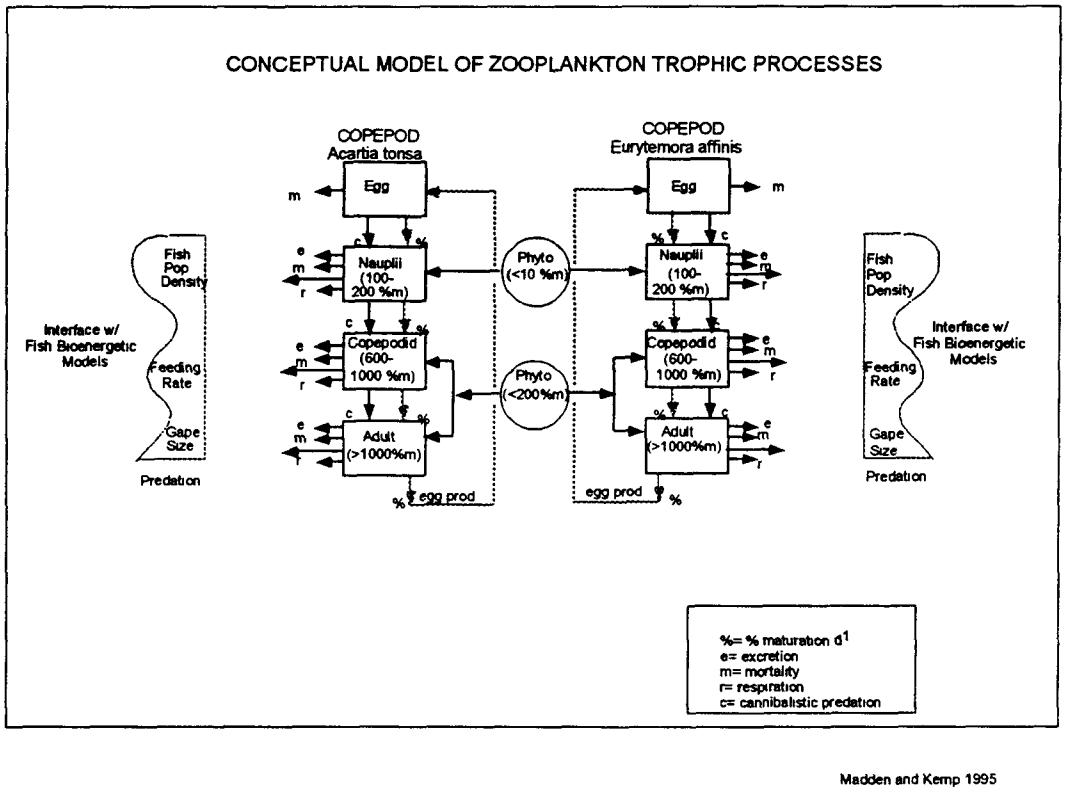

Figure 1

the appropriate point in larval and fingerling development.

The Chesapeake Bay zooplankton database presents an excellent resource for development and calibration of the model. Ongoing monitoring programs provide biweekly or monthly information on species abundances at several sites which will be used for model calibration and validation. At present, the model is uncalibrated. However, it serves an important role as a heuristic tool for testing hypotheses even in its current state.

The Chesapeake Bay ecological model featuring zooplankton trophic dynamics is directed toward answering the following questions:

1) What is the quantitative importance of zooplankton as food for higher trophic levels?
2) What are the critical dimensional considerations in predator-prey relationships in Chesapeake Bay? What size resolution is needed for effective modeling and sampling?
3) What level of model aggregation is needed to achieve reliable model results and calibration?
4) What is the quantitative impact of zooplankton on Chesapeake Bay ecosystem trophic dynamics? On nutrient cycling? On oxygen dynamics?

Several model simulations are planned using zooplankton biomass at different size-frequency distributions to demonstrate the importance of feeding impacts on phytoplankton. Similarly, the species (and size) composition of the phytoplankton will be varied in simulations, while holding total biomass constant. This will allow observation of the impact of size structure on zooplankton productivity.

The resolution of stage-dependent zooplankton development and number of zooplankton life stages required to realistically model total zooplankton biomass/abundance will be investigated using this model. It will explicitly and dynamically quantify relationships between zooplankton and higher trophic levels, such as planktivorous fish and filter feeders. This model uses size-frequency distributions and stage-specific abundances to estimate food availability to planktivorous fish. The size structure of the zooplankton community determined by model calculations will, thus, yield the means to estimate potential fish production based on fish bioenergetic relationships. The high degree of disaggregation of the zooplankton compartment will allow complete analysis of size-regulated transfer efficiencies to piscivorous fish. This aspect of the model represents a first step toward linking the ecosystem process models with fish bioenergetic models and linking nutrient loading to high level living resources.

Model Development

A numerical model was developed using the STELLA II simulation environment on a RISC-based microcomputer. The model consists of a set of 20 difference equations representing state variables for small and larger (>12 micrometer) planktonic algae; ciliates; rotifers; the zooplankter, *Acartia tonsa;* a benthic filter feeder; dissolved inorganic nitrogen (DIN); and sediment particulate organic carbon (POC). Phytoplankton are modeled as two separate state variables, allowing a distinction between functional groups based on differences in nutrient and light response. This strategy allows the model to reflect seasonal succession of spring dominance by diatoms and summer dominance by a mixed flagellate and chlorophyte community. A time-step of 0.25 day, a simulation length of 1-3 yr, and a Runge-Kutta 2 integration scheme are used for model simulations.

The model is spatially averaged, simulating a 1 m^2 unit in the mesohaline littoral region of Patuxent River. Simulations can be run with the water column varying from 1-3 m in depth. The water column in each case is modeled as a single homogeneous layer mixed to the bottom. The shallow depth of the system indicates that benthic filtering of zooplankton could represent a large mortality fraction, and a benthic community is included in the model. Benthic nutrient and carbon compartments are calculated based on a uniform sediment depth of 15 cm. Carbon is tracked in units of mg C m^{-3} and conversion of C to N follows Redfield stoichiometry of 7.2:1 for phytoplankton.

Increases in the phytoplankton compartment include advective import and growth. Growth is modeled as a function of nutrient and light availability. Temperature regulates maximum photosynthetic rate and nutrient uptake is expressed using Monod functions for each nutrient. Light regulates phytoplankton photosynthesis in the model based on P-I (photosynthesis - irradiance) relationships specific for each phytoplankton group. Losses from the phytoplankton community are due to advective export, sinking, natural mortality, and grazing by zooplankton. Additional details of how phytoplankton processes are modeled are discussed in Madden and Kemp, Simulation Model of SAV and Water Quality..., this report.

The zooplankton comprise 13 state variables, representing eggs, six naupliar, and six copepodid developmental stages. Stage-specific feeding and mortality rates are partitioned among each size-class, permitting refined accurate tracking of stage population and size-classes. This allows accurate accounting of size-dependent trophic transfers, as bivalve and fish predation rates can be highly dependent on the size-structure of zooplankton prey. Zooplankton predation on phytoplankton is partially dependent on predator size, and the phytoplankton group that is accessible to the zooplankton predation is determined by the relative size of the zooplankton stage to the phytoplankton equivalent spherical diameter.

Zooplankton growth is a function of recruitment, temperature, food concentration, assimilation efficiency, and diapause egg hatch rate. Recruitment through each of the 12 naupliar and copepodid stages is regulated by temperature and food abundance and converted to biomass using an average mass conversion factor for each stage; conversion factors range from 0.05-4.2 micro-g individual^{-1} as follows:

Egg=0.05	C1=0.33
N1=0.05	C2=0.46
N2=0.05	C3=0.75
N3=0.06	C4=1.8
N4=0.08	C5=2.5
N5=0.12	C6=4.2
N6=0.2	

Egg production is a function of temperature and food available to the female C6 population:

$$Egg=0.5*AC6*5*\ln(AP-40.5)*Tf \quad (1)$$

Egg= #eggs produced m^{-3} d^{-1}; AC6 is the total adult Acartia population; AP is the total prey biomass available to adults (mg m^{-3}); and Tf = an asymptotic sigmoidal temperature function ranging from 0-1 for temperatures ranging from 5-25° C.

Recruitment (maturation of a developmental stage) by zooplankton of each size class to the next higher class occurs based on a stage-specific development rate. This rate is translated to a maturation time period (MT in days) during which the entire cohort occupies the specific class. Each day, a proportion of the cohort moves to the next class based on the reciprocal of the maturation period (*ie.* if MT=5 days, 1/5 of the cohort population advances daily). The rate of development of each zooplankton stage is regulated by different factors, depending on age. For *Acartia* eggs (AE) and first naupliar stage (AN1), development is dependent on temperature only:

$$D1=0.85*(X)*Tf \quad (2)$$

where D1=proportion of cohort (Egg or N1) advancing to next stage (d^{-1}); X=number of individuals in cohort (# m^{-3}); and Tf is the temperature function described above.

For higher stages, development is dependent on temperature and food concentration:

$$D2=XDf \quad (3)$$

where D2=proportion of cohort (N2 through N6) advancing to next stage (d^{-1}); Df is a development function based on temperature and total prey availability, defined as follows:

$$Df=(Tf*0.45*(APn-40)/(APn+100)) \quad (4)$$

where Df = the fraction of cohort maturation (d^{-1}); Tf is defined above and AP=Total prey (mg m^{-3}) available to nauplia, assumed to be the smaller phytoplankton fraction plus ciliates. In the larger zooplankton (C1-C6), APn is replaced by APc, the total prey complex of the zooplankton, which includes APn plus larger phytoplankton forms and rotifers. Thus it is possible (and the norm) to have each developmental stage maturing at different rates in the model. We expect this represents what is actually occurring in nature. The above expression yields a Michaelis-Menton type function for development rate ranging from 0-0.45 d^{-1} with a threshold at 40 mg m^{-3}, half-saturation at 100, and 95% maximum at about 2500. This is the percentage of the cohort state variable (numerical abundance) that passes to the next stage each day. The maximum rate of 0.45 corresponds to a 2.2 day development time for the stage, realizing a 45% recruitment rate for all individuals in the stage per day. Lower prey concentrations result in slower growth, extending recruitment time to infinity. At maximum rates, the entire life cycle is completed in about 24 d from egg to adult.

Zooplankton losses occur from natural mortality, benthic grazing, zooplankton cannibalism, ciliate grazing, respiration, sinking, carbon exudation, and advective export. Losses from each stage combine natural mortality, mortality from filter feeders, and planktivorous fish grazing terms. Because the empirical relationship between food concentration and *Acartia* development rate and recruitment was developed using the number of individuals successfully recruited to the next stage, the formulation yields an extra accumulation of production. Respiration is calculated from these results for purposes of balancing nutrient and carbon flows in other parts of the model, but is not used in calculating carbon loss from the *Acartia* stage, since that is already incorporated in the empirical calculation of cohort recruitment.

Grazing loss (Mzgr) from the zooplankton compartment via planktivorous fish (anchovy) predation relate predator and prey abundance following an Ivlev formulation:

$$Mzgr=Fa*R3*0.11*(1-e^{(-0.01*ACAR)}) \quad (5)$$

where Fa represents predator abundance (g C m^{-3}); R3 is a randomizing term to impart a 25% variability around the anchovy forcing function; and ACAR = total adult zooplankton abundance.

Water column physics are incorporated in the model using relationships of current velocity and wind speed to calculate turbulent energy dissipation rate in a shallow water column. Turbulence in the model has two functions: it modulates predator-prey contact rates via an empirical relationship and it determines the depth of the mixed layer. Turbulent dissipation (TD) is calculated as a quadratic of wind speed, modified by a turbidity index and the air-water thermal gradient as follows:

$$TD=\frac{((0.134*Wind^2-0.000347*Wind+0.00045)}{\text{Depth (m)}} \quad (6)$$

where Wind= wind velocity in m s^{-1}.

An additional term, [$PAR^{-7}*\ln(Kd+1)+ (T_W-T_A)*2E^{-5}$], is subtracted from the above expression to account for the effect of increasing water stability with increasing particulate concentration. Kd is the downwelling attenuation coefficient (measuring turbidity) in m^{-1}; PAR= mean integrated PAR in Ein d^{-1}; T_W-T_A = the gradient between water and air Celsius temperatures. An increase in thermal mass of the upper water column contributes to water column stability. When the model is run using 1-3 m water column depths, the stability term is not relevant because the mixed layer always reaches the bottom, however, future expansion of the model into the deeper tributary channels and mainstem Bay requires this term (in conjunction with a sigma term to account for salinity driven density differences) to adjust the depth of the mixed layer and the degree of contact of the benthic community with the water column.

Results and Discussion

This model is in the process of being calibrated for Chesapeake Bay. Initial pre-calibration runs indicated that carbon flows balanced properly and that the model was stable and within normal ranges for a temperate estuarine system. Forcing functions in the model for preliminary diagnostic execution runs were established using a generalized nitrogen loading cycle similar to that for Chesapeake Bay and initial conditions for state variables based on data from Flemer (1970). The model was run for one, two and three years until stable. Output agreed well with the range expected for temperate estuarine systems.

In standard diagnostic run of the model, a strong pulse of DIN (by forcing function) persisting from January through March months entered the system via runoff from winter precipitation and spring runoff. Water column DIN concentration increased in response to freshwater inputs, peaking in March at 20 μM. Chlorophyll a initially remained at low initial levels, but bloomed in mid-April as light and temperature increased to thresholds required for phytoplankton (particularly diatom) growth; chlorophyll attained values of more than 60 $\mu g\ L^{-1}$ during the spring bloom phase. After the bloom phase, phytoplankton were severely reduced due by top-down control. Analysis of the spring phytoplankton decline indicated that initially, losses in March were due to grazing by pelagic herbivores (*Acartia*, ciliate and rotifer populations), and benthic filter feeders. In early summer, however, DIN often fell below half-saturation concentrations for both spring and summer phytoplankton functional groups. Because the diatoms dominated during spring bloom and smaller phytoplankton were negligible, the adult zooplankton were responsible for all of the pelagic grazing losses through the zooplankton pathway. Juveniles were limited to consuming the smaller phytoplankton fractions and detrital particulate carbon (POC) due to size constraints. Summer phytoplankton group losses were distributed across all zooplankton groups because the smaller average cell size permitted grazing access by all zooplankton (by model parameterization).

During the spring phase of increasing DIN concentration and phytoplankton abundance, a period of rapid growth in the benthic macrofauna compartment occurred, reflected in an increase in bivalve biomass by 50% within a month. After this initial growth period, bivalve biomass steadily declined throughout the summer and fall, despite regularly responding to increases in phytoplankton biomass throughout the summer with short bursts of filtration activity. These short bursts of filtration effectively reducing phytoplankton concentrations and stimulating brief periods of bivalve growth. These episodes occurred periodically, at 5-10 d intervals, as pulses of primary production responded to releases of regenerated nitrogen and intervals of grazing pressure by

bivalves decreased as particle concentrations fell below feeding thresholds. Riverine loading of water and nutrients (via forcing function) was reduced during the summer months and dissolved nutrient concentrations remained low, often limiting phytoplankton growth through November. Under conditions of low summer nitrate input and efficient benthic grazing, model calculations of water column turbidity declined during the growing season, with chlorophyll concentrations ranging to below 10 $\mu g\ L^{-1}$. In preliminary runs without filter feeders, the model showed high levels of phytoplankton productivity, which were ultimately became by nitrogen and biomass in excess of 65 $\mu g\ L^{-1}$, indicating a large degree of top-down control exerted by benthic organisms when present.

An experiment to determine the effect of prey type on zooplankton size distribution was performed by comparing abundances of all stages of the zooplankton (*Acartia* sp.) population under conditions of 50% reduced diatoms, versus 50% reduced chlorophytes. The term "chlorophytes" was used to represent the smaller summer dominant functional group of phytoplankton in the model. Comparison of results of a model run having reduced spring diatom abundance with the reduced chlorophyte run revealed that spring-dominant diatoms seemed less important in determining the ultimate success of the zooplankton community in summer.

Reasons for a stronger reduction in one model population over the other are complex, but a simple explanation may present itself in comparison of output of the juvenile stages in both runs. The initial spring increase in zooplankton abundance was nearly identical in both graphs, indicating that during spring, juvenile zooplankton were probably not limited by food concentrations and may be controlled by grazing, temperature, or initial conditions of adult population and egg abundance. Adult zooplankton seemed slightly reduced in the spring period under the reduced diatom condition. As the summer bloom developed, the two treatments markedly diverged in the adult stages: reduced chlorophytes led to reduced abundance in all zooplankton stages in summer compared with the reduced diatom run. Obviously, because diatoms were concentrated in spring, the forced reduction resulted in lower food availability during spring only; whereas, forced reduction of chlorophytes reduced summer food availability. This was the period when zooplankton were most active and respiratory expenditures were exponentially higher than in spring. This simple model result may indicate an important feature of food availability controlling zooplankton populations via bioenergetics. This represents an area of ongoing study using the model.

Examination of model output of zooplankton abundances by life stage provides insight to rates of zooplankton maturation and development, and may address the above concept of energetics. One important diagnostic of appropriate model functioning is the ability of changes in abundance of younger stages to propagate through the zooplankton stage state variables. Model output indicated that changes in earlier stages were expressed in later stages with appropriate time delays. Moreover, the lags between individual peaks in abundance shorten from spring to summer, then began to lengthen toward fall as temperature and food availability altered the rates of development of each stage. This is simply illustrated with lines drawn which connect cohort peaks in response to population events at various times through the year. The first spring event noted propagated through the population slowly, requiring more than 10 d to reach C-6, while the summer events require 1-3 d at most. These rates reflected total development times (egg to adult) of well over 20 d during the cooler months to less than 10 d in mid-summer. The rates of turnover corresponding to these development times were indicative of the energy required from food to maintain the population and may partially explain the sensitivity of the zooplankton population to food concentration in summer in the experiment described above. Of course, the

population curves were shaped by other forces in addition to development time, such as differential grazing based on size, but the likelihood was that such top-down forces will adjust the size of a peak, but the bottom-up forces control the existence of the peak. The model appeared useful for addressing such questions of trophic control in detail.

Management Implications

Initial results indicated that the highly resolved zooplankton model presented here will be an important complement to the aggregated zooplankton model. Each will allow the investigation of different questions. Eventually, this model should provide a means of linking size-frequency distributions of phytoplankton to feeding efficiencies of zooplankton. The ability to track individual zooplankton stages gives the opportunity to dynamically calculate the size-frequency distribution of the zooplankton community. This will allow the determination of the prey and size classes available to subsequently higher trophic levels such as planktivorous fish.

References

Cushing, D. H. 1958. The effects of grazing in reducing the primary production: A review. Cons. Explor. Mer 144:73-75.

Flemer, D. A. 1970. Primary productivity in the Chesapeake Bay. Chesapeake Science 11:117-129.

Nomenclature

EGG= Acartia Eggs
AN1-AN6= Acartia Nauplia, stages 1 through 6
AC1-AC6= Acartia Copepodids, stages 1 through 6, AC6= Adult Acartia=Total Acartia biomass
AP= Total prey biomass
Tf= Temperature function
Df= Development function
TD= turbulent energy dissipation rate
AEclr= Acartia egg clearance rate by filter feeders
AEmort= Acartia egg natural mortality rate
Xn= Numerical abundance of Stage n
n= Stage number, for N1-C6 n=1-12
Aclr= Acartia mortality clearance rate by Filter feeders
Amort= Acartia natural mortality rate
Astrv= Acartia starvation mortality
Adens= Acartia density dependent mortality
Afg= Acartia grazing mortality by fish
K= Stage specific modification coefficient for reduction of grazing mortality rate due to increased avoidance of Filter feeder clearance
Stage mortality modify= -0.0377*x, where x=

N1	-0.0377
N2	-0.0754
N3	-0.1131
N4	-0.1508
N5	-0.1885
N6	-0.2262
C1	-0.2639
C2	-0.3016
C3	-0.3393
C4	-0.3770
C5	-0.4147
C6	-0.4524

Planktonic-Benthic Interactions in Mesohaline Chesapeake Bay: Model Simulations of Responses to External Perturbations

W. Michael Kemp and Richard D. Bartleson

Horn Point Environmental Laboratory
University of Maryland
Cambridge, MD

Background

Many of the important biological and chemical processes occurring in estuarine ecosystems are controlled by exchanges between planktonic and benthic subsystems (Kemp and Boynton 1990). In most estuaries, autotrophic processes, which tend to be limited to the upper portion of the water column, depend in part on nutrients recycled from benthic metabolism (Kemp and Boynton 1984; Boynton and Kemp 1985). On the other hand, heterotrophic activities, which are concentrated at the sediment surface, depend on the deposition of particulate organic matter (POM) from the overlying water (Hargrave 1973). Quantitatively, nutrient recycling from the benthos is typically sufficient to support more than half of the primary production in the overlying water (Nixon 1981); whereas, growth of benthic animals and metabolism of sediment bacteria in deeper portions of estuaries is largely dependent on inputs of organic matter from plankton above (Parsons *et al.* 1984). The mechanistic interactions that control exchanges of nutrients and POM in estuaries involve a complex assemblage of geochemical, biological and physical processes. These interactions are not readily understood using the information typically generated in field and laboratory experiments.

In recent years, understanding of key processes controlling pelagic-benthic interactions has increased. Dynamic behavior of the benthic subsystem is controlled by numerous factors including inputs of POM from above, sediment redox conditions, as well as macrofaunal grazing and bioturbation (Kemp and Boynton 1990). Rates of deposition of POM are regulated by rates of phytoplankton production and, equally important, by rates of consumption by planktonic bacteria, protozoa and copepods that live in the overlying water (Hargrave 1973). Rates of nutrient recycling are regulated by bacterial decomposition, availability of oxygen, and the activities of benthic macrofauna (Nixon and Pilson 1983). In temperate estuaries such as Chesapeake Bay, seasonal patterns of temperature (and particularly rates of vernal warming) play a major role in determining the proportion of the algal production consumed in the water versus deposited to the sediments. Seasonal temperature patterns also control rates at which POM deposited in winter-spring is metabolized in spring-summer (Westrich and Berner 1984).

Chesapeake Bay is a partially mixed estuary with seasonally varying stratification and reduced exchange between surface and bottom waters. Nutrient loading to the estuary, from the atmosphere and watershed, results in elevated production and consumption of organic matter, which can lead to summertime depletion of oxygen from bottom waters (Officer *et al.* 1984). Nutrient enrichment can also affect the exchange of POM and nutrients between planktonic and benthic subsystems. Increased phytoplankton production associated with higher nutrient loading tends to decrease the proportion of that production deposited to the benthos (Oviatt *et al.* 1986). This may be because, with higher production rates, planktonic consumers become more effective at removing

phytoplankton before they sink to the bottom (Hargrave 1973). Under eutrophic conditions, the structure of the planktonic trophic web may change markedly (Landry 1977), possibly leading to shifts in the timing, quantity and quality of POM deposition (Smetacek 1984).

Eutrophication and associated bottom water hypoxia can lead to dramatic shifts in redox conditions and in microbial metabolism (Kemp *et al.* 1992), as well as seasonal mortality of benthic animals (Holland *et al.* 1977) and associated bioturbation of sediments. These hypoxic conditions also inhibit the coupled benthic process of nitrification-denitrification, which provides a natural mechanism for gaseous removal of excess nitrogen from the estuary (Kemp *et al.* 1990). With the reduction of denitrification under eutrophic/hypoxic conditions, nitrogen is rapidly recycled back to the overlying water where it can support more phytoplankton growth. Given the diversity of interacting processes, it is challenging to predict how changes in nutrient loading to estuarine ecosystems affect the nature of exchanges between water column and sediment subsystems.

Numerical simulation models have successfully dealt with the complexity of interactions characterizing coastal marine ecosystems (*e.g.*, Kremer and Nixon 1978). These models often combine populations of estuarine organisms into aggregated variables, as well as emphasize mechanistic detail concerning factors controlling ecosystem processes. Such models have been used to examine various aspects of aquatic ecology, including: planktonic trophic interactions (Pace *et al.* 1984); planktonic nutrient cycling controls on production (Scavia 1979); dynamics of organic carbon and dissolved oxygen (Summers 1985); factors regulating POM deposition from planktonic systems (Andersen and Nival 1988); sediment nitrogen cycling (Billen and Lancelot 1988); and benthic suspension-feeding effects on phytoplanktonic biomass (Gerritsen *et al.* 1994). None of these models focused on pelagic-benthic coupling by combining processes associated with simultaneous flows of organic carbon, inorganic nutrients and dissolved oxygen.

An ecosystem simulation model was used to examine the role of planktonic-benthic interactions and system responses to bottom-up and top-down external perturbations in the mesohaline region of Chesapeake Bay. The primary objectives were to investigate the system responses to changes in: 1) POM deposition; 2) bottom-water oxygen concentrations; and 3) bottom-up and top-down external perturbation.

Model Development

Overall Model Structure

The model was developed using finite difference equations which describe the temporal rates of change of the system state variables. The simulations were conducted on an Apple Macintosh computer using the STELLA simulation software (High Performance Systems, Inc.). Simulation time for an annual cycle was approximately 7 minutes when integrations were performed by Euler rectangular approximation using a time-step of 3 hours.

This model simulated ecological processes for an average square meter area of the mesohaline Bay. This square meter was separated into three layers in the vertical dimension: upper photic layer of the water column; lower aphotic layer of water; and sediments. The total volume modeled was 12.19×10^9 m^3. Average depth of the upper layer was 10 m in deep water and 4.4 m where depth was less than 10 m. The lower layer depth averaged 6.08 m. The surface area was 527×10^6 m^2. Mass movement of materials into and out of the system, and through the pycnocline, was determined by mass balance calculations and adjacent upstream and downstream salt concentrations.

The planktonic-benthic interactions model included 40 state variables detailing planktonic and benthic processes in the mesohaline portion of the Chesapeake Bay. The water column was divided by the pycnocline into two sections. The ecosystem was defined in terms of its state variables, external forcing functions and interactions among variables. The equations used to define this model employed well-established relationships from the scientific literature. For example, ammonium effects on nitrification were described using a hyperbolic Michaelis-Menten expression (Henriksen and Kemp 1988). The use of such widely accepted relationships in structuring the model insured a high degree of generality, making the model applicable for a broad range of conditions and Bay regions.

Pelagic state variables were represented in both upper and lower layers. Phytoplankton (PP) were divided into two groups, large diatoms (DIA) and other algae dominated by nannoplankton (OP); these two groups had distinctly different seasonalities and physiological characteristics. Phytoplankton assimilated dissolved inorganic nitrogen (DIN) and were grazed by copepods (ZP) and protozooplankton (MP). Protozooplankton fed mostly on smaller phytoplankton (OP) (Heinbokel 1978) but also grazed diatoms, bacteria (Sherr and Sherr 1987) and suspended particulate organic carbon (POC). Copepods also consumed protozoa and POC. Bacterioplankton (BP) assimilated both dissolved organic matter (DOM) generated from phytoplankton exudation, as well as ZP and MP excretion and sloppy feeding. BP also assimilated DIN in varying stoichiometries, depending on the DOM sources. Ctenophores and fish fed on copepods and phytoplankton. Respiration in the water column consumed oxygen.

The benthic subsystem was averaged over the upper 10 cm of sediments, where most of the biological activity was concentrated. Particulate organic matter (POM) was separated into labile (LPOM) and refractory (RPOM) fractions, based on the ability of the organic matter to be decomposed (Billen *et al.* 1988). POM was deposited to the sediments from the overlying water in proportion to the POC and phytoplankton pools. The POM was consumed by deposit-feeding macrofauna and by both aerobic and anaerobic bacterial respirations. Rate coefficients for biological utilization of labile and refractory fractions were based on geochemical experiments (*e.g.* Westrich and Berner 1984). Suspension-feeding macrobenthos fed on POC in the bottom layer of the water column and in the portion of the surface layer that was in direct contact with the benthos. Both macrofaunal groups excreted feces to POM and nitrogenous wastes to dissolved inorganic nitrogen (DIN), as well as consumed oxygen in respiration. These metabolic processes were described by hyperbolic functions of food consumption and biomass. Iron and iron sulfide complexes were included because they played a role in sediment oxygen flux. Benthic algae played a role in oxygen production and nutrient uptake at the surface of shallow euphotic sediments.

Forcing functions included photosyntheticly active radiation (PAR) (Pers. comm., Tom Fisher, Horn Point Environmental Lab, University of Maryland), particulate carbon, Si concentrations, water temperature and salinity. For the most part, these data were generated from 1986-1989, for the same region of the mainstem Bay (between the mouths of the Choptank and Patuxent Estuaries). Studies were supported by the Maryland Department of the Environment (MDE) Bay Monitoring Program, National Oceanic and Atmospheric Administration (NOAA)/Sea Grant, National Science Foundation, and the Environmental Protection Agency (EPA)/MDE Sediment Data Collection Program.

Process Description

Phytoplankton carbon fixation was modeled as a function of temperature, light, and nutrients. The effect of temperature was assumed to be exponential with a Q_{10} of 1.7 for diatoms and 2 for PO.

This formulation was used by Kremer and Nixon (1978) and supported by several published values (Fasham *et al.* 1983, Bannister 1974). Enzyme inhibition occurs at high temperatures among single species, but the assumption was made that it didn't occur among the whole assemblage of phytoplankton at normal summer temperatures. Because phytoplankton size varied inversely with temperature (Malone *et al.* 1991), an allometric formulation was used for this relationship. The phytoplankton community is capable of adapting to the seasonal change in temperature and growth may be independent of temperature (Sheridan and Ulik 1976, Davison 1987). Maximum growth rates and temperature coefficients for PD and for PO are calibrated within the range of reported values (Talling 1957, Eppley 1972, Ojala 1993, etc.). Production of picoplankton (< 1-3 μM) is low (1 μg C μg Chl^{-1} h^{-1}) below 20° C but exceeds 10 μg C μg Chl^{-1} h^{-1} at higher temperatures (Malone *et al.* 1990).

The effect of light on maximum photosynthesis was calculated by using a formulation for depth-integrated photosynthesis modified for the effect of self-shading. This expression did not incorporate photoinhibition, which was assumed to be unimportant in the relatively turbid waters of the mid-bay. An attenuation coefficient for self-shading of 0.002 per mg phytoplankton C was used (Steemann-Nielsen 1962). Light availability at the base of the pycnocline was assumed to be negligible and if mixing rate was small, production also would be negligible.

The effect of dissolved nitrogen (DIN) on photosynthesis was modeled as a hyperbolic function with a half-saturation coefficient (K_s) of 10 mg m^{-3} for PO (Goldman and Glibert 1983 obtained a K_s value of 7 μg l^{-1}) and 30 mg m^{-3} for PD (Scavia 1980). Diatom growth additionally was controlled by silica concentrations (forcing function) with a K_s of 0.2 μM (Conley and Malone 1992). Inputs of phytoplankton were determined by assuming a ratio of 70 mg C mg Chl^{-1} (Malone 1982).

Phytoplankton losses occurred due to respiration; grazing by fish, copepods and protozoa (Capriulo and Carpenter 1983, Burkhill *et al.* 1987, Gallegos 1989); sinking; exudation; natural mortality; and downstream export. Respiration was modeled as a function of temperature (Scavia *et al.* 1976), biomass and production. Reported specific respiration rates range from 0.02 to 1.2 d^{-1} (Geider 1992), or about 10% of maximum photosyntetic rate (Parsons *et al.* 1984). Respiration rates for flagellated species may be quite high, relative to the diatoms due to their active nature (Geider and Osborne 1989). Grazers of phytoplankton included copepods, protozoa, and menhaden. Copepods preferentially graze diatoms and, although protozoans preferred other algal taxons (Burkhill *et al.* 1987), they still ingested significant amounts of diatoms. The model assumed that copepods preferred diatoms 5 to 1 over PO. Copepod grazing loss included a percentage due to inefficient feeding. Menhaden biomass was a forcing function that peaked at 50 mg C m^{-3} in November 1989 (Brandt 1990) and consumed from 5 to 40% of their weight per day, depending on temperature.

To establish initial values for model variables and equation coefficients, data were compiled from published and unpublished reports on research in the mid-Bay. For the most part, these data were generated from 1986-1989, for the mainstem Bay between the mouths of the Choptank and Patuxent Estuaries, in the same studies cited above for the forcing functions.

Results and Discussion

Seasonality of POM deposition and bottom O_2 balance

Phytoplankton dominated the sinking particulate matter in spring; whereas, detrital matter dominated in summer through fall (Figure 1). This was partly due to the fact that the spring diatoms were large and sank faster, and partly due to the deficiency of grazing in the spring. Two scenarios examined the effect of timing of POM deposition: (1) a 50% increase in inputs of POM from upstream in winter-spring; and (2) the same increase in summer-fall. If sedimentation rate was increased, production decreased, so the effect seen wasn't exclusively the result of POM deposition change. With increased POM total sedimentation decreased, so the increased winter sedimentation rate resulted in lower sedimentation; this resulted in slightly less ammonium flux and higher lower-layer dissolved oxygen concentrations. The nitrification-denitrification equation is parameterized to fit some seasonal data, but effects of oxygen on this process are not well described. Thus, related simulations may not be realistic.

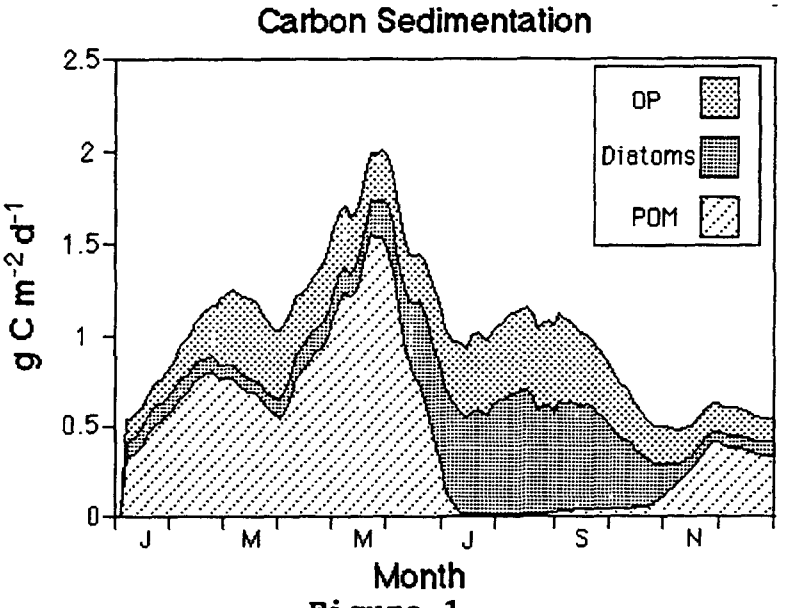

Figure 1

The seasonal O_2 balance showed that inputs from mixing become important in the summer when upstream concentrations were reduced (Figure 2). Pelagic respiration dominated the losses in the summer.

Nutrient input/output balance

The seasonal nitrogen-balance from model output (Figure 3) showed that most of the nitrogen came from river flo in the spring and from regeneration in the summer, with most of the regeneration occurring in the water column. As nutrient inflow increased, outflow increased to a lesser extent. During the summer, the effect of increased nutrients wasn't seen in the outflow, due to the high demand.

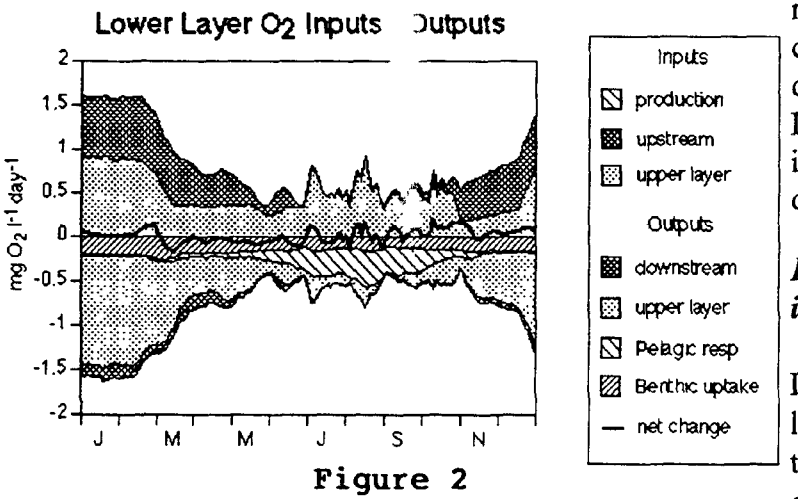

Figure 2

Responses to variations in nutrient inputs

Increasing landward or seaward DIN inputs by 100 mg m^{-3} d^{-1} removed N limitation. Production was controlled by temperature, dissolved silica concentrations and light availability.

Regardless of the source of additional DIN, phytoplankton biomass, sedimentation and lower-layer dissolved oxygen all changed by the same amount. A difference may have been detectable at a lower addition rate.

Effect of benthic bioturbation

The physical activities of benthic deposit feeders influence the oxygen concentration in the sediments in proportion to their feeding rate. When we increased the effect of bioturbation on sediment oxygen the nitrification-denitrification rate increased. Previous experimental and modeling studies have reported similar effects of animal burrowing on nitrification (Henriksen and Kemp 1988). NH_4+ and sulfide fluxes were not affected by bioturbation.

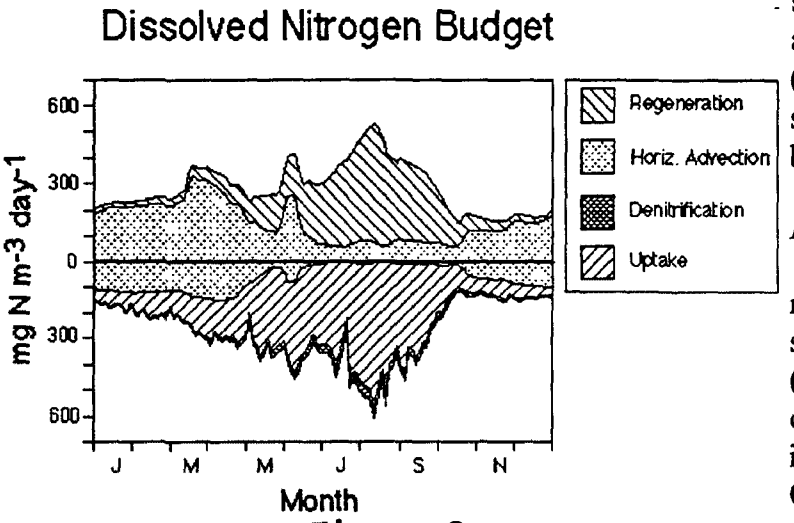

Figure 3

Effects of fish grazing

Increased menhaden ingestion reduced summer phytoplankton slightly in summer and substantially during October (Figure 4, left panels). Dissolved nitrogen concentration in the upper layer was increased slightly in early summer and October. Sedimentation changed only slightly before October, when it decreased with phytoplankton biomass. Increased anchovy feeding rates resulted in reduced copepod populations and increased spring phytoplankton biomass and sedimentation. However, increased anchovy feeding had little effect on model behavior the rest of the year. If fish were hypothesized to control copepod biomass and predation is decreased, there was a decrease in spring phytoplankton and sedimentation, but an increase in fall phytoplankton and sedimentation. Although grazing increased, the increased nutrient release stimulated production.

Effect of benthic suspension feeders

If oxygen concentrations remained above 2 mg l^{-1} the standing stock of benthic suspension-feeders (oysters, clams, tunicates and polychaetes) could be much higher than the levels in the base run. The increased activities of suspension-feeding would result in increased benthic metabolism and would impact the dissolved oxygen concentration. We ran two scenarios to examine this impact. In one scenario, biomass and ingestion rates of both shallow and deep suspension feeders were increased. In the second, just the shallow suspension feeder biomass and ingestion rate were increased. Both scenarios reduced phytoplankton biomass and sedimentation (Figure 4, right panels). When both suspension-feeder groups were increased, the summer lower-layer oxygen concentrations were basically the same as the base run. Thus, although sedimentation decreased, total input to the deep sediments was not significantly changed because the suspension-feeders contributed feces to the sediments. Lower layer oxygen increased slightly in the second scenario since inputs to the deep sediments were increased.

Conclusions and Future Directions

There are many interactions to consider when modeling a complex natural system, such as Chesapeake Bay. By keeping track of carbon and providing some feedback effects, the results of this model were more useful than "back of the envelope" computations. In the future, flows will be determined by hydrodynamic models and the spatial resolution will be increased.

The model shows that various processes can affect sedimentation of organic carbon and dissolved oxygen in the deeper waters of the Bay. Increasing nitrogen did not substantially increase hypoxia, even though sedimentation increased 30%. This may be due to reduced sediment respiration rate at low oxygen concentrations, or the lack of feedback from the southern portion of the Bay. Decreased nitrogen inflows also resulted in only a small increase in lower layer dissolved oxygen. A larger change occurred if particulates were also reduced.

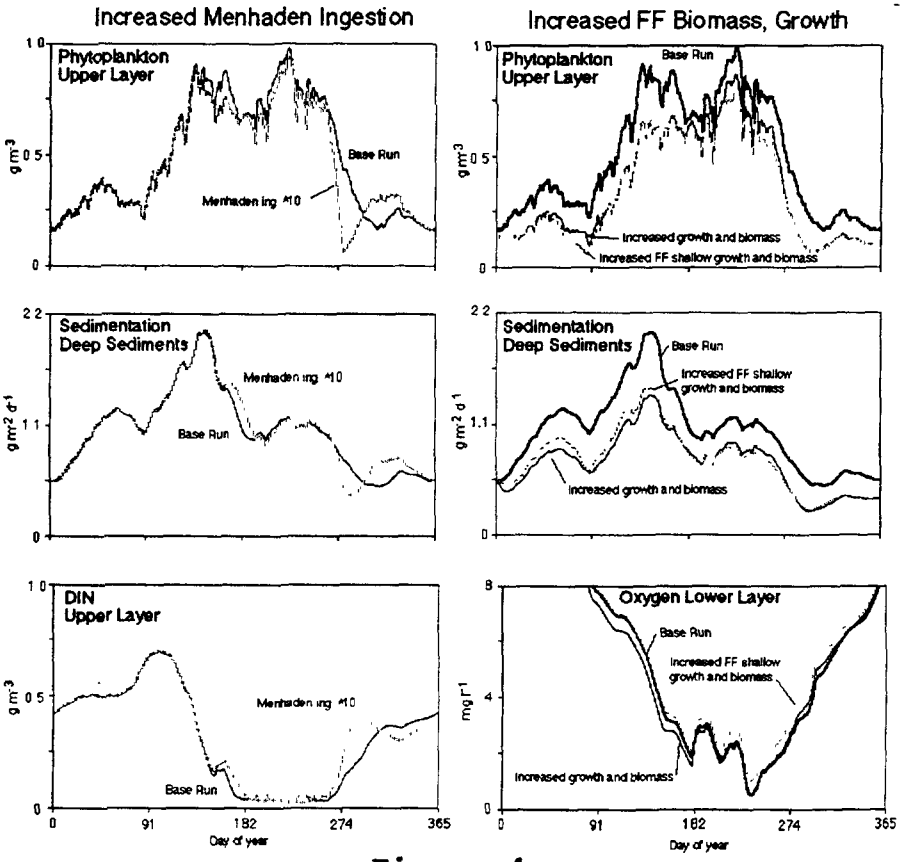

Figure 4

Fish, whether feeding on benthos, copepods or plankton, had little effect on production or sedimentation; whereas, benthic suspension feeders potentially had a significant effect. Because beds of submerged aquatic vegetation (SAV) can also remove particulate material from the water column, it is possible that increased SAV biomass will have a similar influence. Freshwater inflow can affect both POM deposition and mixing rates, which have a significant impact on lower-layer dissolved oxygen concentrations.

References

Andersen, V., and P. Nival. 1988. A pelagic ecosystem model simulating production and sedimentation of biogenic particles: Role of salps and copepods. Mar. Ecol. Prog. Ser. 44: 37-50.

Bannister, T. T. 1974a. Production equations in terms of chlorophyll concentration, quantum yield, and upper limit to production. Limnol. Oceanogr. 19: 1-12.

Billen, G., S. Dessery, C. Lancelot, and M. Maybeck. 1989. Seasonal and interannual variations of nitrogen diagenesis in the sediments of a recently impounded basin. Biogeochem. 8: 73-100.

Boynton, W. R. and W.M. Kemp. 1985. Nutrient regeneration and oxygen consumption by sediments along an estuarine salinity gradient. Mar. Ecol. Progr. Ser. 23: 45-55

Brandt, S.B. 1990. Acoustic quantification of fish abundance in the Chesapeake Bay: applications to power plant siting and evaluation. Progress Report to: Maryland Department of Natural Resources, Power Plant Research Program, Tawes State Office Building, B-3, Annapolis, Maryland 21401 {UMCEES} CBL 90-047

Burkill, P. H., R.F. Mantoura, C. Llewellyn, and C.A. Owens. 1987. Microzooplankton grazing and selectivity of phytoplankton in coastal waters. Mar. Biol. 93: 581-590

Capriulo, G. M., and E.J. Carpenter. 1983. Abundance, species composition and feeding impact of tintinnid microzooplankton in central Long Island Sound. Mar. Ecol. Prog. Ser. 10: 277-288

Davison, I. R. 1987. Adaptation of photosynthesis in *Laminaria saccharina* (Phaeophyta) to changes in growth temperature. J. Phycol. 23: 273-283.

Eppley, R. W. 1972. Temperature and phytoplankton growth in the sea. Fishery Bull. 1063-1085.

Fasham, M. J. R., P. M. Holligan, and P. R. Pugh. 1983. The spatial and temporal development of the spring phytoplankton bloom in the Celtic Sea, April 1979. Prog. Oceanogr. 12: 87-145.

Gallegos, C. L. 1989. Microzoplankton grazing on phytoplankton in the Rhode River, Maryland: nonlinear feeding kinetics. Mar. Ecol. Prog. Ser. 57: 23-33

Geider, R. J. 1992. Respiration: Taxation without representation. In: Falkowski, P. G. and Woodhead, A. D. (eds.) Primary productivity and biogeochemical cycles in the sea. Plenum Press, New York, p. 333-360

Geider, R. J., and B.A. Osborne. 1989. Respiration and microalgal growth: A review of the quantitative relationship between dark respiration and growth. New Phytol. 112: 327-340

Gerritsen, J., A. F. Holland, and D. E. Irvine. 1994. Suspension-feeding bivalves and the fate of primary production: An estuarine model applied to Chesapeake Bay. Estuaries 17: 403-416.

Goldman, J. C., and P.M. Glibert. 1983. Kinetics of inorganic uptake by phytoplankton. In: Carpenter, E. J. Capone, D. G. (eds.) Nitrogen in the marine environment. Academic Press, New York, p.

Hargrave, B. T. 1973. Coupling carbon flow through some pelagic and benthic communities. J. Fish. Res. Board Can. 30: 1317-1326

Heinbokel, J. F. 1978. Studies on the functional role of tintinnids in the Southern California Bight. I. Grazing and growth rates in laboratory cultures. Mar. Biol. 47: 177-189.

Henriksen, K., and W. M. Kemp. 1988. Nitrification in estuarine and coastal marine sediments: Methods, patterns and regulating factors. *In* T. H. Blackburn and J. Sørensen [eds.], Nitrogen cycling in coastal marine environments. John Wiley

Holland, A. F., N.K. Mountford, and J.A. Mihursky. 1977. Temporal variations in upper bay mesohaline benthic communities: I. The 9-m mud habitat. Chesapeake Sci. 18: 370-378

Kemp, W. M., and W.R. Boynton, W. R. 1984. Spatial and temporal coupling of nutrient inputs to primary production: The role of particulate transport and decomposition. Bull. Mar. Sci. 35: 522-535

Kemp, W. M., and W.R. Boynton. 1990. Benthic-pelagic interactions: Coupling of nutrient input and recycling processes to plankton production and oxygen depletion. In: Leffler, M. Smith, D. (eds.) Dissolved oxygen dynamics in Chesapeake Bay. Maryland Sea Grant College Publ., College Park, MD, p. 1-40

Kemp, W.M., P.A. Sampou, J.C. Caffrey, M. Mayer, K. Henriksen, and W.R. Boynton. 1990. Ammonium recycling versus denitrification in Chesapeake Bay sediments. Limnol. Oceanogr. 35: 1545-1563

Kemp, W.M., P.A. Sampou, J. Garber, J. Tuttle, and W.R. Boynton. 1992. Seasonal depletion of oxygen from bottom waters of Chesapeake Bay: roles of benthic and planktonic respiration and physical exchange proce es. Mar. Ecol. Prog. Ser. 85: 137-152

Kremer, J. N., and S.W. Ni n. 1978. A coastal marine ecosystem simulation and analysis. 1 ed. Ecological Studies. Sprin er-Verlag, New York

Landry, M.R. 1977. A revie of important concepts in the trophic organization of pelagic ecosystems. Helgolander wiss. Meeres. 10: 8-17

Malone, T.C. 1982. Phytoplankton photosynthesis and carbon-specific growth: light-saturated rates in a nutrient-rich environment. Limnol. Oceanogr. 27: 226-235

Malone, T.C., and H.W. Ducklow. 1990. Microbial biomass in the coastal plume of Chesapeake Bay: Phytoplankton-bacterioplankton relationships. Limnol. Oceanogr. 35: 296-312

Malone, T. C., H.W. Ducklow, E.R. Peele, and S.E. Pike. 1991. Picoplankton carbon flux in Chesapeake Bay. Mar. Ecol. Prog. Ser. 78: 11-22

Nixon, S.W. 1981. Remineralization and nutrient cycling in coastal marine ecosystems. In: Estuaries and nutrients. B. J. Nielson. and. L. E. Cronin (eds.) Humana, p. 111-138

Nixon, S.W., and M.E.Q. Pilson. 1983. Nitrogen in estuarine and coastal marine ecosystems. In: Carpenter, E. J. Capone, D. G. (eds.) Nitrogen in the marine environment. Academic Press, New York, p. 565-649

Odum, H. T. 1971. Environment, power and society, John Wiley Publ.

Officer, C.B., R.B. Biggs, J.L. Taft, L.E. Cronin, M.A. Tyler, and W.R. Boynton. 1984. Chesapeake Bay Anoxia: Origin, development and significance. Science 223: 22-27

Ojala, A. 1993. Effects of temperature and irradiance on the growth of two freshwater photosynthetic cryptophytes. J. Phycol. 29: 278-284.

Oviatt, C.A., A.A. Keller, P.A. Sampou, L.L. Beatty. 1986. Patterns of productivity during eutrophication: A mesocosm experiment. Mar. Ecol. Progr. Ser. 28: 69-80

Pace, M. L., J.E. Glasser, L.R. Pomeroy. 1984. A simulation analysis of continental shelf food webs. Mar. Biol. 82: 47-63

Parsons, T.R., M. Takahashi, and B. Hargrave. 1984. Biological Oceanographic Processes. Third Edition ed. Pergamon Press, New York

Scavia, D., B. J. Eadie, and A. Robertson. 1976. An ecological model for the Great Lakes. *In* W. R. Ott [eds.]. Environmental modeling and simulation. EPA 600/9-76-016 (U. S. Environmental Protection Agency).

Scavia, D. 1979. Examination of phosphorus cycling and control of phytoplankton dynamics in Lake Ontario with an ecological model. J. Fish. Res. Board Can. 36: 1336-1346

Scavia, D. 1980. An ecological model of lake Ontario. Ecol. Modelling 8: 49-78

Sheridan, R.P., and T. Ulik. 1976. Adaptive photosynthesis responses to temperature extremes by the thermophilic cyanophyte *Synechococcus lividus*. J. Phycol. 12: 255-261

Sherr, E. B., and B. F. Sherr. 1987. High rates of consumption of bacteria by pelagic ciliates. Nature 325: 710-711

Smetacek, V. 1984. The supply of food to the benthos. In: Fasham, M. J. (eds.) Flows of energy and materials in marine ecosystems. Theory and practice. Plenum Press, New York, p. 517-547

Steemann-Nielsen, E. 1962. On the maximum quantity of plankton chlorophyll per surface unit of a lake or the sea. Int. Rev. ges. Hydrobiol. 47: 333-338

Summers, J. K. 1985. A simulation model of carbon and oxygen dynamics in a reservoir. Ecol. Model. 28: 279-309

Talling, J. F. 1957. Photosynthetic characteristics of some freshwater plankton diatoms in relation to underwater radiation. New Phytol. 56: 29-50

Westrich, J.T., and R.A. Berner. 1984. The role of sedimentary organic matter in bacterial sulfate reduction: The *G* model tested. Limnol. Oceanogr. 29: 236-249

Fish Bioenergetics: Relating Nutrient Loading to Production of Selected Fish Populations

Jiangang Luo, Stephen B. Brandt, Kyle J. Hartman,
Melinda A. Gerken, and Michael T. Weimer

Great Lakes Center, Buffalo State College
State University of New York
Buffalo, NY

Background

Fish production depends on two factors: (1) changes in the number of individuals in the population over time, which are caused by mortality, migration, and recruitment; and (2) growth rates of individuals within the population. The growth rate of an individual fish is a highly pliant, species- and size-specific response to habitat conditions and food availability. Because fish growth is influenced by both natural variability and anthropogenic causes of ecosystem change, it has been used as an indicator of aquatic ecosystem health. The ability of a fish to achieve its maximum growth potential is a relative measure of fish well-being and its ultimate survival. Growth rate is also closely linked to reproductive potential, because larger females often produce more and larger eggs, which can enhance larval survival (Zastrow *et al.* 1991; Monteleone and Houde 1990).

Fish growth rates are very sensitive to water temperature and food supply (Bartell *et al.* 1986). Thus, bioenergetics models are useful for evaluating the effects of changes in temperature and prey abundances on growth, consumption, and ultimately, trophic interactions (Brandt and Hartman 1993). Bioenergetics models are simply energy budgets that can be used to estimate how much food was consumed, based on observed growth rates, thermal history, and diets of fish. They simulate growth rates for fish "grown" under different conditions of diet, prey availability, or water temperature. Bioenergetics models were used to evaluate the growth rate potential of a fish under given environmental conditions.

In the years ahead, Chesapeake Bay Program managers will require an integrated ecological framework that can guide decisions and priorities. Information from modeling and analysis of ecosystem processes enables managers to direct efforts toward an ecosystem-based management program. Management scenarios produced from the ecosystem models will be applied over the next two years to answer specific scientific and resource management questions. Questions concerning physical habitat alterations, living resource exploitation, and nutrient input reduction will be addressed. For example, such models could be used to consider how implementation of the Baywide 40% nutrient reduction strategy will change the production of recreationally important fishes in Chesapeake Bay (Kemp *et al.* 1992). The fish bioenergetics models provide detailed analyses of how environmental conditions (*e.g.*, temperature, food, dissolved oxygen) affect fish production and consumption. Bioenergetics modeling techniques were recently applied to fish species inhabiting estuaries such as the

Hudson River and Chesapeake Bay (Brandt and Kirsch 1993; Luo and Brandt 1993; Hartman and Brandt 1993).

A key aspect of the ecosystem modeling program is effective integration of the modeling approaches. The ecosystem process models use nutrient loading and other inputs to predict the quality and quantity of food and habitat available to fish populations. The fish bioenergetics models use these outputs as inputs to predict the potential production of striped bass, bluefish, weakfish, bay anchovy, menhaden, spot, and white perch. The models will be combined to directly incorporate ecological feedbacks associated with top-down control of fish predators on their prey and on other components of the ecosystem, such as SAV and water quality. The simultaneous evolution of the two types of mechanistic models (fish bioenergetics models and ecosystem process models) for Chesapeake Bay provides an unprecedented opportunity to merge and link the two essentially different modeling frameworks into a unified management tool which encompasses ecosystem processes from nutrients and habitat quality to the highest level living resources.

Atlantic menhaden

Model Development

The Atlantic menhaden (*Brevoortia tyrannus*) is an abundant and commercially important fish in the Chesapeake Bay estuary and nearshore habitats of the eastern United States (U.S. Nat. Mar. Fish. Serv. 1978). Menhaden account for nearly half the total east coast fishery harvest (Peters and Schaaf 1991). The menhaden is also consumed by many commercially and recreationally important species such as bluefish, striped bass, and weakfish (Hartman and Brandt 1995a). On the other hand, the menhaden consume mostly phytoplankton; it converts primary production (phytoplankton and plant detritus) directly into fish production (growth and reproduction) (Peter and Schaaf 1991, Rippetoe 1993). The Chesapeake Bay is the major nursery ground of Atlantic menhaden. Menhaden spawn in coastal ocean water during later fall and winter. The larvae enter Chesapeake Bay in winter and spring and use Chesapeake Bay as an important nursery ground in summer and fall.

The main objective of this study was to link an Atlantic menhaden bioenergetics model with the 3-D Water Quality Model in Chesapeake Bay. The model can be used to evaluate growth rate potential of young-of-year (YOY) Atlantic menhaden in the Bay, to quantify the habitat quality of YOY Atlantic menhaden in the Bay, and to estimate the carrying capacity of YOY Atlantic menhaden in the Bay.

Menhaden Foraging Model

Menhaden of 50 mm or larger are mostly filter feeders on phytoplankton (Rippetoe 1993). The consumption rate of a filter feeding organism can be estimated as:

$$con = (phy * vol) * eff \quad (1)$$

$$vol = gap * u \quad (2)$$

where, con = the consumption rate (g/s); phy = the phytoplankton density (g/m^3); vol = the filtration rate (m^3/s); eff = the phytoplankton retention efficiency; gap = mouth open area (m^2); and u = swimming speed (m/s).

The swimming speed of menhaden was modeled as function of body length and water temperature (Figure 1). The filtration retention efficiency (Figure 2) was modeled as function of body length. Atlantic menhaden of different sizes were sampled in Chesapeake Bay and brought back to the laboratory. The height, the width of the mouth and the total length of menhaden were measured with a caliber to nearest 0.1 mm. The shape of the mouth was a close approximate of an ellipse. Therefore, the height and width was used to estimate the mouth open area as an ellipse, then we modeled the mouth open area as an exponential function of total body length (Figure 3).

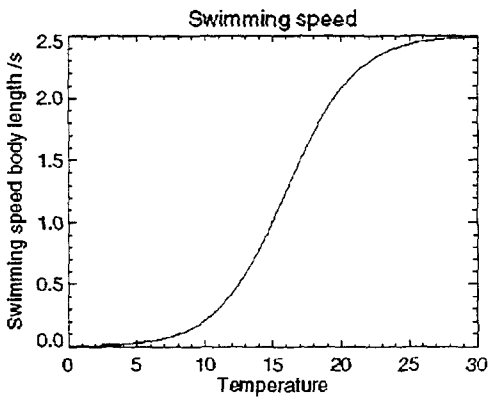

Figure 1

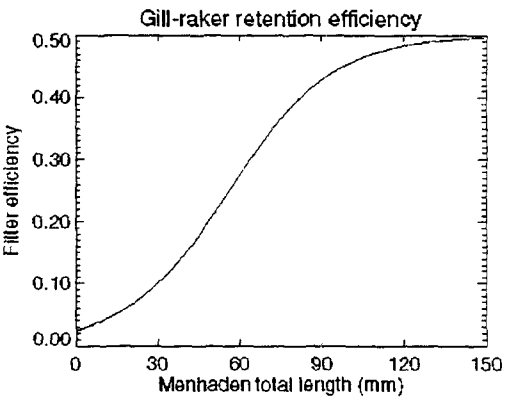

Figure 2

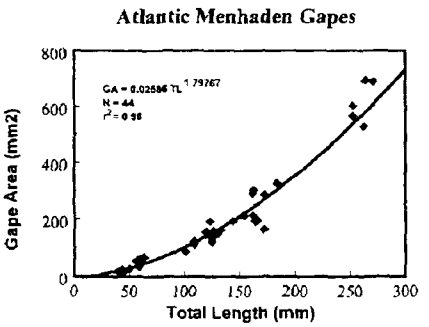

Figure 3

Bioenergetics Model

The bioenergetics model for Atlantic menhaden was developed with parameters derived by Rippetoe (1993). In the model, the YOY menhaden were started on Julian day 152 (June 1) at 50 mm total length. The growth rate was modeled as function of temperature, its physiological constraint, and phytoplankton biomass density. Temperature and fish physiology determined the maximum potential consumption of phytoplankton by menhaden, but phytoplankton density determined the amount of food that a menhaden could retain by filtering the water through its gill rakers. The maximum

consumption for a 1 g menhaden at the optimal temperature for consumption was 1.294 g/g/d. The exponent for the weight dependence of the consumption was -0.312. The temperature-dependence of consumption was defined by the Thornton-Lessem algorithm (Thornton and Lessem, 1978), which included two sigmoid curves: one fit the increasing portion of the water temperature dependence curve; the other fit the decreasing portion. The optimal temperature for maximum consumption was about 28 °C and the maximum limit of temperature for consumption was about 33 °C. Respiration rate was modeled as an allometric function of body weight, water temperature, fish activity level, and specific dynamic action. The rate for standard respiration of a 1g menhaden at the optimal respiration temperature was 0.003301 g O_2 /g/d. The exponent for the weight dependence of respiration was -0.2246. The temperature-dependence of respiration was defined by a non-linear function in Kitchell *et al.* (1977). The slope for temperature dependence of respiration was 2.07. The optimum temperature for respiration was 33 °C and the maximum limit of temperature for respiration was 36 °C. The activity multiplier was modeled as a function water temperature. Specific dynamic action coefficient, defined as the metabolic cost of digestion, absorption and deposition of consumed energy, was equal to 10% of assimilated energy. Egestion was modeled as a constant 20% of consumed food, and excretion was modeled as a constant 10% of assimilated food.

Spatially Explicit Model of Growth Rate Potential

Traditional models of population production are normally based on average conditions over large areas and assume homogeneity and constancy of the environment. As fragmentation and decrease of natural habitat occurred, scientists and managers realized that traditional modeling techniques were no longer reliable tools to assess and manage any complex ecosystem. Recent work suggested that spatial patchiness of density-dependent and density-independent processes could significantly affect population processes, including predator-prey interactions, trophic efficiency, and system-level production (Kareiva and Anderson 1988; Possingham and Roughgarden 1990).

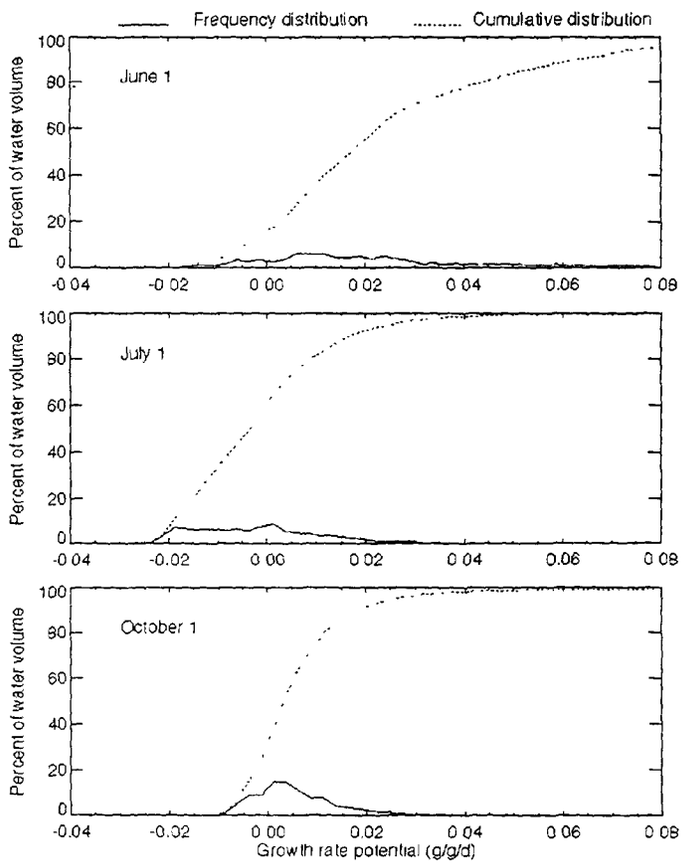

Figure 4

A three-dimensional Chesapeake Bay geographic information system (GIS) program (developed at State University of New York (SUNY) as part of the EPA project) was used to link the ecological processes and fish bioenergetics models to the Chesapeake Bay Water Quality Model. This spatially explicit model demonstrated how the spatial patterning of the environment affected species-specific consumption and growth rates. In spatially explicit modeling, the aquatic habitat was modeled as an explicit feature of environment by subdividing the pelagic habitat into small homogeneous units that defined a cube for a geographical coordinate system and water depth. Each cubic cell represented a small volume of water that was characterized by a specific set of attributes, including prey density, prey size, water temperature and dissolved oxygen (DO) that were measured in the field or were simulated (*e.g.* Chesapeake Bay Water Quality Model).

The conceptual framework of the three-dimensional fish growth and production model was similar to the two-dimensional, spatially explicit models (Brandt *et al.* 1992, Brandt and Kirsch 1993, Luo and Brandt 1993, Mason and Patrick 1994). Fish production was determined by the relationship of the supply of prey resources to the amount of prey that the fish required for growth (predator demand). This relationship depended on the particular temperature-dependent physiological needs and growth rate potential of the predator and on the ability of the predator to make use of the prey supply. Process-oriented simulation models of the same model structure were run in each cell, but were parameterized differently, according to the habitat conditions of each cell and the specific size and species of fish being modeled. A foraging submodel estimated consumption rate by converting measured prey densities and sizes into prey availability for the predator. The bioenergetics submodel estimated the growth rate of the predator from consumption rate and was based on the physiology of the predator and habitat conditions in the cell. The result was a 3-D representation of Atlantic menhaden growth rate potential for each day of the year. The growth rate potential integrated the physiological response and the needs of the predator and, thus, could be interpreted in the context of habitat quality. Volumetric analyses of the growth rates over the entire Bay defined the proportion of the Bay volume that could support various levels of fish growth. The frequencies below zero growth were cumulated and plotted with the dates to demonstrate the seasonal change of menhaden growth habitat.

Spatially Explicit Carrying Capacity Estimation for Menhaden

Carrying capacity is the maximum number of individuals or inhabitants that a given environment can support without detrimental effects. Traditionally, carrying capacity was estimated as a singular value of a given environment. For example, we would say "the carrying capacity of herring in the North Sea", or "the carrying capacity of striped bass in Chesapeake Bay". This type of estimation usually could be derived from quantitative study of energy flow in a whole ecosystem. It required information on standing stocks of the living and nonliving ecosystem components, diets of the feeding species, and rates at which ingested materials were used, transferred among various entities in the food web. Most early studies of ecosystem dynamics assumed processes occurred over a homogeneous environment — both spatially and temporally (*e.g.* Baird and Ulanowicz 1989). Recent studies in spatial ecology (Brandt *et al.* 1992, Brandt and Kirsch 1993, Luo and Brandt 1993, Mason and Patrick 1994) indicated that spatial heterogeneity could have significant effects on overall results, because most ecological processes occurred within a short time-period and at small spatial scales. For

example, a school of planktivore fish will not interact with a patch of zooplankton 10 km away.

In this study, the carrying capacity of the Atlantic menhaden was estimated as spatially and temporally explicit features of the environment, based on the spatially explicit model of growth rate potential. The carrying capacity (CC_{ij} , g/m^3) was estimated for each cell (i, 1 - 4073) and for each day (j, 1 - 365) as:

$$CC_{ij} = (fp*pb_j*phy_{ij}/cons_{ij})*f_{ij}(g)*f_{ij}(do)$$

where, fp = the fraction of phytoplankton production (10%) that can be consumed by the menhaden; pb_j = daily phytoplankton production and biomass ratio (Nixon 1981) on day j; phy_{ij} = hytoplankton biomass density (g/m^3) for cell i and on day j; $cons_{ij}$ = weight specific consumption (g/g/d) for cell i and on day j; $f_{ij}(g)$ = a growth rate dependent scaler for cell i and on day j (Figure 4); and $f_{ij}(do)$ = a dissolved oxygen dependent scaler for cell i and on day j.

Results of Menhaden Modeling

Growth Rate Potential

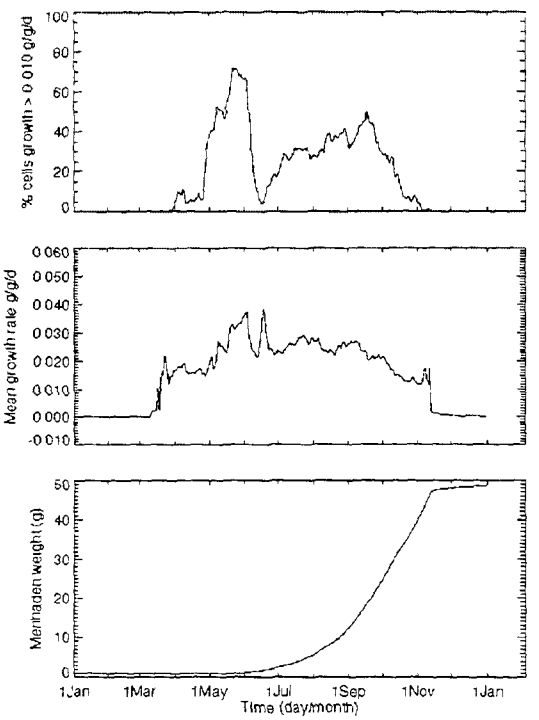

Figure 5

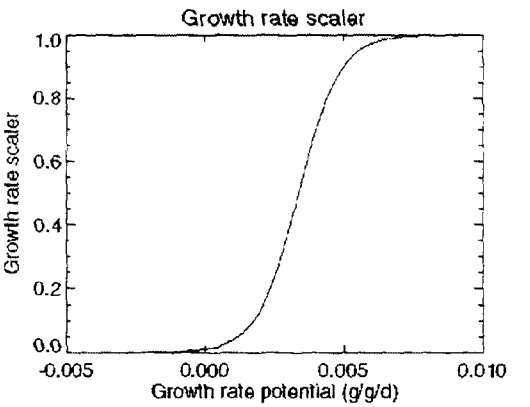

Figure 6

Atlantic menhaden growth rate potential varied over space and time. Growth rate potential ranged from -0.02 to 0.08 g/g/d over the entire bay in early summer (Figure 5, top panel), and more than 80 % of the Bay had positive growth rate potential. On July 1 (Figure 5, middle panel), maximum growth rate potential was less than 0.04 g/g/d and

50% of the Bay had negative growth rate potential (*i.e.* menhaden would loose weight if they remained in these areas). On October 1 (Figure 5, bottom panel), growth rate potential ranged from -0.01 to 0.04 g/g/d and over 70% of the Bay had positive growth rate potential.

If it was assumed that menhaden would only stay in cells with growth rate greater than a given value, the percentage of those cells would define the quantity of menhaden habitat. At menhaden growth rates greater than 0.0 g/g/d, which represents a positive growth rate (Figure 6), the percentage of menhaden habitat in Chesapeake Bay ranged from 20 to 90 % of the Bay and the average growth rate ranged from 0.01 to 0.02 g/g/d during summer and fall. A 50 mm (about 0.5 g) menhaden growing under these conditions would only reach 10 g (98 mm) by the end of the year. At growth rate greater than

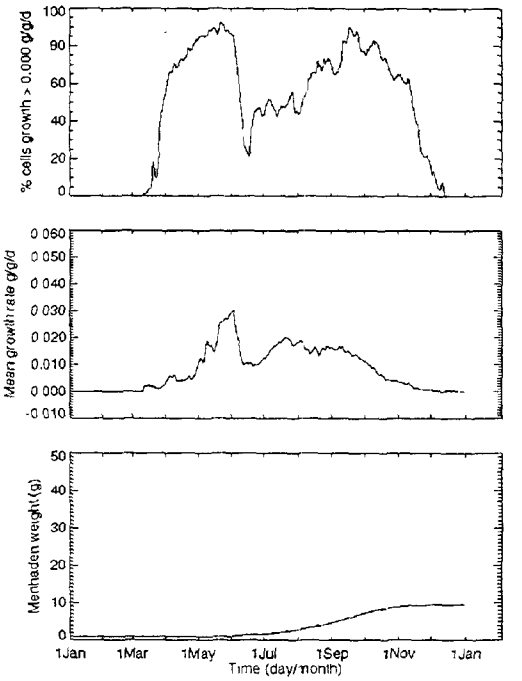

Figure 7

0.005 g/g/d (Figure 7), the percentage of habitat ranged from 10 to 75% of the Bay and the average growth rate ranged from 0.015 to 0.025 g/g/d during summer and fall. The same fish would reach 20 g (120 mm) by the end of the year. At growth rates greater than 0.01 g/g/d (Figure 8), the percentage of habitat was reduced to 5 to 50 % of the Bay and the average growth rate increased to 0.02-0.035 g/g/d. A 50 mm (about 0.5 g) menhaden growing under this condition would reach about 50 g (157 mm) by the end of the year. Trawl survey data from Virginia Institute of Marine Sciences (VIMS), (Bonzek *et al.* 1992) showed that the sizes of YOY menhaden ranged from 120 mm to 160 mm in November and December. Therefore, the menhaden habitat could be defined as the cells with growth rate potential equal or greater than 0.005 g/g/d.

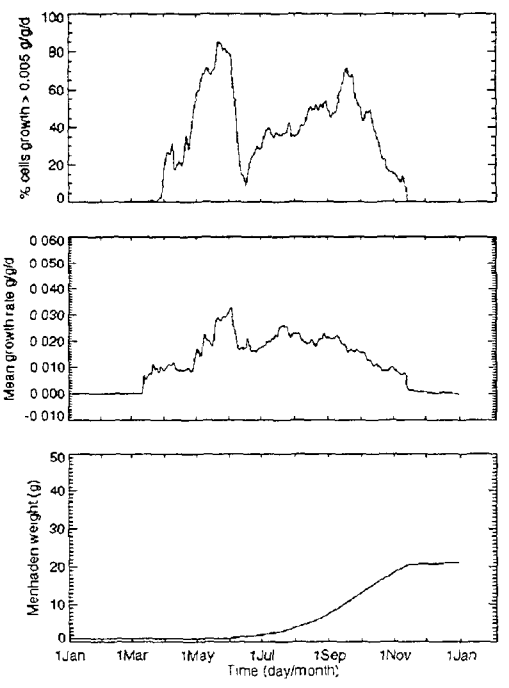

Figure 8

Carrying Capacity

Results indicated a great degree of patchiness in carrying capacity, with carrying capacity varying over space and time. High carrying capacity occurred in early summer, which sharply declined in mid-June. A second peak occurred in mid-July and gradually declined in later summer and fall. In early summer (Figure 9, top), carrying capacity ranged from 0 to 3.5 g/m^3 over the entire Bay; 75% of the bay had carrying capacity greater than 2.0 g/m^3. On July 1 (Figure 9, middle), 60% of the bay had no carrying capacity; whereas, 25% of the Bay had carrying capacity greater than 3.0 g/m^3. In fall, the capacity differences between cells decreased; 30% of the bay had no carrying capacity and 99% of the bay had carrying capacity less then 2.0 g/m^3 (Figure 9, bottom). Another measurement of menhaden habitat quantity was the percentage of the Bay with greater than zero carrying capacity. During summer and fall, the minimum habitat volume occurred in mid-June and the maximum habitat volume occurred in mid-September (Figure 10, top).

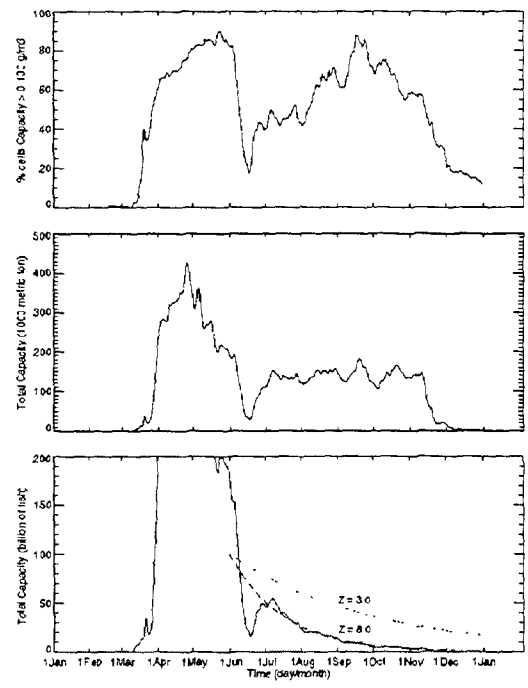

Figure 9

Integrating the carrying capacity of each cell over the entire Bay, for each day, produced the total carrying capacity (on weight base) of Chesapeake Bay for each day (Figure 10, middle). The weight-based carrying capacity was not a good measurement in an ecological sense, however, because mortality and migration were operating on an individual organism. The individual-based carrying capacity can be derived by dividing the weight-based carrying capacity with the average weight of fish on each day (Figure 10, bottom).

Discussion

Results indicated large spatial and temporal variations in growth rate potential and carrying capacity for the Atlantic menhaden in Chesapeake Bay. Compared with the traditional estimate of carrying capacity (a singular value for a given environment), the spatially explicit carrying capacity had many advantages. Spatial patchiness of growth rate potential and carrying capacity characterized the quality and quantity of the Atlantic menhaden habitat in Chesapeake Bay. Temporal changes in growth rate potential and carrying capacity portrayed the dynamics of the Chesapeake Bay ecosystem.

Comparing predicted growth with the growth of Atlantic menhaden observed from field, suggested that menhaden should choose water bodies where growth rates were no less then 0.005 or 0.01 g/g/d. Observed differences in menhaden sizes (20 g to 50g, Figure 11, bottom) at the end of year could be contributed to small differences in growth rates (0.003-0.004 g/d/d, Figure 11, middle).

Comparing predicted carrying capacity in Chesapeake Bay from this study with estimated recruitment of YOY (at age 0.5) menhaden calculated for the entire East coast (Ahrenholz *et al.* 1987), suggested that Chesapeake Bay could nurse the recruits of the entire Atlantic menhaden stock. Ahrenholz *et al.* (1987) estimated the number of recruits at age 0.5 for the entire stock from 1955 to 1979 from a virtual population analysis method. The maximum number of recruits was 18.6 billion in 1958, and the minimum number of recruits was 1.5 billion in 1967. During the late 1970's, the number of recruits ranged from 6 to 10 billion. The current Atlantic menhaden landings were very close to those of late 1970's. Therefore, current number of recruits can be assumed at a similar level, about 10 billion. Spawning peak of Atlantic menhaden occurs in December, therefore, age 0.5 occurs in June. Results from this study showed a maximum carrying capacity of over 150 billion in early June and a minimum of 20 billion in mid-June (Figure 10, bottom), which was greater than the maximum recruits (18.6 billion) of the entire Atlantic menhaden stock. This minimum dip of carrying capacity is the bottle-neck of menhaden recruitment level. No matter how large the carrying capacity was in earlier and later months, this bottle-neck will limit the recruitment level.

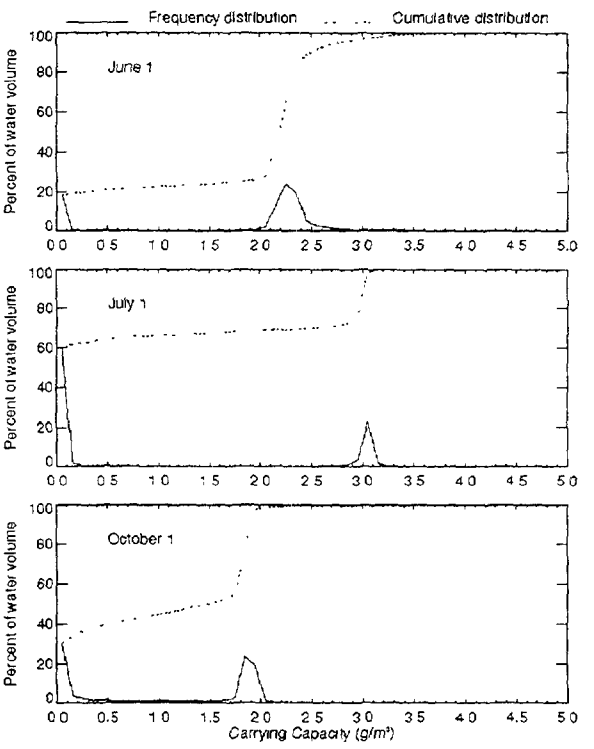

Figure 10

The gradual decline of carrying capacity in later summer and fall can be described by the natural succession of the ecosystem. As the menhaden grow larger in the fall, each individual fish will consume more food and require more space than the fish in early season. Therefore, the system would hold fewer individuals later in the season. As the season progressed, many fish would be eaten by large predators such as striped bass, bluefish and weakfish, or would migrate out of the Bay. The decline of capacity can be quantified by an exponential function: $N_t = N_o e^{-8t}$ (Figure 10 bottom).

Currently proposed nutrient reductions in Chesapeake Bay may not decrease the recruitment level of the entire Atlantic menhaden population and might increase the recruitment level. If overloaded nutrients (mostly, nitrogen and phosphate) produced excess primary production that sank to the bottom in spring, two negative effects would occur in summer. First, excess primary production would deplete the limiting nutrients (e.g. silicon) and cause the sharp decline in primary production in summer. Second, the decaying of the over-produced primary production on the bottom could deplete the water column oxygen concentration in summer, thus, degrading the habitat quality and decreasing the quantity of habitat available to fish. Therefore, reducing nutrient loadings in spring may increase the primary production and dissolved oxygen level in Chesapeake Bay in summer. This would reduce the bottle-neck effect on the menhaden recruitment level and might increase the recruitment level.

The modeling approach described above is still at its frontier development stages with many simplified assumptions and no time dynamics. Information from this type modeling and analysis of ecosystem processes may enable managers to direct their efforts toward an ecosystem-based management program, considering model predictions of the effects of habitat quality changes and resource management options on different trophic levels in the ecosystem. In the future, the bioenergetics model and the spatially explicit model need to dynamically linked with the Water Quality Model to better relate nutrient levels to habitat volumes and prey production.

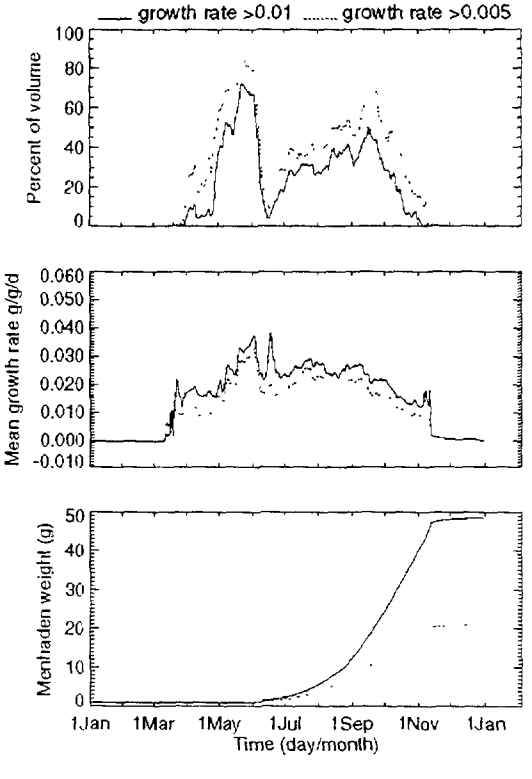

Figure 11

Bay Anchovy Model

A major revision on the STELLA bay anchovy model (*Anchoa mitchilli*) was made (eg. Luo and Brandt 1993). Most progress was made at the population level of the model (immigration and emigration) and simulation time. In the previous version of the model, the model could only simulate a one-year period, because only the growth of individual growhorts (fish hatched within a time-period; 15 days in this case) was modeled for a year. Also, recruitment processes were not included. In the new version, the growth of each growhort was followed for up to two years (Figure 2). Spawning, immigration and emigration were added to the model. The model can be now run for a number of consecutive years. The recruitment for each growhort was assumed to occur at the same time each year. At

present, the level of recruitment was set at a constant value. In the next step, the recruitment level will be modeled as a biomass density-dependent function.

Spatial Planktivore Forage Model

Planktivorous fish can be very effective at altering the size distribution and abundances of zooplankton in aquatic systems (Brooks and Dodson 1965, Hutchinson 1971, Sprules 1972, Lynch 1979, O'Brien 1979, Vanni 1986, MacDonald *et al.* 1990). Changes in size structure of the zooplankton community can permeate throughout the food web and change production dynamics and rates of nutrient cycling (Stein *et al.* 1988). Predicting the size-selectivity of a planktivore becomes critical to evaluating the effect of planktivory on the zooplankton community as well as the relationship of zooplankton resources to planktivore production.

Many studies have sought to determine prey size selection or preference by comparing the size composition of zooplankton in the diet to the size composition of ambient prey measured in the field (Baird and Hopkins 1981, Scott and Murdoch 1983, Mikheev 1984, Magnhagen 1985, Main 1985, Collie 1986, Grover and Olla 1986, Khadka and Ramakrishna 1986, Schmitt 1986, Confer *et al.* 1990, Forrester *et al.* 1994). Other studies have suggested that apparent size and encounter frequency were the determinant of prey size selection (Werner and Hall 1974; Confer and Blades 1975; O'Brien *et al.* 1976, 1985; Eggers 1977, 1982; Pastorok 1981). A typical index of feeding electivity was usually calculated in the form of an "odds ratio" or "forage ratio" (Fleiss 1973, Jacobs 1974, Chesson 1978, Gabriel 1979, Johnson et al. 1990) that compares the percent of the size class in the plankton to that in the diet. Such indices, however, are not really an electivity index from the fish's perspective; they are more appropriately called size-difference indices. The actual prey size distribution perceived by a fish may be very different from that measured.

In this study, a spatial simulation model was developed from the fish's perspective of the size distribution of prey. Field data from the planktivorous bay anchovy,*(Anchoa mitchilli)* was used to test the model. The bay anchovy is the most abundant planktivorous visual feeder in Chesapeake Bay and the nearby coastal areas (Johnson *et al.* 1990, Klebasko 1991, Luo 1991). Previous studies showed that patches of high consumption by the bay anchovy could occur even though the average consumption was relatively low (Klebasko 1991, Luo and Brandt 1993). First, the model performance was tested with hypothetical prey size frequencies. Then, model-predicted size distributions of the prey were compared with the diet of the bay anchovy.

Results and Discussion

Bay anchovy predation was simulated with a 3-D spatial model that also provided an animated visualization during simulation runs. The input size-frequency distributions of prey was compared with the size-frequency distributions of prey encountered, selected, and captured under different assumptions. The size-frequencies of prey encountered did not differ with number of time-steps (Figure 6A) and differed only slightly with prey densities (Figure 6B), light attenuation coefficient (Figure 6C), capture efficiencies (Figure 6D), predator's speeds, and reactive distances (Figure 7). The distance distribution of prey (Figure 8) did differ and most prey were located somewhere in the middle distance of its visual field (Figure 8A) depending on types of prey size distribution (Figure 8D).

Results showed that reactive distance and predator speed affected the size-frequency of prey encountered (Figure 7). An increase of reactive distance and predator speed will increase the encounter rate of prey (Gerritsen and Strickler 1977). However, it has not been demonstrated how changes in reactive distance and predator speed will affect the size frequency of prey encountered. If the reactive distance was held as a constant and predator's speed increased, the predator would encounter more, larger prey (Figure 7A-C). But, if predator's speed was held as a constant and the reactive distance increased, the predator would encounter more, smaller prey (Figure 7D). An encounter was determined by both visual acuity (function of reactive distance) and predator swimming speed.

The size-frequencies of prey eaten were compared for assumptions of "Random choice" (RC) and "apparent size choice" (AC) for different prey densities, reactive distances and predator's speeds were compared (Figure 9). There was no difference between the two choices at different prey densities, if the reactive distance and predator's speed were assumed to be equal (Figure 9A-B). However, there were significant differences between the two choices when the predator's speed was below the reactive distance (Figure 9C-D). The prey distance distribution between the two assumptions of prey choices was also compared (Figure 8). At low prey density (N=250, Figure 8A), there was no obvious differences of prey distance distribution between the two assumptions. At higher prey densities (Figure 8B, C), if the predator selected prey according to the "AC" assumption, more prey would be selected at a closer distance than if the predator selected prey by random choice. At low prey density, the predator rarely saw two prey at the same time therefore no choice was needed; the predator attacked what it saw. In contrast, at higher prey density, the predator might see two or more prey at the same time and must choose; the predator attacked the preferred prey. From an energenetics point of view, a predator should use the "AC" model to select prey. Selecting prey at closer distance not only saved energy in reaching the prey but also could increase the capture efficiency. This phenomenon may help explain why larval fish need higher prey densities to survive (Lasker 1975, 1978; Houde 1978) even though the expected encounter rates are high enough for survival at lower prey densities.

Prey size selection by the bay anchovy was evaluated by running the model with the zooplankton data collected in mid-Chesapeake Bay during April, May, August, and October 1990 with different combinations of swimming speed, reactive distance, and capture efficiency. Then, the predicted size distribution was compared with the dietary size distribution of the bay anchovy collected at the same site and time. The Kolmogorov-Smirnov goodness of fit test (Table 1) was used. The dietary prey size distributions were from bay anchovies ranging in size from 40 to 60 mm total length (Figure 10). The model predicted diet size frequencies quite well for most of the observed patterns of prey size selection by the bay anchovy even though errors could have occurred in zooplankton sampling (missing small size by net, missing large size by pump), the patchiness of zooplankton, or in measuring preserved zooplankton, in measuring partially digested prey from fish stomachs.

This 3-D spatial foraging model (SFM) has good potential for the study of planktivore and plankton interactions in aquatic environment. This model will provide a link between anchovy predation and size-dependent mortality of zooplankton. Future model developments include changing the assumption of randomness regarding prey and predator movements, allowing predation to alter the prey density and size distribution through time, incorporating other environmental parameters (e.g. temperature which may affect swimming speeds) and

running the model in a spatially heterogeneous environment (Brandt and Kirsch 1993, Mason and Patrick 1993) .

Table 1. Kolmogorov-Smirnov goodness of fit test for comparing model predicted prey size frequencies with prey size frequencies found in bay anchovy stomachs in April, May, August, and October, 1990 in mid-Chesapeake Bay. Rd is the reactive distance (mm) to a 1-mm prey; v is bay anchovy speed (mm/s); CE is the capture efficiency; x is prey size (mm); dmax is the test statistics (Zar 1984); values in parenthesis are P values. A P value less than 0.05 indicates that predicted frequency is statistically different from the observed frequency.

Rd	v	CE	April dmax	May dmax	August dmax	October dmax
100	100	1	8.66 (0.21)	11.98 (0.051)	20.05 (0.001)	11.02 (0.075)
100	100	1-0.5x	13.51(0.015)	7.07 (0.40)	15.72 (0.004)	7.24 (0.40)
100	50	1	18.52 (0.001)	4.24 (0.70)	10.00 (0.10)	7.03 (0.40)
100	50	1-0.5x	24.15 (0.001)	8.67 (0.25)	7.68 (0.35)	14.17 (0.01)
200	100	1	9.88 (0.11)	8.70 (0.25)	16.06 (0.003)	11.10 (0.075)
200	100	1-0.5x	14.71 (0.004)	3.97 (0.75)	11.51 (0.065)	7.04 (0.40)
200	150	1	11.68 (0.06)	8.50 (0.26)	16.34 (0.003)	9.34 (0.16)
200	150	1-0.5x	18.02 (0.001)	4.45 (0.70)	10.31 (0.08)	7.93 (0.30)

Incorporation of Fish Bioenergetics Model into the Ecosystem Process Models

The Atlantic menhaden and bay anchovy models were linked with the ecosystem process models developed at the University of Maryland (see SAV, plankton-benthos and zooplankton models in this document) . Because the ecosystem process models used different mass balance units (carbon) than the fish bioenergetics model (calories), unit conversions had to be made before the models could be coupled. For example, to convert zooplankton to fish, the biomass of zooplankton in mg carbon/m3 was first converted into gram wet weight /m^3 by 40% carbon from dry weight and 15% dry weight from wet weight. Then, gram wet weight /m^3 was converted into calories/m^3 by the caloric density of zooplankton (average for copepoda was 650 cal/g). In reverse, wet fish weight was converted to dry weight at 20%, then the dry fish weight was converted into carbon at 40%. These conversion coefficients were set as constant for convenience, but in reality, they varied both seasonally and ontogenetically.

In this combined planktivore-ecosystem model, bay anchovy production was linked with copepod production by relating copepod abundance to the proportion of maximum consumption that a bay anchovy could achieve in a day. Menhaden production was linked with phytoplankton production by relating phytoplankton abundance to the proportion of maximum consumption that a menhaden can obtain in a day. Fish grazing had negative effects

on both phytoplankton and zooplankton production by taking a proportion of daily production, and positive effects by returning the egestion and excretion into the particular organic matter (POM) and dissolved organic matter (DOM) pools.

In preliminary simulations, the fish-ecosystem model ran for a four-year time period. The results showed that all variables followed consistent annual cycles, indicating a steady state of the model (Fig. 3, Fig. 4, Fig. 5). The dissolved inorganic nitrogen concentration (DIN) peaked in early spring, followed by diatoms (DIA), which peaked in mid spring. Other phytoplankton (OP) then peaked in late spring and late summer (Fig. 3). The zooplankton biomass density peaked in spring and fall (Fig. 4), which matched quite well with the observed data in 1984 and 1985. The bay anchovy population had two peaks (Fig. 2), a small one in spring as a result of immigration; and a larger one in fall as a result of production. The Atlantic menhaden population biomass sharply increased in summer and peaked in fall as a result of rapid growth of individual fish. It then quickly decreased in late fall and winter as a result of emigration (Fig. 1). At the bottom of the water column, the deposit feeder biomass peaked in summer and the benthic filter feeder peaked in fall (Fig. 5).

In the next steps of the project, the piscivore bioenergetics models for striped bass and bluefish will be coded into the STELLA models. The planktivore-ecosystem model will also be refined. The piscivore models will be incorporated into the planktivore-ecosystem model to form the piscivore-planktivore-ecosystem model. When this model is completed, managegement simulations will be able to examine such features as bottom-up controlling process by reducing the nutrients input and top-down controlling processes by increasing the piscivore abundance (or reducing the fishing mortality).

Striped Bass Model

Effect of Hypoxia on Striped Bass Growth and Consumption

Laboratory experiments were conducted to test the effect of hypoxia on striped bass (*Morone saxatilis*) growth and consumption (as part of a MD Sea Grant-sponsored project). Low (dissolved oxygen) DO can be a limiting factor in many aquatic ecosystems (Coutant 1985; 1990). In particular, fish distributions, growth, consumption, and metabolic rates can be significantly affected by the amount of DO available. In systems with a long history of cultural eutrophication, such as Chesapeake Bay, low DO can limit striped bass production during the summer when stratification occurs. Striped bass consumption and growth were measured over a two-week time period, at three oxygen levels and four temperatures. Both consumption and growth decreased significantly as DO levels decreased. Some interactions between temperature and oxygen concentrations were present. Laboratory results were used to develop equations to modify existing bioenergetics models of striped bass in Chesapeake Bay. The bioenergetics models were then used to examine trade-offs between temperature, prey availability, and oxygen levels across Chesapeake Bay. These results will be applied in the spatially explicit model to test how the intensity of hypoxia in Chesapeake Bay will affect the striped bass growth and habitat volume.

Field Verification of a Bioenergetics Model for Striped Bass

Verification of bioenergetics modeling with independent field estimates of consumption or growth produced mixed results, often differing by 50-200% between field and model estimates. One outcome of these mixed verification results was a recommendation that model results for untested models be accepted with caution pending field validations. In earlier work, a bioenergetics model for striped bass in Chesapeake Bay was developed and laboratory-validated. Independent laboratory experiments indicated the striped bass bioenergetics model provided good estimates of growth and consumption. During October 1993, age-0 striped bass were collected with bottom trawls every 2.5 hours over two 24-h periods from near Pooles Island in Chesapeake Bay. Fish were frozen in water for later analysis. In the laboratory, stomach content weights were estimated using standard methods. Daily ration estimates were calculated with a gastric evacuation model for age-0 striped bass derived from laboratory experiments. Field measures of consumption and growth were similar (within 20%) to those estimated with the bioenergetics model. The results of this field verification suggested that the Hartman and Brandt (1995) age-0 striped bass model was a robust model that provided realistic estimates of growth and consumption in field applications.

The successful testing of this bioenergetics model for striped bass with field estimated consumption and growth will allow this model to be used with confidence by managers and researchers. This model can be used by managers and researchers to predict the feeding requirements of striped bass with commonly obtained information such as the growth of these fish. The bioenergetics models will allow managers to determine if sufficient prey fishes are present to support stocking of striped bass into reservoirs. Such information will also allow a better understanding of the importance of striped bass in aquatic food webs.

Changes in Habitat Suitability for Bluefish and Striped Bass in Mid-Chesapeake Bay

Fish growth rate potential was previously defined as a measure of the habitat suitability for fish (Brandt *et al.* 1992; Brandt and Kirsch 1993; Goyke and Brandt 1993). Growth rate potential is the expected growth rate of a predator if placed in a particular volume of water with known physical and biological characteristics. Fish growth rate potential combines foraging and bioenergetics models with spatially explicit field measures of temperature, prey density and prey size to arrive at the potential growth rate a predator may experience if constrained within the spatial cell. Thus, growth rate potential (GRP) provides a measure of habitat quality from the fish's perspective. However, previous work on spatial modeling of fish GRP examined only single sizes (adults) of predators (Brandt 1992; Brandt and Kirsch 1993; Goyke and Brandt 1993; Mason *et al.* 1995).

As fish age, the type and size of prey typically changes (Mathur and Robbins 1971; Knight *et al.* 1984; Setzler-Hamilton and Hall 1991; Hartman and Brandt 1995a). Many fish species begin life as planktivores and switch to a piscivorous feeding mode with aging. Maximum prey size and size ranges of prey consumed also usually increase with age in piscivores (Knight *et al.* 1984; Hartman and Brandt 1995a). Due to these changes in prey sizes with age, the available prey field may differ among different sized predators of the same species. Thus, depending upon the size distributions of prey, food availability may differ dramatically among different sized predators.

Striped bass, *Morone saxatilis*, and bluefish, *Pomatomus saltatrix*, represent an interesting ecological contrast. Both also support valued sport and commercial fisheries (Setzler *et al.* 1980; Mid-Atlantic Fishery Management Council 1989). Striped bass and bluefish are the dominant predators in Chesapeake Bay and represent two families (Percichthyidae and Pomatomidae, respectively) from the order Perciformes). Striped bass are resident in Chesapeake Bay until about age-6 (Kohlenstein 1981); whereas, bluefish are seasonal residents, using the bay as a nursery and growing area during summer (Norcross *et al.* 1974; Kendall and Walford 1979; McBride and Conover 1992). Feeding strategies also differ among the two species-- bluefish are cruising predators with teeth that permit searing detention (Baird 1873; Bigelow and Schroeder 1953); striped bass feed both as sit-and-wait and cruising predators (Setzler *et al.* 1980). Both predators commonly feed on the same species such as bay anchovy *(Anchoa mitchilli)*, Atlantic menhaden *(Brevoortia tyrannus)* and spot *(Leiostomus xanthurus)*(Grant 1962; Homer and Boynton 1978; Friedland *et al.* 1988; Hartman and Brandt 1995a,c).

Growth rates of fish are mediated by body size, temperature, and prey availability. Because water temperatures and available prey sizes and abundance (prey spectrum) are heterogeneously distributed, the conditions for growth of a predator will also be patchily distributed. Similarly, temperatures and prey spectrum changes seasonally, so conditions for growth of a predator may differ among seasons. Due to the complex interaction of spatial, seasonal, biotic, abiotic, and ontogenetic changes in growth conditions for fish, an adequate evaluation of habitat quality for any fish species would require a seasonal and ontogenetic analysis of fish growth rate potential. In this study, spatially explicit modeling was used to combine previously developed bioenergetics models of bluefish and striped bass (Hartman and Brandt 1995b) with quantitative acoustic measurements of prey spectra to evaluate habitat suitability for the two piscivores in the mid-Chesapeake Bay.

Results and discussion

The perception of habitat quality, or growth rate potential, changes with fish species, fish size, and season. Within a season and species, spatial maps of fish growth rate potential substantially differed across fish sizes (Fig. 6). This was largely due to different prey size ranges that resulted in different prey spectrums and, in part, to differing thermo-physiological constraints on consumption and metabolic rates (Hartman and Brandt 1995b). Small (10 g) predators usually had the lowest percentages of cells that supported positive growth, probably due to the low availability of the smaller prey sizes these predators could consume. The large predators consumed a wider range of prey sizes which led to a wider prey field. Thus, larger predators tended to have higher percentages of cells that supported positive growth rate potential (Fig. 7, 8). The exception to this generalization was during winter, when 10 g striped bass had slightly higher possible growth rates and a greater percentage of cells with positive growth than 2000 g striped bass.

Water column averages of growth rate potential suggested that fall and spring provided the best, and summer and winter the worst overall habitat quality for striped bass and bluefish (Table 2). For each predator, highest averages of water column GRP occurred in fall. Striped bass average GRP was +0.0039 (10 g) to +0.0209 g g^{-1} d^{-1} (100 g) in fall. Bluefish average GRP was -0.0099 g g^{-1} d^{-1} for 10 g, but increased to +0.0187 g g^{-1} d^{-1} for 2000 g fish (Table 2). Poorest average growth was in summer for 10 g fish (-0.0146 to -0.0327 g g^{-1} d^{-1}), but all

predators had poorest average growth of any season in summer. In winter and spring, 2000 g predators had higher average GRP than smaller conspecifics, with average spring GRPs of +0.0034 to +0.0096 g g^{-1} d^{-1} estimated for bluefish and striped bass, respectively (Table 2).

Table 2. Seasonal whole water-column averages of growth rate potential (x 100) for 10, 100, and 2000 g striped bass and bluefish in Chesapeake Bay. Standard deviations of mean values (x 100) are given parenthetically.

Predator	Winter	Spring	Summer	Fall
Striped Bass				
10 g	-0.08	-0.03	-1.46	+0.39
	(0.33)	(0.65)	(0.67)	(1.84)
100 g	-0.09	+0.05	-1.06	+2.09
	(0.25)	(0.60)	(0.47)	(2.28)
2000 g	-0.06	+0.96	-0.26	+1.54
	(0.12)	(1.11)	(0.86)	(1.12)
Bluefish				
10 g	-0.70	-0.94	-3.27	-0.99
	(0.14)	(0.54)	(0.73)	(1.79)
100 g	-0.38	-0.48	-1.69	+0.25
	(0.07)	(0.34)	(0.59)	(1.76)
2000 g	-0.17	+0.34	-0.29	+1.87
	(0.03)	(0.52)	(1.20)	(1.23)

Measures of habitat quality (spatial growth potential) supported the concept that fish use of the Bay may be driven by both thermal physiology and prey availability. Striped bass were much better suited to the thermal regimes and prey fields available during winter and spring than were bluefish. Growth potential for both species during winter was limited by low water temperatures. Bluefish of any size would lose weight in all cells during winter; whereas, some small growth was possible for striped bass. Growth rate was also suppressed for bluefish during spring, with a small volume of water supporting growth for 10 or 100 g bluefish (Fig. 7). Positive GRP was available in 25% of cells for 10 and 100 g striped bass and 2000 g fish had positive GRP in over 65% of all cells (Fig. 8).

Given the differing growth maps for striped bass and bluefish during winter and spring, it was not surprising that bluefish are not found in Chesapeake Bay during those seasons (when spring data were collected; Norcross *et al.* 1974; Kendall and Walford 1979) and that striped bass are annual residents of the Chesapeake Bay (Kohlenstein 1981). Bluefish overwinter in the coastal waters off North Carolina, from November to May, where temperatures, and in all

likelihood prey availability, exceed those found in Chesapeake Bay during that time (Norcross *et al.* 1974; Kendall and Walford 1979).

Spatial maps of growth rate potential of small (10 g) fish may be less representative of growth conditions for these predators (than for larger predators) in Chesapeake Bay. First, we have considered only pelagic fish as possible prey for small striped bass and bluefish. Actual diets of these small predators often include a large variety of abundant prey not accessible to our hydroacoustic instruments such as benthic invertebrates, shrimps, and some benthic fishes (Boynton *et al.* 1981; Friedland *et al.* 1988; Hartman and Brandt 1995a). Second, the frequency of the acoustic transducer (120 kHz) did not effectively sample very small organisms, thus any prey less than 12 mm were not included in the prey field. Therefore, prey fields of the small fish in the model were probably less accurate than for larger fishes which fed primarily on larger pelagic fishes (Grant 1962; Schaefer 1970; Texas Instruments 1976; Homer and Boynton 1978; Gardinier and Hoff 1982; Rulifson and McKenna 1987; Hartman and Brandt 1995a).

Water temperatures and prey densities combined to limit the maximum growth rate and ranges of growth rates for striped bass and bluefish. Within a season, water temperatures fell within a restricted range ($\pm$ 4°C). Thus, GRP was moderated more by the absolute density of prey than by temperatures within a season. Across seasons, maximum prey densities within a cell were similar (although spatial patterning and seasonal prey densities differed greatly, prey densities of over 5 g m^{-3} were found in all seasons) and the resulting GRP was limited by temperature. This suggested that across seasons, temperature limited the maximum growth rate potential of predators; but, within a season, the distribution of prey density limited the proportion of cells providing favorable growth conditions.

Expansion of the concept of fish growth rate potential to include different sized predators with careful consideration of each predator's size-specific prey field improved understanding of ecosystem function and the importance of spatial patterning in the physical and biological habitat upon available habitat for a species throughout it's ontogenetic development. These models allowed evaluation of habitat quality in a comparative nature, across species and sizes of fish. This modeling has shown that habitat quality and the spatial patterning of habitat in the environment (as assessed by fish growth rate potential) can be quantified from the fish's perspective and that it changed seasonally and with age for striped bass and bluefish.

Weakfish

Spatial Analyses of Predator Growth Potential: Biotic and Abiotic Influences

Chesapeake Bay is a nursery and growing area for weakfish. In summer, hypoxic mesohaline waters may affect distributions, migrations, and growth of these fish. Growth is influenced by biotic variables (*e.g.* prey availability and size) and abiotic variables (temperature, D.O., salinity). These biotic and abiotic factors vary in time and space. A spatial model was developed that used field-derived measures of abiotic variables and hydroacoustically derived prey size, density, and distribution arrays. These arrays were combined with weakfish bioenergetics and foraging models to predict growth potential. Fish growth potential represented the growth rate of a fish if constrained within a spatial cell (about

0.5 m depth by 30 m cross-sections) with prey and physical attributes inherent to that cell. Modeling results showed DO may play a key role in summer growth patterns of weakfish, particularly age-0 fish. Weakfish growth potential (all ages) was generally highest near the surface where anchovy densities were greatest. Anchovies are a primary food source for weakfish (Hartman and Brandt 1995a). A sequential analysis of the physical data showed that DO and temperature were more important than salinity in influencing growth potential. These results suggested that DO levels might limit weakfish production; therefore weakfish habitat could be improved by continued nutrient control programs in Chesapeake Bay.

The spatial modeling in this study permited a better understanding of the importance of temperature, salinity, DO, and food availability upon habitat quality for weakfish in Chesapeake Bay. The spatial maps of fish growth rate potentials illustrated how habitat quality compared across different sections of the water column and the importance DO levels, relative to available temperatures -- if you were a weakfish! These types of color maps help to illustrate the importance of reducing nutrients for future management of coastal waters.

White perch

Trophic Dynamics: Diet, Growth, and Bioenergetics

A bioenergetics model for the white perch (*Morone americana*) is currently being developed. The white perch is an abundant benthic feeder in the freshwater and mesohaline portions of the Chesapeake Bay estuary and may have significant effects on the macrobenthic community of the bay. White perch are fished commercially and recreationally in many coastal waters. They provide a prey resource to larger piscivores, such as striped bass and bluefish. To define the role of the white perch in the Bay's food web, diet, growth, and bioenergetics of this species were examined. White perch were sampled at four different seasons of the year (April, June, October, and December 1995) over a 24-hour period with bottom trawls. Fish lengths, wet weights, and ages were assessed. The main diets of white perch consisted of amphipods (Gammarid spp.), copepods, and cladocerans. Consumption estimates will be derived from a bioenergetics model and compared to direct measures of diel and seasonal predation rates on various prey types. Overall, white perch appear to play a dominant role in the benthic food web interactions in Chesapeake Bay.

Future Objectives

During the next year, the principle objective will be to emphasize the development of biologically complex and spatially explicit models. An important task is to couple the fish bioenergetics models with the ecosystem process models and with the water quality model. The connections of ecosystem process and fish bioenergetics models accomplished during previous years will be defined and used to assess the effects of patchiness and spatial resolution on model results and predictions for water quality and habitat improvement. A range of policy scenarios will be simulated using the individual and integrated models to provide resource managers with a unique tool for relating fish production to proposed and planned nutrient

reductions. An assessment will be made to determine the water quality improvements needed to achieve targeted habitat and species restoration goals and to identify the associated sensitive biological components. The combination of ecosystem process models and fish bioenergetics models will provide the capability to predict potential fish production from nutrient loading and to simulate management scenarios.

References

Ahrenholz, D.W., W.R. Nelson, and S.P. Epperly. 1987. Population and fishery characteristics of Atlantic menhaden, *Brevoortia tyrannus*. Fish. Bull., U.S. 85:569-600.

Aksnes, D. L., and J. Giske. 1993. A theoretical model of aquatic visual feeding. Ecol. Model. 67:233-250

Baird, R. C. and T. L. Hopkins. 1981. Trophodynamics of the fish *Valenciennellus tripunctulatus*. 2. Selectivity, grazing rates and resource utilization. Mar. Ecol. Prog. Ser. 5:11-19.

Baird, R.M. and R.E. Ulanowicz. 1989. The seasonal dynamics of the Chesapeake Bay ecosystem. Ecol. Monogr. 59:329-364.

Baird, S. F. (1873). Natural history of some of the more important food fishes of the south shore of New England. II. The bluefish, *(Pomatomus saltatrix)* (Linn.). Rep. U.S. Fish. Comm. for 1871-1872: 235-252.

Bartell, S.M., J.E. Breck, R.H. Gardner and A.L. Brenkert. 1986. Individual parameter perturbation and error analysis of fish bioenergetics models. Can. J. Fish. Aq. Sci. 43:160-168.

Beamish, F. W. H. 1978. Swimming capacity. Pages 101-189 in W. S. Hoar, and D. J. Randall, editors, Fish Physiology. 7. Locomotion. Academic Press, New York, USA.

Bigelow, H. B., and W.C. Schroeder. 1953. Fishes of the Gulf of Maine. U.S. Fish Wild. Ser., Fish. Bull. 53.

Blaxter, J. H. S., and R. S. Batty. 1985. Herring behaviour in the dark: responses to stationary and continuously vibrating obstacles. J. Mar. Biol. Assoc. U.K. 66:1031-1049.

Boynton, W. R., Polgar, T. T., and H.H. Zion. 1981. Importance of juvenile striped bass food habits in the Potomac Estuary. Trans. Am. Fish. Soc. 110:56-63.

Bonzek, C.F., P.J. Geer, J.A. Colvocoresses and R.E. Harris. 1992. Juvenile finfish and blue crab stock assessment program. Virginia Institute of Marine Science. Special science report No. 124. Vol. 1992.

Brandt, S. B. (1992). Acoustic quantification of fish abundance in the Chesapeake Bay. Final Report to Maryland Department of Natural Resources, Power Plant Topical Research Program, [UMCEES]CBL 92-054, Annapolis.

Brandt, S.B., D.M. Mason and E.V. Patrick. 1992. Spatially explicit models of fish growth rate. Estuaries 17(2):23-35.

Brandt, S.B. and K.J. Hartman. 1993. Innovative approaches using bioenergetics models: Future applications to fish ecology and management. Trans. Amer. Fish. Soc. 122:731-735.

Brandt, S.B. and J. Kirsch. 1993. Spatially explicit models of striped bass growth in the mid-Chesapeake Bay. Trans. Amer. Fish. Soc. 122:845-869.

Brooks, J. L. and S. I. Dodson. 1965. Predation, body size, and composition plankton. Science 150:28-35.

Chesson, J. 1978. Measuring preference in selective predation. Ecology. 59:211-215.

Collie, J. S. 1987. Food selection by yellowtail flounder (*Limanda ferruginea*) on Georges Bank. Can. J. Fish. Aquat. Sci. 44:357-367.

Confer, J. L. and P. I. Blades. 1975. Omnivorous zooplankton and planktivorous fish. Limnol. Oceanogr. 20:571-579.

Confer, J. L, E. L. Mills, and L. O'Bryan. 1990. Influence of prey abundance on species and size selection by young yellow perch (*Perca flavescens).* Can. J. Fish. Aquat. Sci. 47:882-887.

Coutant, C.C. 1990. Temperature-oxygen habitat for freshwater and coastal striped bass in a changing climate. Trans. Am. Fish. Soc. 119:240-253.

Coutant, C.C. 1985. Striped bass, temperature, and dissolved oxygen: a speculative hypothesis for environmental risk. Trans. Am. Fish. Soc. 114:31-61.

Day, J. W., Jr., Hall, C. A. S., Kemp, W. M., Yanez-Araniciba, A. (1989). Estuarine Ecology. John Wiley and Sons, Inc. New York.

Eggers, D. M. 1982. Planktivore preference by prey size. Ecology. 63:381-390.

Eggers, D. M. 1977. The nature of prey selection by planktivorous fish. Ecology. 58:46-59.

Fleiss, J. L. 1973. Statistical methods for rates and proportions. John Wiley and Sons, New York.

Forrester, G. E., J. G. Chace and W. McCarthy. 1994. Diel an density-related changes in food consumption and prey selection by brook charr in a New Hampshire steam. Env. Bio. Fish. 39:301-311.

Friedland, K. D., Garman, G. C., Bedja, A. J., Studholme, A. F., Olla, B. (1988). Interannual variation in diet and condition in juvenile bluefish during estuarine residency. Trans. Am. Fish. Soc. 117: 474-479.

Gabriel, W. L. 1979. Statistics of selection. In: Lipovsky, S. J., Simenstad, C. A. (eds). Gutshop 1978: fish food habits studies. Proc. 2nd Pacific Northwest technical workshop. Washington Sea Grant, Seattle, p. 62-66.

Gardinier, M. N., Hoff, T. B. 1982. Diet of striped bass in the Hudson River Estuary. N. Y. Game Fish J. 29: 152-165.

Gerritsen, J. and J. R. Strickler. 1977. Encounter probabilities and community structure in zooplankton: a mathematical model. J. Fish. Res. Board Can. 34:73-82.

Goyke, A. P., and S.B. Brandt. 1993. Spatial models of salmonine growth rates in Lake Ontario. Trans. Am. Fish. Soc. 122: 870-883.

Grant, G. C. 1962. Predation of bluefish on young Atlantic menhaden in Indian River, Delaware. Ches. Sci. 3:45-47.

Grover, J. J. and B. L. Olla. 1986. Morphological evidence for starvation and prey size selection of see-caught larval sablefish, *Anoplopoma fimbria*. Fish. Bull. 84:484-489.

Harding, L W. Jr. 1994. Long-term trends in the distribution of phytoplankton in Chesapeake Bay: roles of light, nutrients and streamflow. Mar. Ecol. Prog. Ser. 104:267-291.

Hartman, K. J. 1994. Striped bass, bluefish, and weakfish in the Chesapeake Bay: energetics, trophic linkages, and bioenergetics model applications. PhD thesis. The University of Maryland, College Park, MD, USA. 336 pp.

Hartman, K. J., and S.B. Brandt. 1995a. Trophic resource partitioning, diets and growth of sympatric estuarine predators. Trans. Am. Fish. Soc. 124: 520-537.

Hartman, K. J., and S.B. Brandt. 1995b. Comparative energetics and the development of bioenergetics models for sympatric estuarine piscivores. Can J. Fish. Aq. Sci. 52: 1647-1666.

Hartman, K. J., and S.B. Brandt. 1995c. Predatory demand and impact of striped bass, bluefish, and weakfish in the Chesapeake Bay: applications of bioenergetics models. Can J. Fish. Aq. Sci. 52: 1667-1687.

Hartman, K.J. and S.B. Brandt. 1993. A bioenergetics model for age 0 striped bass: evaluation of parameter accuracy and precision. Trans. Amer. Fish. Soc. 122:912-926.

Hofmann, E. E. and J. W. Ambler. 1988. Plankton dynamics on the outer southeastern U.S. continental shelf. Part II: A time-dependent biological model. J. Mar. Res. 46:883-917

Homer, M., and W.R. Boynton. 1978. Stomach analysis of fish collected in the Calvert Cliffs region, Chesapeake Bay - 1977. Final Rep. to MDNR, PPS Progress, Annapolis, MD. Ref. No. UMCEES 78-154..

Houde, E. D. 1978. Critical food concentrations for larvae of three species of subtropical marine fishes. Bull. Mar. Sci. 28:395-411.

Hutchinson, B. P. 1971. The effect of fish predation on the zooplankton of ten Adirondack lakes, with particular reference to the alewife, *Alosa pseudoharengus*. Trans. Am. Fish. Soc. 100:325-335.

Jacobs, J. 1974. Quantitative measurement of food selection: a modification of the forage ratio and Ivlev's electivity index. Oecologia (Berl.) 14:413-417.

Jobling, M. 1982. Food and growth relations of the cod, Gadus morhua L., with special reference to Balsfjorden, north Norway. J. Fish Biol. 21: 357-363.

Johnson, W. S., D. M. Allen, M. V. Ogburn and S. E. Stancyk. 1990. Short-term predation responses of adult bay anchovies *Anchoa mitchilli* to estuarine zooplankton availability. Mar. Ecol. Prog. Ser. 64:55-68.

Kareiva, P. and M. Anderson. 1988. Spatial aspects of species interactions: The wedding of models and experiments. pp. 38-54, In: Hastings, A. (ed.), Community Ecology, Springer-Verlag, New York.

Kemp, W.M., S.B. Brandt, W.R. Boynton, R. Bartleson, J. Hagy, J. Luo and C.J. Madden. 1992. Ecosystem models of the Patuxent River Estuary relating nutrient loading to production of selected fish populations. Final Rept, Year 1. Maryland Dept. Nat. Res. Tidewater Admin., Chesapeake Bay Research and Monitoring Division, Annapolis MD 21401.

Kendall, A. W., and L.W. Walford. (1979). Sources and distribution of bluefish *Pomatomus saltatrix,* larvae and juveniles off the east coast of the United States. Fish. Bull. 77: 213-227.

Khadka, R. B. and R. T. Ramakrishna. 1986. Prey size selection by common carp (*Cyprinus carpio var. communis*) larvae in relation to age and prey density. Aquaculture. 54:89-96.

Kitchell, J.F., D.J. Stewart and D. Weininger. 1977. Applications of a bioenergetics model to yellow perch (*Perca flavescens)* and walleye (*Stizostedion vitreum).* J. Fish. Res. Bd. Can. 34:1922-1935.

Kitchell, J. F., D.J. Stewart, and D. Weininger 1977. Applications of a bioenergetics model to yellow perch (*Perca flavescens)* and Walleye (Stizostedion vitreum vitreum). J. Fish. Res. Board. Can. 34:1922-1935.

Klebasko, M. J. 1991. Feeding Ecology an daily ration of bay anchovy (*Anchoa mitchilli*) in the mid-Chesapeake Bay. MS. thesis, Univ. of Maryland, College Park. 103 p.

Knight, R. L., F.J. Margraf, and R.F. Carline. 1984. Piscivory by walleyes and yellow perch in western Lake Erie. Trans. Am. Fish. Soc. 113:677-693.

Kohlenstein, L. C. (1981). On the proportion of the Chesapeake Bay stock of striped bass that migrates into the coastal fishery. Trans. Am. Fish. Soc. 110:168-179.

Lasker, R. 1975. Field criteria for survival of anchovy larvae: the relation between inshore chlorophyll maximum layers and successful first feeding. U. S. Fish. Bull. 73:453-462.

Lasker, R. 1978. The relation between oceanographic conditions and larval anchovy food in the California Current: Identification of factors contributing to recruitment failure. Rapports et Proces-Verbaux des Reunions du Conseil International pour l'Exploration de la Mer 173:212-230.

Lippson, A. J. 1985. The Chesapeake Bay in Maryland - an atlas of natural resources. Johns Hopkins University Press, Baltimore, Maryland.

Luo, J. and S.B. Brandt. 1993. Bay anchovy, Anchoa mitchilli, production and consumption in mid-Chesapeake Bay based on a bioenergetics model and acoustical measures of fish abundance. Mar. Ecol. Prog. Ser. 98:223-236.

Luo, J. 1991. The life history of the bay anchovy, *Anchoa mitchilli,* in Chesapeake Bay. Ph. D. dissertation, College of William and Mary, Williamsburg, VA. 108 p.

Lynch, M. 1979. Predation, competition, an zooplankton community structure: an experimental study. Limnol. Oceanogr. 24:253-274.

MacDonald, M. E., L. B. Crowder and S. B. Brandt. 1990. Changes in Mysis and Pontoporeia populations in southeastern Lake Michigan: A response to shifts in fish community.

Magnhagen, C. 1985. Random prey capture or active choice? An experimental study on prey size selection in three marine fish species. Oikos. 45:206-216.

Main, K. L. 1985. The influence of prey identity and size on selection of prey by two marine fishes. J. Exp. Mar. Biol. Ecol. 88:145-152.

Mason, D. M. and E. V. Patrick. 1993. A model for the Space-time dependence of feeding for pelagic fish populations. Trans. Am. Fish. Soc. 122:884-901.

Mason, D. M., Goyke, A., and S.B. Brandt. 1995. A spatially-explicit bioenergetics measure of habitat quality for adult salmonines: Comparison between Lakes Michigan and Ontario. Can. J. Fish. Aq. Sci. 52: 1572-1583.

Mathur, D., and R.W. Robbins. 1971. Food habits and feeding chronology of young white crappie, Pomoxis annularis, Rafinesque, in Conowingo Reservoir. Trans. Am. Fish. Soc. 100:307-317.

McBride, R. S., and D.O. Conover. 1992. Recruitment of young-of-the-year bluefish *Pomatomus saltatrix* to the New York Bight: variation in abundance and growth of spring- and summer-spawned cohorts. Mar. Ecol. Prog. Ser. 78: 205-216.

McHugh, J. L. 1967. Estuarine nekton. In: Lauff, G.. H. (ed.), Estuaries. Am. Assoc. Advanc. Sci., Publ. No. 83, Washington, DC, pp 581-620.

Mid Atlantic Fishery Management Council, Atlantic States Marine Fisheries Commission, National Marine Fisheries Service, New England Fishery Management Council, South Atlantic Fishery Management Council. 1989. Fishery management plan for the bluefish fishery. 76 pp.

Mikheev, V. N. 1984. Prey size and food selectivity in young fishes. J. Ichthyol. 24:66-76.

Miller, T. J, L. B. Crowder, and J. A. Rice. 1993. Ontogenetic changes in behavioural and histological measures of visual acuity in three species of fish. Environmental Biology of Fishes **37**:1-8.

Monteleone, D.M. and E.D. Houde. 1990. Influence of maternal size on survival and growth of striped bass *Morone saxatilis* (Walbaum) eggs and larvae. J. Exp. Mar. Biol. Ecol. 140:1-11.

Nixon, S. W. 1981. Freshwater inputs and estuarine productivity. In R. D. Cross and D. L. Williams (Eds), Proceedings of the National Symposium on Freshwater Inflow to Estuaries. U.S. Fish and Wildlife Service, Office of Biological Service, FWS/OBS-81/04, Washington, D. C., Vol. 1, pp 31-57.

Norcross, J. J., S.L. Richardson., W.H. Massmann, E.B. Joseph. 1974. Development of young bluefish (*Pomatomus saltatrix)* and distribution of eggs and young in Virginia coastal waters. Trans. Am. Fish. Soc. 103:477-497.

O'Brien, W. J. 1979. The predator-prey interaction of planktivorous fish and zooplankton. Am. Sci. 67:572-581.

O'Brien, W. J., B. Evans and C. Luecke. 1985. Apparent size choice of zooplankton by planktivorous sunfish: exceptions to the rule. Env. Bio. Fish. 13:225-233.

O'Brien, W. J., N. A. Slade, and G. L. Vinyard. 1976. Apparent size as the determinant of prey selection by bluegill sunfish (*Lepomis Macrochirus*). Ecology. 57:1304-1310.

Officer, C.B., R.B. Briggs, J.L Taft, L.E. Cronin, M.A. Tyler, and W.R. Boynton. 1984. Chesapeake Bay anoxia: origin, development and significance. Science 223:22-27.

Park, S. K. and K. W. Miller. 1988. Random Number Generators: Good ones are hard to find. Communication of the ACM, 31:1192-1205.

Pastorok, R. A. 1981. Prey vulnerability and size selection by Chaoborus larvae. Ecology. 62: 1311-1424.

Peters, D. S. and W. E. Schaaf. 1981. Empirical Modelof the Trophic Basis for Fishery Yield in Coast Waters of the Eastern USA.

Possingham, H.P. and J. Roughgarden. 1990. Spatial population dynamics of a marine organism with a complex life cycle. Ecology 71:973-985.

Rippetoe, T.H. 1993. Production and energetics of Atlantic menhaden in Chesapeake Bay. Master's thesis, Univ. of Maryland, College Park. 113 pp.

Rulifson, R. A., McKenna, S. A. 1987. Food of striped bass in the upper Bay of Fundy, Canada. Trans. Am. Fish. Soc. 116:119-122.

Schaefer, R. H. 1970. Feeding habits of striped bass from the surf waters of Long Island. N.Y. Game Fish J. 17:1-17.

Schmitt, P. D. 1986. Prey size selectivity and feeding rate of larvae of the northern anchovy, *Engraulis mordax Girard*. Rep. CCOFI. 27:153-161.

Scott, M. A. and W. W. Murdoch. 1983. Selective predation by the backswimmer, *Notonecta*. Limnol. Oceanogr. 28:352-366.

Setzler, E. M., plus eight others. 1980. Synopsis of biological data on striped bass, *Morone saxatilis* (Walbaum). NOAA Tech. Rep., NMFS Circular 433. FAO Synopsis No. 121. 69 pp.

Setzler-Hamilton, E. M., Hall, L., Jr. 1991. pp 13-1 to 13-25, In: Habitat Requirements for Chesapeake Bay Living Resources. S. L. Funderburk, J. A. Mihursky, S. J. Jordan, and D. Riley (eds.), Chesapeake Research Consortium, Solomons, Maryland.

Sprules, W. G. 1972. Effects of size-selective predation and food competition on high altitude zooplankton communities. Ecology 53:375-386.

Stein, R. A., S. T. Threllkeld, C.D. Sandgren, W. G. Sprules, L. Persson, E. E. Werner, W. E. Neill, and S. I. Dodson. 1988. Size-structured interactions in lake communities. In: Complex interactions in lake communities, Carpenter, S .R. (ed). 161-179. Springer-Verlag New York.

Texas Instruments. 1976. Predation by bluefish in the lower Hudson River. Final Report to Consolidated Edison Company of New York.

U.S. National Marine Fisheries Service. 1978. Fishery statistics of the United States, 1977. U.S. National Marine Fisheries Service Current Fishery Statistics, No. 7500. 112 pp.

Vanni, M. J. 1986. Fish predation and zooplankton demography: indirect effects. Ecology 67:337-354.

Werner, E. E. and D. J. Hall. 1974. Optimal foraging and the size selection of prey by the bluegill sunfish (*Lepomis macrochirus*). Ecology 55: 1042-1052.

Zastrow, C.E., and E.D. Houde, and L.G. Morin. 1991. Spawning, fecundity, hatch-date frequency and young-of-the-year growth of bay anchovy *Anchoa mitchilli* in mid-Chesapeake Bay. Mar. Ecol. Prog. Ser. 73:161-171.